NASA CR-120888
Contract NAS3-12023

Final
Report

March 1972

Composite Overwrapped Metallic Tanks

MARTIN MARIETTA CORPORATION

1. Report No.	2. Government Accession No.	3. Recipient's Catalog No.
NASA CR-120888		

4. Title and Subtitle	5. Report Date
COMPOSITE OVERWRAPPED METALLIC TANKS	March 1972
	6. Performing Organization Code

7. Author(s)	8. Performing Organization Report No.
C. L. Caudill and R. L. Kirlin	-
	10. Work Unit No.

9. Performing Organization Name and Address	11. Contract or Grant No.
Martin Marietta Corporation P.O. Box 179 Denver, Colorado 80201	NAS3-12023
	13. Type of Report and Period Covered Contractor Report Feb 28, 1970 to Dec 17, 1971
12. Sponsoring Agency Name and Address	14. Sponsoring Agency Code
National Aeronautics and Space Administration Washington, D.C. 20546	

15. Supplementary Notes

Project Manager, James R. Barber, Liquid Rocket Technology Branch,
NASA Lewis Research Center, Cleveland, Ohio

16. Abstract

The purpose of this program was to design, fabricate, and test glass-fiber-reinforced (GFR) titanium pressure vessels suitable for the containment of helium at cryogenic temperatures and up to 160°F.

The first two portions of this four-part effort are covered in the interim report, NASA CR-72765, MCR-70-350. That document includes a detailed report on Task I, Titanium Properties Determination, and Task II, Pressure Vessel Design. This volume will deal with Task III, Vessel Fabrication, and Task IV, Test Program.

Difficulties encountered in the tank liner fabrication phase involved explosive forming, vacuum annealing, chemical milling and electron beam welding. While each of these processes and the nondestructive test methods employed are normally considered to be individually reliable, the combination of poor material together with fabrication and development reversals prevented the full achievement of the desired end results.

Eight tanks plus a prototype and tool proofing article were produced. Six of the vessels failed during the hydrostatic sizing operation. One of the remaining tanks was hydrostatically pressurized to burst and the other was pressurized repeatedly at 75°F from 100 psi to the operating pressure until failure occurred. As a result, it is not possible to draw firm conclusions as to the true value of the design concept due to the problems encountered in the program.

17. Key Words (Suggested by Author(s))	18. Distribution Statement
titanium 5Al-2.5 Sn explosive forming pressure vessels composite overwrap electron-beam welding chemical milling	Unclassified-Unlimited

19. Security Classif. (of this report)	20. Security Classif. (of this page)	21. No. of Pages	22. Price*
Unclassified	Unclassified	138	$3.00

* For sale by the National Technical Information Service, Springfield, Virginia 22151

FOREWORD

This report is submitted by the Martin Marietta Corporation in fulfillment of Contract NAS3-12023 and covers Task III, Vessel Fabrication, and Task IV, Test Program. These tasks were accomplished between February 28, 1970, and December 17, 1971.

The program was performed under the cognizance of the Structures and Materials Research Organization, Mr. James A. Sterhardt, Mr. B. Lee Bogema, and Mr. William F. Barrett, Department Managers. Dr. Arthur Feldman was Program Manager for Tasks I and II, with Dr. Alvin Holston responsible for the computer program revision and vessel design. The results of the Task I and II efforts are reported in *Composite Overwrapped Metallic Tanks, Interim Report*, NASA CR-72765, dated October 1971.

Mr. Charles Caudill replaced Dr. Feldman as Program Manager shortly after the initiation of Task III, Vessel Fabrication. Mr. Ronald Kirlin became Project Engineer and Dr. Holston continued to provide the necessary computer revisions. Acknowledgement is due Dr. Feldman for consultation, Mr. Donald Stang, Composites Laboratory, who performed overwrapping operation, and Mr. Bernie Bandelin of the Baltimore Division for electron beam welding, hot sizing, and other fabrication efforts. Dr. Jimmy Mote was responsible for explosive forming and Mr. Don Dulaigh was Project Test Conductor for sizing, burst, and cyclic tests. Mr. Russell McCord provided the Quality Engineering and Control support.

CONTENTS

ABSTRACT

The purpose of this program was to design, fabricate, and test glass-fiber-reinforced (GFR) titanium pressure vessels suitable for the containment of helium at cryogenic temperatures and up to 160°F.

The first two portions of this four-part effort are covered in the interim report NASA CR-72765, MCR-70-350. That document includes a detailed report on Task I, Titanium Properties Determination, and Task II, Pressure Vessel Design. This volume will deal with Task III, Vessel Fabrication, and Task IV, Test Program. As may be seen herein, many fabrication and development reversals prevented the full achievement of the desired end results. It is not possible to draw firm conclusions as to the true value of the design concept due to the problems encountered in the program.

SUMMARY

The following three paragraphs cover the portion of effort accomplished in Task I, Titanium Properties Determination, and Task II, Pressure Vessel Design. The results of these tasks were reported in the interim report, NASA CR-72765.

To better use the strength of fiberglass in a pressure vessel application, NASA originated the concept of forcing a metal liner to exist in a compressive stress state with zero internal pressure. This investigation tested the concept first by examining the behavior of the candidate liner material, 5Aℓ-2.5Sn titanium (ELI) under various loading conditions, temperatures, and subjecting it to several manufacturing processes. Second, an existing computer program for the design of vessels operating this way was revised to account for a liner of variable thickness in the domes, thus distributing the stresses in a more favorable fashion and increasing the possible weight savings over an all-metal vessel.

The liner material tests performed were uniaxial tensile tests at room temperature, liquid nitrogen temperature (-320°F), and liquid hydrogen temperature (-423°F); biaxial tensile tests at these temperatures of specimens that had been chem-milled, electron-beam-welded, tungsten-inert gas welded, and explosively formed; compressive "creep" tests of specimens that had been electron-beam-welded and overwrapped with fiberglass/epoxy; and uniaxial tensile tests of specimens that had been chem-milled, and mechanically milled. The conclusion drawn from these tests was that, although some of the processes reduced the ductility of the liner material, sufficient ductility remained so pressure vessel performance was not degraded.

Successful revision of the computer program to account for a variable liner thickness permitted studies to be made concerning the functional form the thickness variation should take. A piecewise linearly varying liner was chosen for its generality and seemed to produce an effective design and a good distribution of liner overwrap stress. Studies of the effect of manufacturing tolerance on vessel weight and performance indicated that a tradeoff must be made between the cost of increased care in manufacturing and the cost of either lessened efficiency or lessened reliability of the vessel.

The remaining paragraphs of this section summarize the efforts of Task III, Vessel Fabrication, and Task IV, Test Program.

As a result of the favorable tests and evaluations realized during the first two tasks described above, raw material and an explosive-forming die were ordered. By the time the raw material had been received and the explosive-forming die finish-machined, the program had been rescheduled and the completion of tank fabrication (Task III) was one year behind the original schedule. In addition to this problem, the development of explosive-forming for full-scale domes resulted in a combination of broken domes and failure of the domes to meet contour requirements. Subsequent metallurgical surveys revealed that the plate material had a highly textured alpha microstructure that rendered it unsuitable for forming. Since this material was the only 5Aℓ-2.5Sn titanium of this thickness available and the delivery of replacement material would take several months, it was determined that a proper annealing cycle that would yield an equiaxial grain structure would have to be developed. An annealing cycle was developed and all of the remaining material was reannealed. Explosive forming continued with some success, but was still plagued with variations in response to identical explosive charges. The number of shots required varied from two to four and a similar number of process vacuum anneals was required. Unfortunately, the vacuum furnace had contaminated a large portion of the domes. The cause and effect are discussed in the appropriate section of this document. Ultimately, this contamination problem reduced the number of usable domes to 19. A maximum effort was made to assure that the tank liners were of high quality, but the incompatibility of poor explosive-forming tolerance control and the sensitivity of electron beam welding to poor tolerance control resulted in premature failure of the overwrapped tanks.

I. INTRODUCTION

The objective of this program was to develop a fiberglass overwrapped titanium pressure vessel for cryogenic service. Although techniques for filament winding solid-fueled missile cases have been developed, there has been a significant lag in the development of techniques for successfully applying filament winding to fabrication of glass-fiber/epoxy pressure vessels for gas or liquid containment. Considering the very attractive strength-to-density properties of filament-wound materials, it is essential that the techniques necessary to make pressure vessels using this fabrication method be developed.

The principal difficulty that has prevented success in applying filament winding to pressure vessels is the lack of a reliable liner system for both room-temperature storable and cryogenic propellants. A liner is needed because the organic matrix materials used in filament winding are permeable. For room-temperature application, elastomeric liners would suffice except for problems of chemical compatibility; for cryogenic service the elastomeric liners are not suitable because of their brittle behavior. Therefore, metal liner systems are required.

The principal problem with the metal liner is one of mechanical compatibiity, i.e., the strain imparted to the liner during pressurization and the attendant deformation of the glass-fiber vessel must be reabsorbed during depressurization of the vessel. Furthermore, it must be reabsorbed for each cycle without liner malfunction in spite of the fact that full utilization of the overwrap may require the liner to experience some plastic straining.

Recent work* with overwrapping relatively thick Inconel metal load-bearing liners has indicated that this overwrapping concept reliably provides a significant weight saving. The principle involved in overcoming the mechanical compatibility problem is to place the metal liner under compression during fabrication to increase the strain range though which the liner may operate. At the same time, the glass-fiber/epoxy overwrap is placed in tension. Matching the overwrap tension properly to the liner compression results in the operation of the overwrap at an efficient stress level while the liner remains elastic. The creep and biaxial strain properties of the liner material must be considered when the zero-pressure stress levels are chosen so this prestressed state is not seriously diminished with time. Otherwise the inelastic strain to which the liner would be subjected in each cycle would degrade the metal's fatigue resistance.

*NASA CR-72224 and NASA CR-54855 (Contract NAS3-6292). Aerojet Liquid Rocket Company, Sacramento, California.

The performance factor (pressure x volume/weight) of a vessel thus designed is between that of an all-metal vessel and that of a glass-fiber/epoxy filament-wound vessel with a thin, nonload-bearing metal liner. Until a nonload-bearing liner is developed, the overwrapped load-bearing liner can provide weight savings. These savings strongly depend on the elastic strain/weight ratio for the liner material. Titanium promises to provide even higher performance factors than Inconel, especially if a liner of non-uniform thickness is used to approximate a uniform stress state.

The objective of this program was pursued with the effort divided into four major tasks as tabulated.

Task No.	Effort
I	Titanium Properties Determination
II	Design Computer Program Revision Pressure Vessel Design
III	Manufacture Explosive Forming Development Liner Fabrication Pressure Vessel Winding and Sizing
IV	Test Design and Fabrication of Test Fixtures Burst and Cyclic Tests

The narrative and data above were extracted from the interim report, NASA CR-72765.* This final report covers the details of Task III, Vessel Fabrication, and Task IV, Test Program.

Because of premature failures in fabrication and testing, the program did not completely prove or disprove the design concept of the overwrapped titanium tank. Poor materials, incompatibility of the interrelated manufacturing processes, and less than positive nondestructive test methods are felt to be the primary causes for the premature test failures. Details of these problems may be found in the body of the text.

*_Composite Overwrapped Metallic Tanks, Interim Report._ Martin Marietta Corporation, Denver, Colorado, October 1971.

II. DESIGN

The design for the tankage developed in Task II was reported in *Composite Overwrapped Metallic Tanks, Interim Report*, NASA CR-72765. The original design plan was to mechanically machine the domes to close tolerance for weight control. This became impossible because of dome contour variations. Other changes discussed in this chapter were minor in nature and were made, for the most part, to facilitate fabrication. The specific details of these changes will be discussed in the following sections.

A. DESIGN DESCRIPTION

The titanium (5Aℓ-2.5Sn, ELI) tank liner consisted of two ellipsoidal domes, a rolled and welded narrow cylindrical barrel section, and two end boss fittings machined from bar stock (Fig. 1).

The completed tank liner was overwrapped with epoxy-preimpregnated fiberglass (20 end roving S-994) in both the hoop and polar directions. The engineering drawings for the tank are included in the appendix of this report.

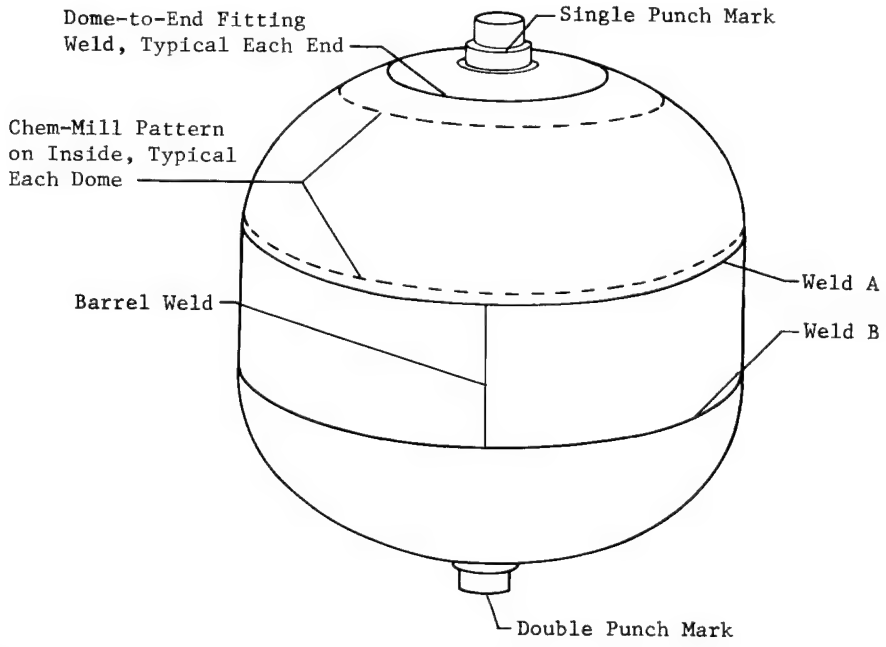

Figure 1 Weld Designation and Location Schematic, Titanium Tank Liner

B. TANK MATERIALS

The original tank liner materials used in the Task I tests were titanium 5Aℓ-2.5Sn (ELI) as supplied by both the Titanium Metals Corporation of America and Reactive Metals, Inc. The overwrap material, epoxy-impregnated (18 to 23% solids by weight) 20 end S-HTS/E-796, was supplied by the U.S. Polymeric Corporation. The material used in biaxial and creep tests was from the Titanium Metals Corporation, and the material for coupon tests was supplied by Reactive Metals, Inc.

The titanium procured for the full-scale tank liners was produced by Reactive Metals, Inc. because of their stated capability to produce the entire lot of plates from a single heat of material.

Fiberglass roving S-994/HTS impregnated with EPON 828/DSA/EMPOL BDMA was procured from Fiberite Corporation because of cost and schedule considerations.

C. DOMES

The design of the original configuration was changed to provide for chemical milling in two zones on the inside of each dome for weight reduction. The original design had called for a tapered cross section to be machined mechanically. Since the variations in contour resulting from springback and bounceback in explosive forming in many instances exceeded the thickness of the dome wall, mechanical machining could not be performed and it became necessary to reduce the wall section by chemical milling (Fig. 2). The results of a computer program for selecting proper wall thickness and comparing a chem-milled stepped liner with a continuously varying liner are shown in the appendix.

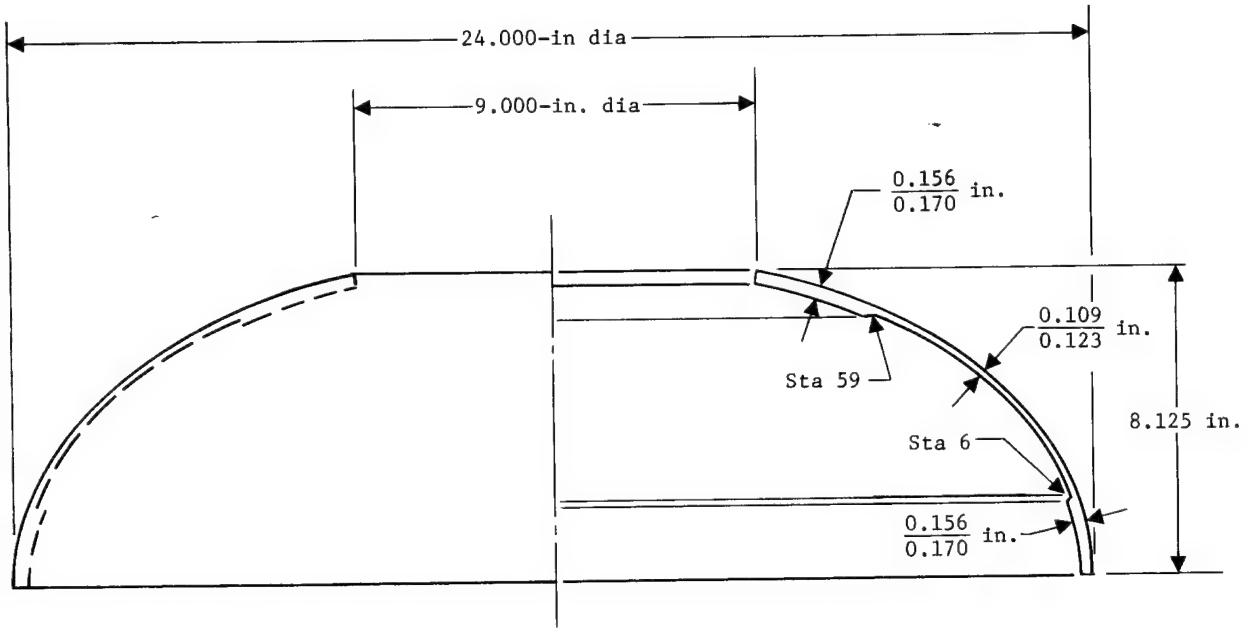

Figure 2 Chemically Milled Dome Configuration Design

D. END BOSS

The original design appeared to include closer tolerances than absolutely necessary. A redesign that relaxed certain radii and noncritical thickness tolerances is now reflected in Drawing FWL-69002 (see appendix).

E. CYLINDRICAL SECTION

The only change in this area was a revision to include a circumferential flat butt joint that replaced the original step joint. The width of several cylindrical sections was reduced when they were separated from previously welded liners to allow for reweld-ing.

F. OVERWRAP

The design for overwrapping was corrected to change the angle of the wrap from the computer-generated angle of 6°39' to the actual of 10°15' (refer to Drawing FWL-69002 in the appendix). This angle revision was necessary because the computer assumed the ribbon width to be zero whereas it is actually 2.1 inches.

G. WEIGHT VARIATIONS

The estimated and actual weights are tabulated.

	Estimate, lb (kg)	Actual, lb (kg)	
		Minimum	Maximum
Tank Liner	41.2 (18.7)	40.6 (18.4)	45.0 (20.4)
Overwrap	24.3 (11.0)	26.1 (11.8)	30.0 (13.6)
Tank	65.5 (29.7)	68.0 (30.8)	73.0 (33.1)

The weights varied more than anticipated. The total weight of the completed tank was a function of both the liner and the overwrap variations.

The liner variations were due to several items:

1) Chemical milling thickness variations were dependent on explosively formed parts that had thickness variations up to 20%;

2) Several of the tanks were disassembled and rewelded at the girth after remachining.

The overwrap variations were due to:

1) The variations in resin content on the preimpregnated roving;

2) Addition of fiberglass doilies or extra wraps to reduce liner joint mismatch or weld bead height;

3) Added hoop wraps when migration of the roving moved from the cylindrical section toward the dome;

4) The weight of the polar wrap was a direct function of the dome surface area. Domes that most nearly met the proper contour possessed more surface area than those that did not properly fill out in the explosive-forming process.

H. CONCLUSIONS

The design concept itself was neither proved nor disproved at completion of the program. This was due in most part to a series of interrelated problems. These began with poor material and an unusual number of reversals in what were initially thought to be reliable manufacturing and inspection processes.

The major area in which the design itself contributed to the difficulties was the lack of an access port that would permit internal weld tooling and/or nondestructive tests, i.e., single-wall X-ray, die penetrant, and visual inspection.

III. FABRICATION

A. MATERIALS

1. Titanium Bar

The raw material from which the end fittings were machined was received in the proper annealed condition and no fabrication problems were encountered.

2. Titanium Plate

The raw material as received from the supplier contained numerous surface defects and, even though bought to commercial standards, part of the shipment was returned to the supplier for poor workmanship. The variations in flatness from the edge to the center of a sheet, though within specification requirements, made it very difficult to work in the explosive-forming process. Attempts to machine the surfaces to a close tolerance were not successful because of the inability to hold the material flat. In general, it is concluded that the poor quality of the material (see Section B) had a major bearing on the program's lack of success (Fig. 3, 4, and 5).

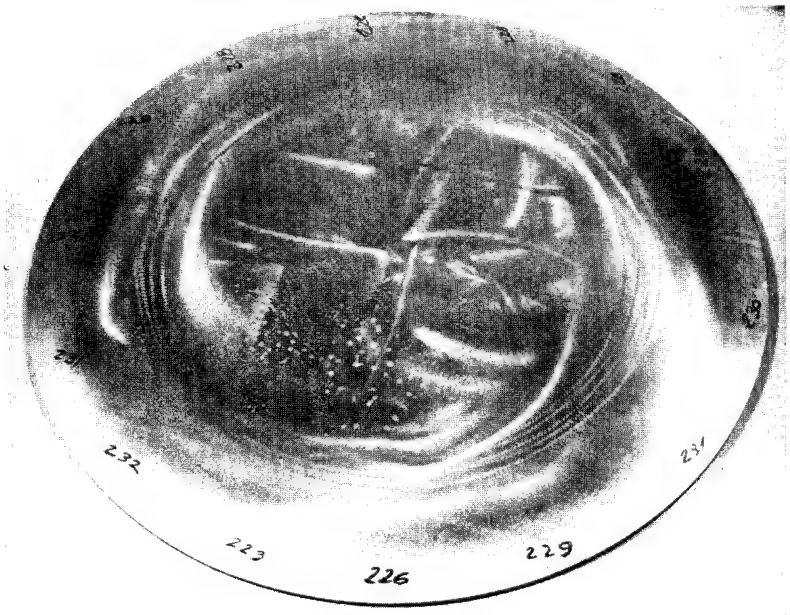

Figure 3 Explosive-Forming Titanium Blank Showing Rolled-In Defects and Surface Pitting Remaining After Attempts to Grind the Surface under a Coolant

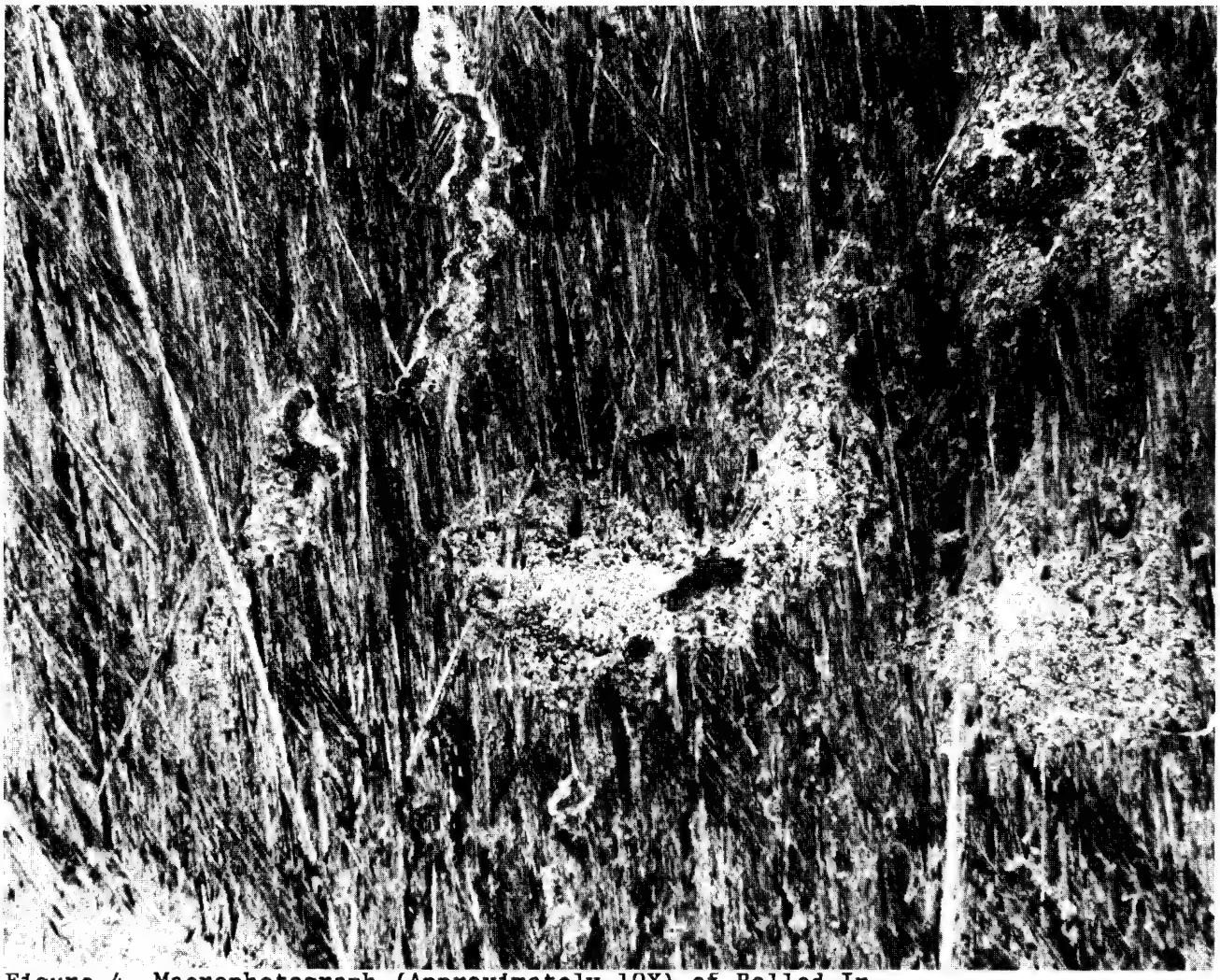

Figure 4 Macrophotograph (Approximately 10X) of Rolled-In Surface Defects in Titanium Plate Shown in Figure 3

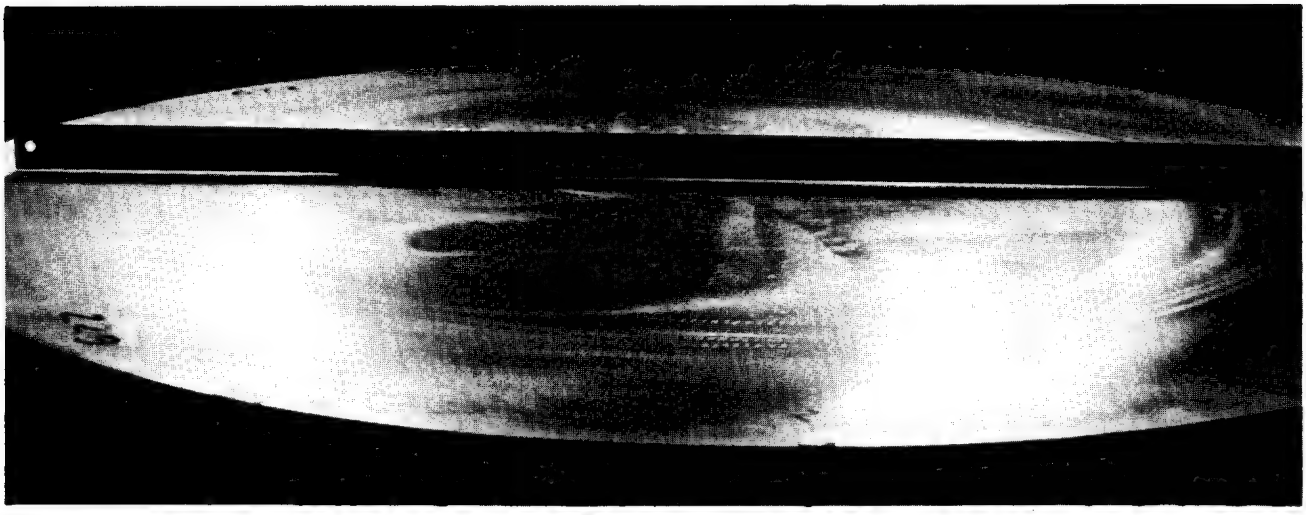

Figure 5 Explosive-Forming Blank (Same as Fig. 3 and 4) Illustrating Deviation From Flatness

The plate material was ordered in May 1969 and delivery was promised on July 15, 1969. Eleven sheets of the 14 ordered were received in September. One was rejected for poor-quality surface and substandard workmanship. The remaining four were delivered in January 1970 and did not show a marked improvement in quality. Thus, the philosophy of obtaining all the material from the same heat for maximum uniformity was negated by the supplier.

B. EXPLOSIVE-FORMING DEVELOPMENT, INCLUDING ANNEALING AND CLEANING OF DOMES

The full-scale explosively formed dome development activity began on February 16, 1970. The dome shape is shown in Figure 6. Six blanks were cut from two plates, and as may be seen in Table 1, one dome was fractured in the first series. Even though several combinations of explosive-forming parameters were tried, none produced a satisfactory dome because of excessive contour deviations. The last shot of this series was completed on February 25, 1970, and the final forming parameter recommendations were completed on March 9, 1970. After considerable discussion as to the proper parameters for forming, it was determined that a second series of domes would be shot to prove repeatibility. One of the recommendations from the Explosive-Forming Group was that the blanks should be machined to uniform flatness and thickness. To give the process the greatest likelihood of success, one plate (3 blanks) was machined. Three dome blanks of each condition (machined and as-received) were put into the repeatibility test with first shot charges of 8100 grains. One blank of each group failed and production was halted after the second failure, leaving one of the six blanks unformed (Table 2).

A metallurgical investigation as to the cause of failures was then undertaken. The normal cause for forming failures in titanium (a hard face-oxidized surface and contamination) was suspect. Investigation revealed that improper annealing by the producer rather than contamination was the cause. Mill records were studied and it was determined that one group of the plates had been annealed at 1500°F for 30 minutes and the second group at 1500°F for 15 minutes. While normal tensile tests did not reveal the lack of a proper anneal, the photomicrographs left no doubt as to the material condition. Photomicrographs (Fig. 7 and 8) show the heavily textured grain structure with no indication of alpha surface scale. All the formed domes listed in Tables 1 and 2 exhibited crosshatched microcracks (Fig. 9). The crosshatched microstructure automatically scrapped all domes that had been produced to this point even though they did not indicate conditions of surface cracking. The normal equiaxial grain structure for this alloy is shown in Figure 10.

Table I Experimental Explosive-Forming Data - First Series

Dome Designation	Explosive Shot Sequence	Explosive Size, grains	(grams)	Standoff Height, in.	(cm)	Draw Depth, in.	(cm)
A3	1	7680	(496.89)	3	(7.62)	7.75	(19.68)
	2	4000	(258.80)	4	(10.16)	10.00	(25.40)
B3	1	8020	(518.89)	3	(7.62)	7.81	(19.81)
	2	4500	(291.15)	4	(10.16)	10.00	(25.40)
A2	1	8360	(540.89)	3	(7.62)	7.92	(20.11)
	2	3200	(207.04)	4	(10.16)	10.00	(25.40)
	3	2500	(161.75)	7	(17.78)	10.00	(25.40)
B2	1	9000	(582.30)	3	(7.62)	Broke	
B1	1	8300	(540.89)	3	(7.62)	7.97	(20.24)
	2	4500	(291.15)	7	(17.78)	10.00	(25.40)
A1	1	8360	(540.89)	3	(7.62)	8.123	(20.63)
	2	2560	(165.63)	4	(10.16)	10.00	(25.40)
	3	2000	(129.40)	4	(10.16)	10.00	(25.40)

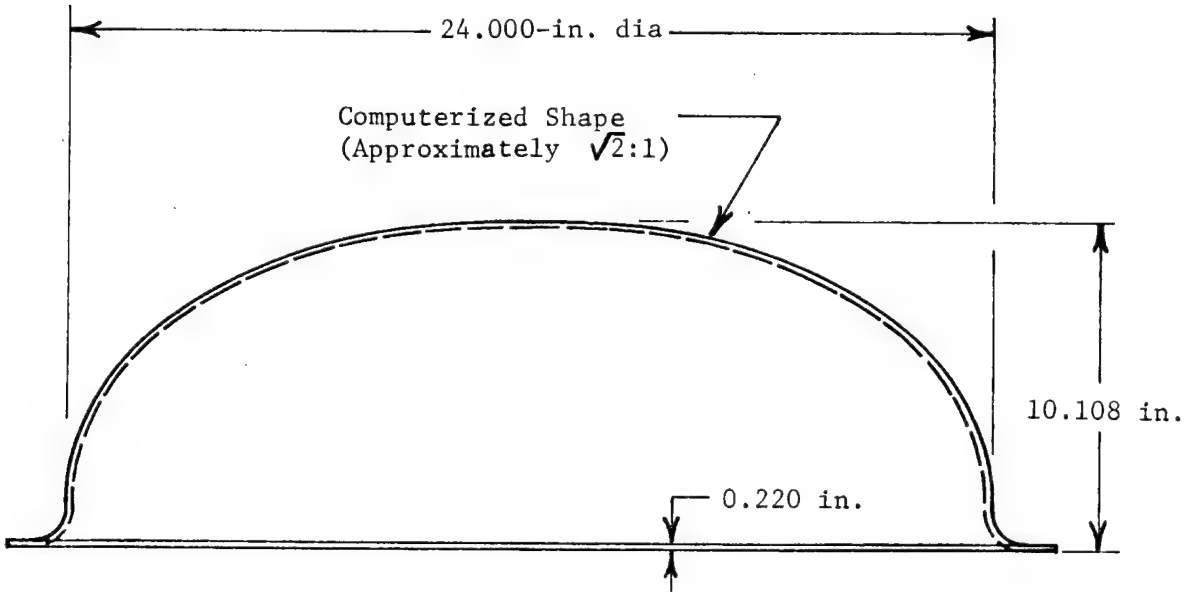

Figure 6 Explosively Formed Dome Shape

Table 2 Experimental Explosive-Forming Data - Second Series

Dome Designation	Explosive Shot Sequence	Explosive Size, grains	(grams)	Standoff Height, in.	(cm)	Draw Depth, in.	(cm)
C2	1	8100	(524.07)	3	(7.62)	7.93	(20.14)
C1	1	8100	(524.07)	3	(7.62)	Broke	
C3	1	8100	(524.07)	3	(7.62)	7.94	(20.16)
D1	1	7700	(498.19)	3	(7.62)	7.88	(20.01)
D3	1	8100	(524.07)	3	(7.63)	Broke	

Figure 7 Photomicrograph of Cross Section at 100X from Failure Area of Dome C-2 Showing Hot Roll Texture

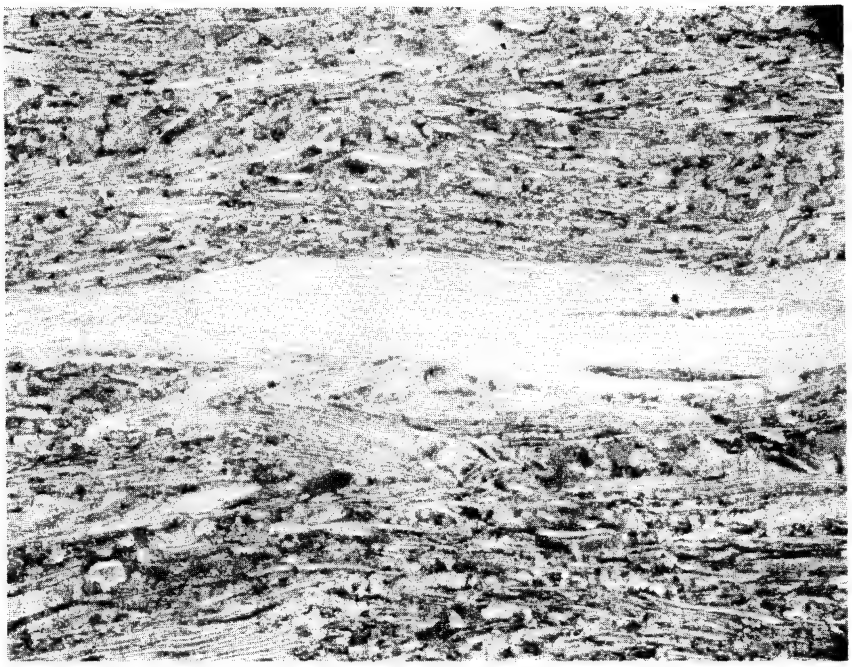

Figure 8 Photomicrograph of Longitudinal Cross Section at 100X of As-Received "C" Plate

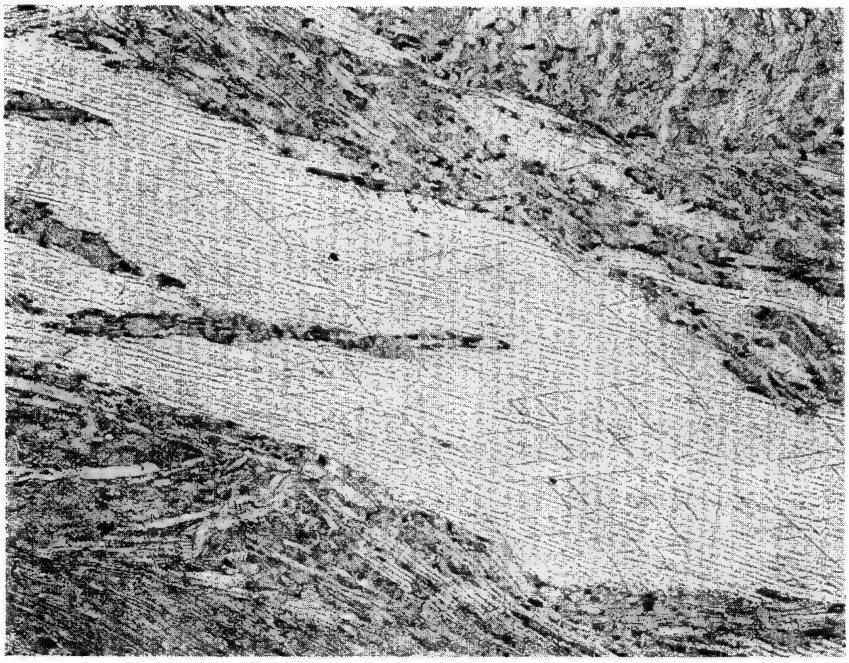

Figure 9 Photomicrograph of Cross Section at 100X from Failure Area of Dome D-3 Showing Crosshatch Cracking

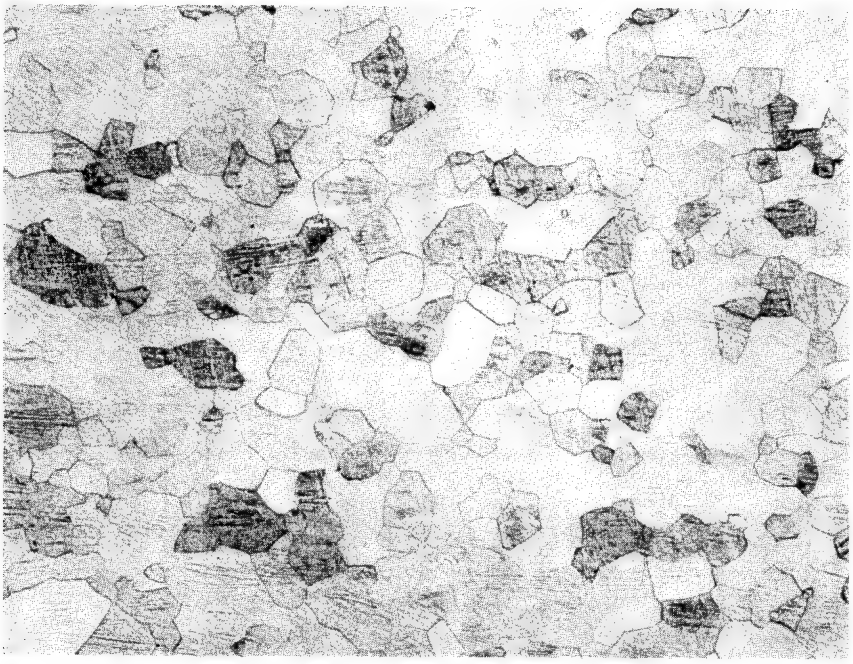

Figure 10 Photomicrograph of Properly Annealed Ti-5Aℓ-2.5Sn (ELI)

Attempts to return the material to the producers were fruitless and, since replacement appeared out of the question, it was determined that a proper annealing cycle must be developed to salvage the remaining material. This was accomplished, and a period of four hours at 1650°F in a vacuum followed by a furnace-cool proved to be the optimum cycle. The full report of the failure analysis and supporting technical data may be found in the appendix. The ABAR vacuum furnace at the Denver Division facility was not large enough to economically anneal the blanks. The only other suitable, certified vacuum furnace in the area was located some 60 miles away in Colorado Springs at the Proto Shop. This furnace, an Ipsen, contained automatic controls, proper temperature and pressure readouts, and recording equipment. After thoroughly discussing the problem, arrangements were made with the very cooperative Proto Shop management to give the titanium annealing effort first priority. A maximum effort to properly anneal the material for explosive forming and to provide "in process" annealing between shots was undertaken. The annealing for the remaining supply of blanks began on April 23 and was completed on May 23. In the meantime, blanks were being given their first explosive-forming shots, process annealing, and second shots, etc, as rapidly as

possible per the program flow chart (Fig. 11). Of the six blanks put into the explosive-forming operation, one failed and damaged the die face (see Table 3). This occurred on April 24 when an excessive charge of 9300 grains was tried to determine if the new annealing process might allow a larger first charge to improve the contour control. After a few more first shots were made, it was determined that damage to the die face was sufficient to cause potential problems when the domes, receiving their last shot, would strike the scarred surface of the die.

Table 3 Experimental Explosive-Forming Data - Third Series

Dome Designation	Explosive Shot Sequence	Explosive Size, grains	(grams)	Standoff Height, in.	(cm)	Draw Depth, in.	(cm)
AA1	1	9000	(582.30)	3	(7.62)	8.93	(22.68)
	2	3100	(200.57)	4	(10.16)	9.87	(25.06)
AA2	1	8500	(549.95)	3	(7.62)	8.65	(21.97)
	2	3100	(200.57)	4	(10.16)	9.99	(25.37)
AA3	1	9300	(601.71)	3	(7.62)	Broke	
BB1	1	8500	(549.95)	3	(7.62)	8.66	(21.99)
	2	2900	(187.63)	6	(15.24)	9.93	(25.22)
	3	2900	(187.63)	12	(30.48)	9.98	(25.34)
BB2	1	8500	(549.95)	3	(7.62)	8.63	(21.92)
	2	3100	(200.57)	4	(10.16)	9.99	(25.37)
BB3	1	8500	(549.95)	3	(7.62)	8.69	(22.07)
	2	3100	(200.57)	4	(10.16)	9.99	(25.37)

Coincidentally with the die surface problem, it was observed that excessive dome springback was occurring. Since the contour of the die face did not include a springback factor, the springback data were analyzed and a new contour developed. The die was returned to the machining vendor for corrective machining.

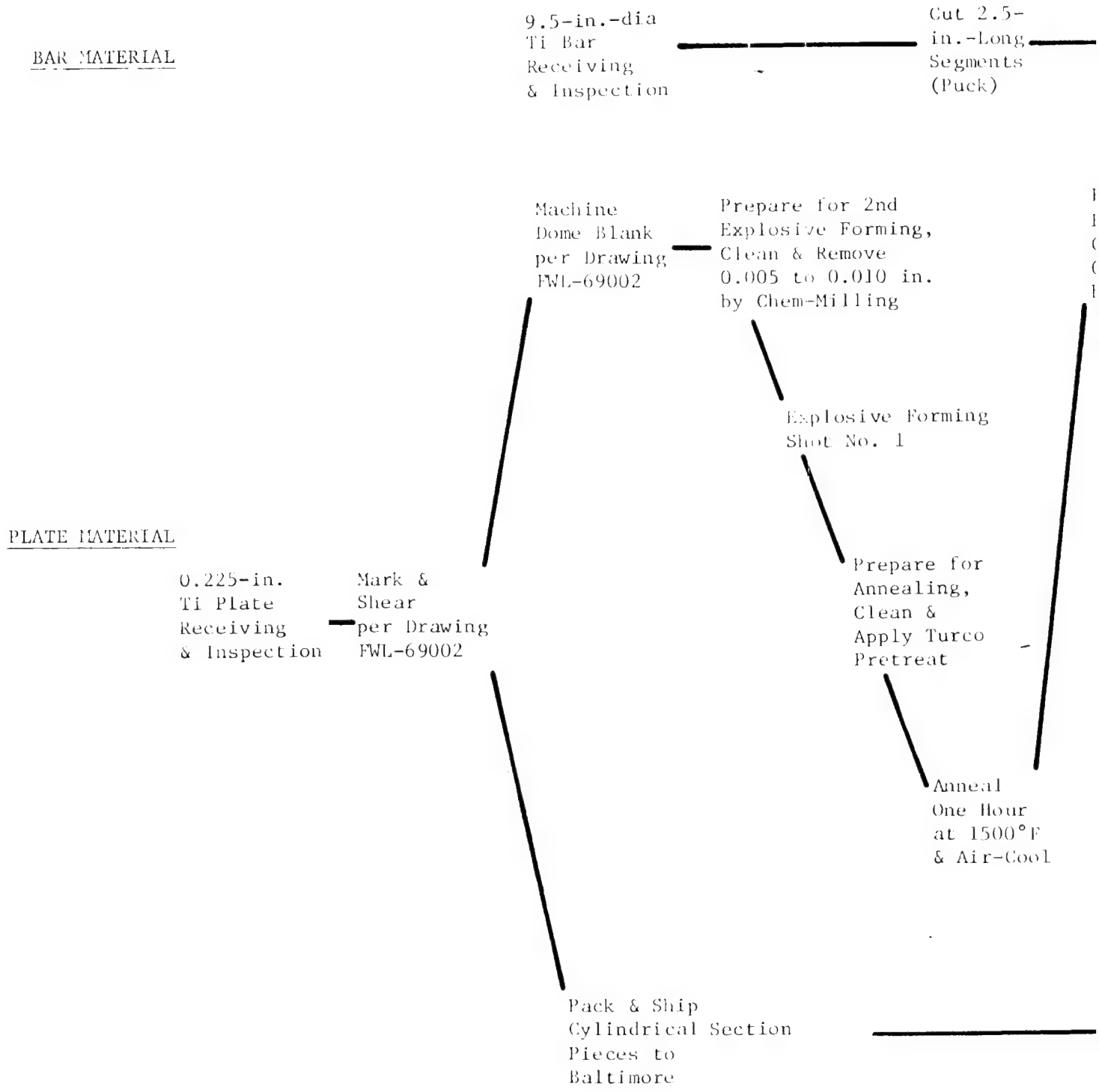
BAR MATERIAL
9.5-in.-dia Ti Bar Receiving & Inspection
Cut 2.5-in.-Long Segments (Puck)
Machine Dome Blank per Drawing FWL-69002
Prepare for 2nd Explosive Forming, Clean & Remove 0.005 to 0.010 in. by Chem-Milling
Explosive Forming Shot No. 1
PLATE MATERIAL
0.225-in. Ti Plate Receiving & Inspection
Mark & Shear per Drawing FWL-69002
Prepare for Annealing, Clean & Apply Turco Pretreat
Anneal One Hour at 1500°F & Air-Cool
Pack & Ship Cylindrical Section Pieces to Baltimore

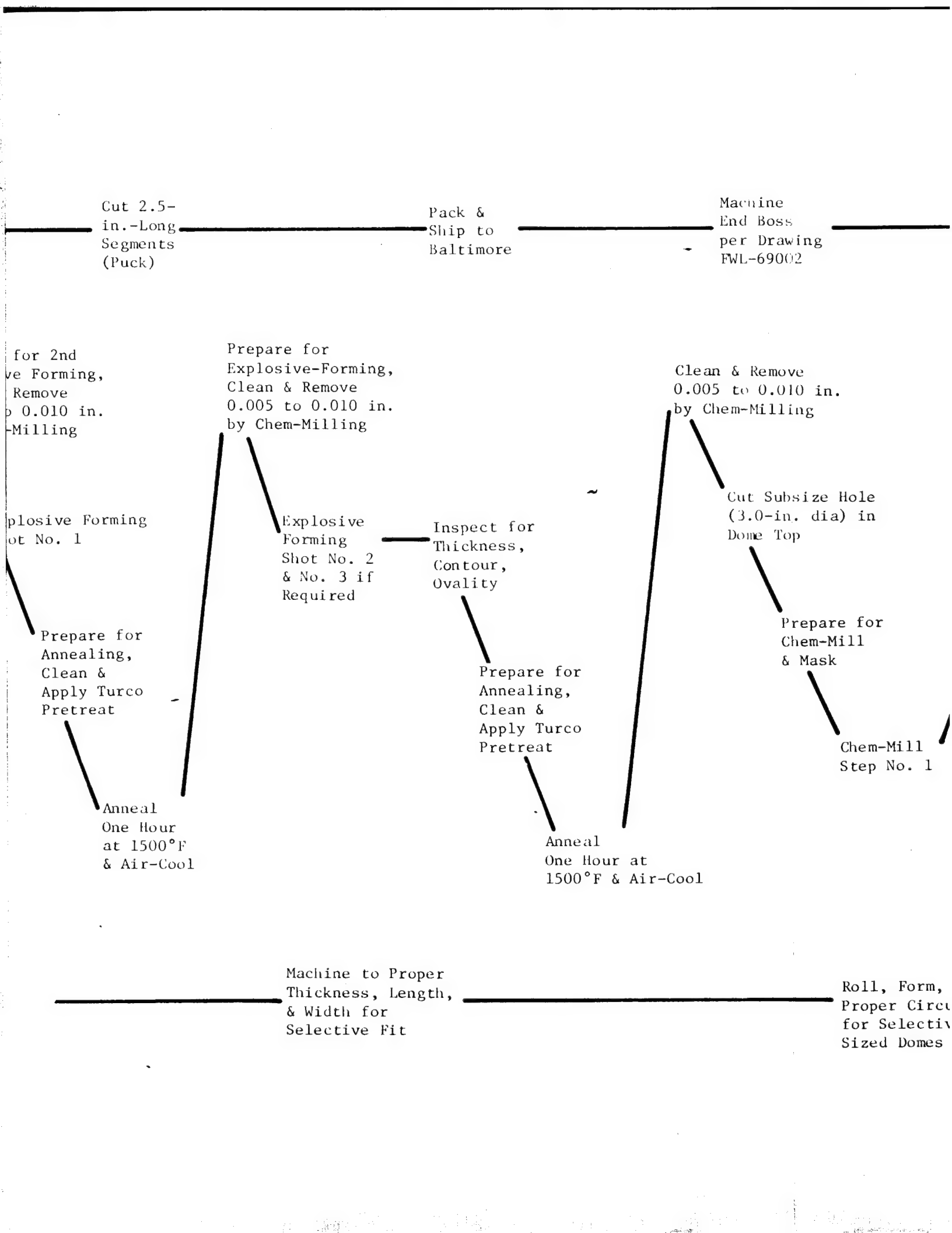
Cut 2.5-in.-Long Segments (Puck)
Pack & Ship to Baltimore
Machine End Boss per Drawing FWL-69002
for 2nd ve Forming, Remove 0.010 in. -Milling
Prepare for Explosive-Forming, Clean & Remove 0.005 to 0.010 in. by Chem-Milling
Clean & Remove 0.005 to 0.010 in. by Chem-Milling
plosive Forming ot No. 1
Explosive Forming Shot No. 2 & No. 3 if Required
Inspect for Thickness, Contour, Ovality
Cut Subsize Hole (3.0-in. dia) in Dome Top
Prepare for Annealing, Clean & Apply Turco Pretreat
Prepare for Annealing, Clean & Apply Turco Pretreat
Prepare for Chem-Mill & Mask
Chem-Mill Step No. 1
Anneal One Hour at 1500°F & Air-Cool
Anneal One Hour at 1500°F & Air-Cool
Machine to Proper Thickness, Length, & Width for Selective Fit
Roll, Form, Proper Circu for Selectiv Sized Domes

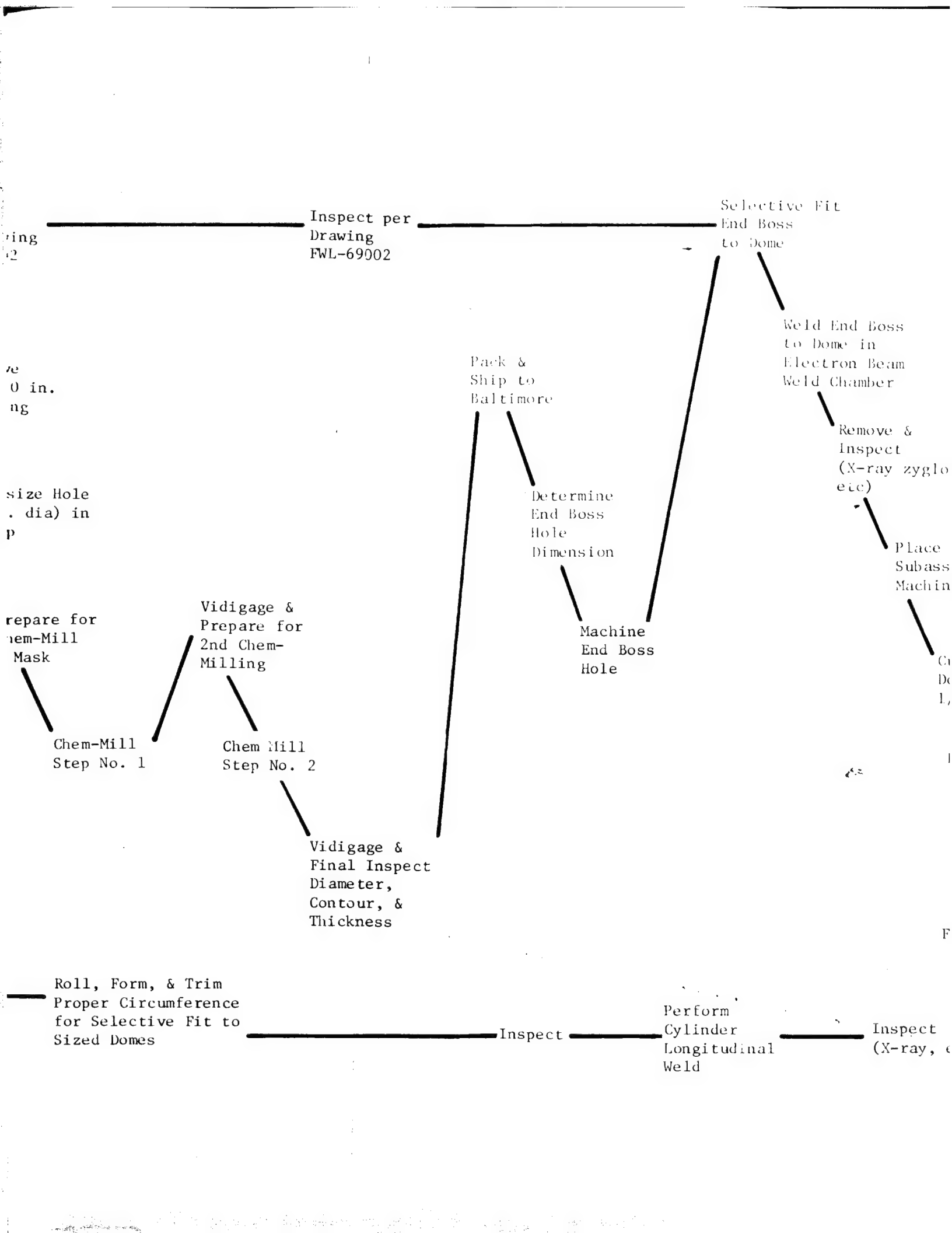
ring
2
Inspect per Drawing FWL-69002
Selective Fit End Boss to Dome
Weld End Boss to Dome in Electron Beam Weld Chamber
Remove & Inspect (X-ray zyglo etc)
Place Subass Machin
Pack & Ship to Baltimore
Determine End Boss Hole Dimension
Machine End Boss Hole
e
0 in.
ng
size Hole
. dia) in
p
repare for
hem-Mill
Mask
Vidigage & Prepare for 2nd Chem-Milling
Chem-Mill Step No. 1
Chem Mill Step No. 2
Vidigage & Final Inspect Diameter, Contour, & Thickness
Roll, Form, & Trim Proper Circumference for Selective Fit to Sized Domes
Inspect
Perform Cylinder Longitudinal Weld
Inspect (X-ray,

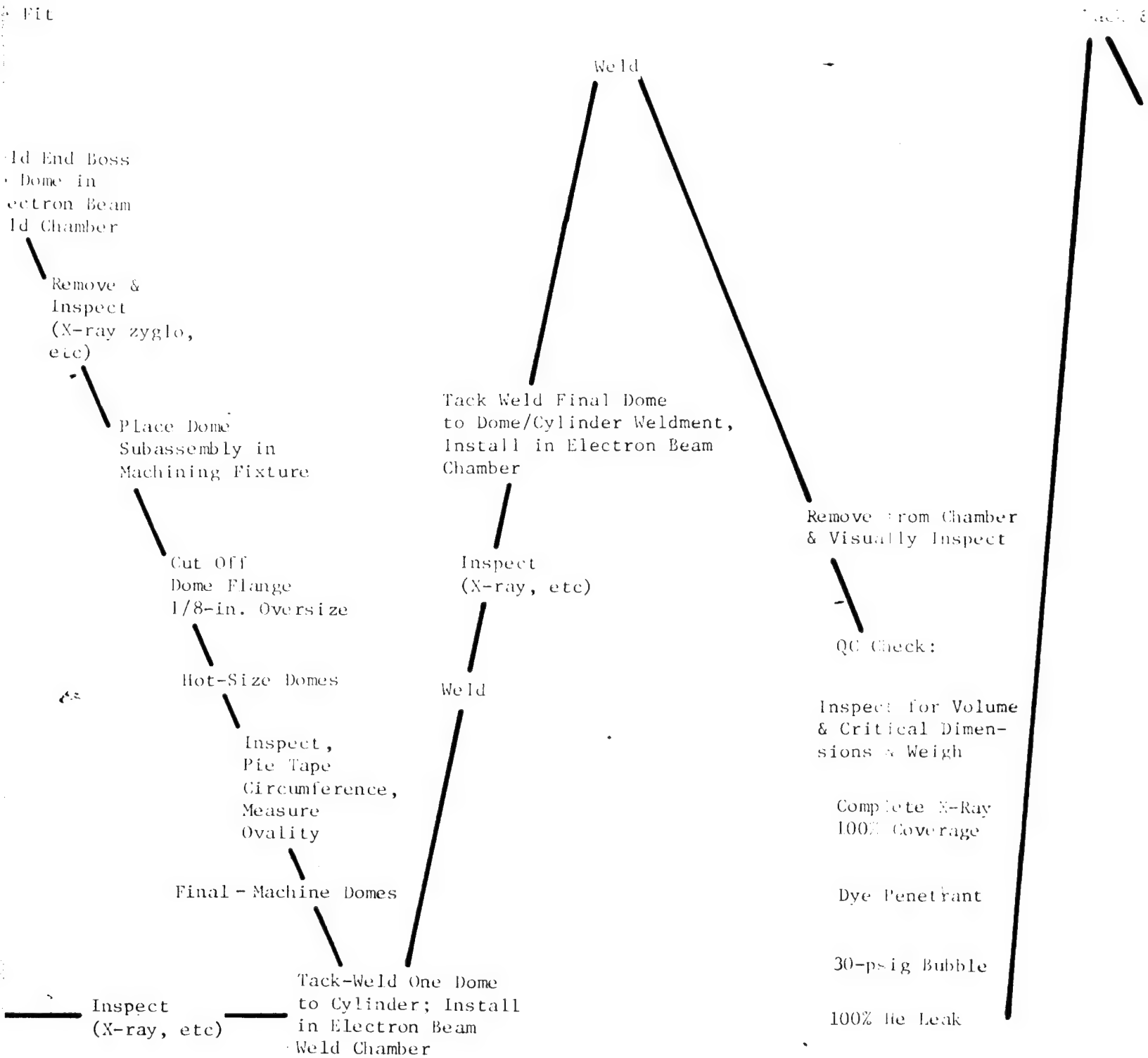

Figure 11 Titaniu

III-9 and 1

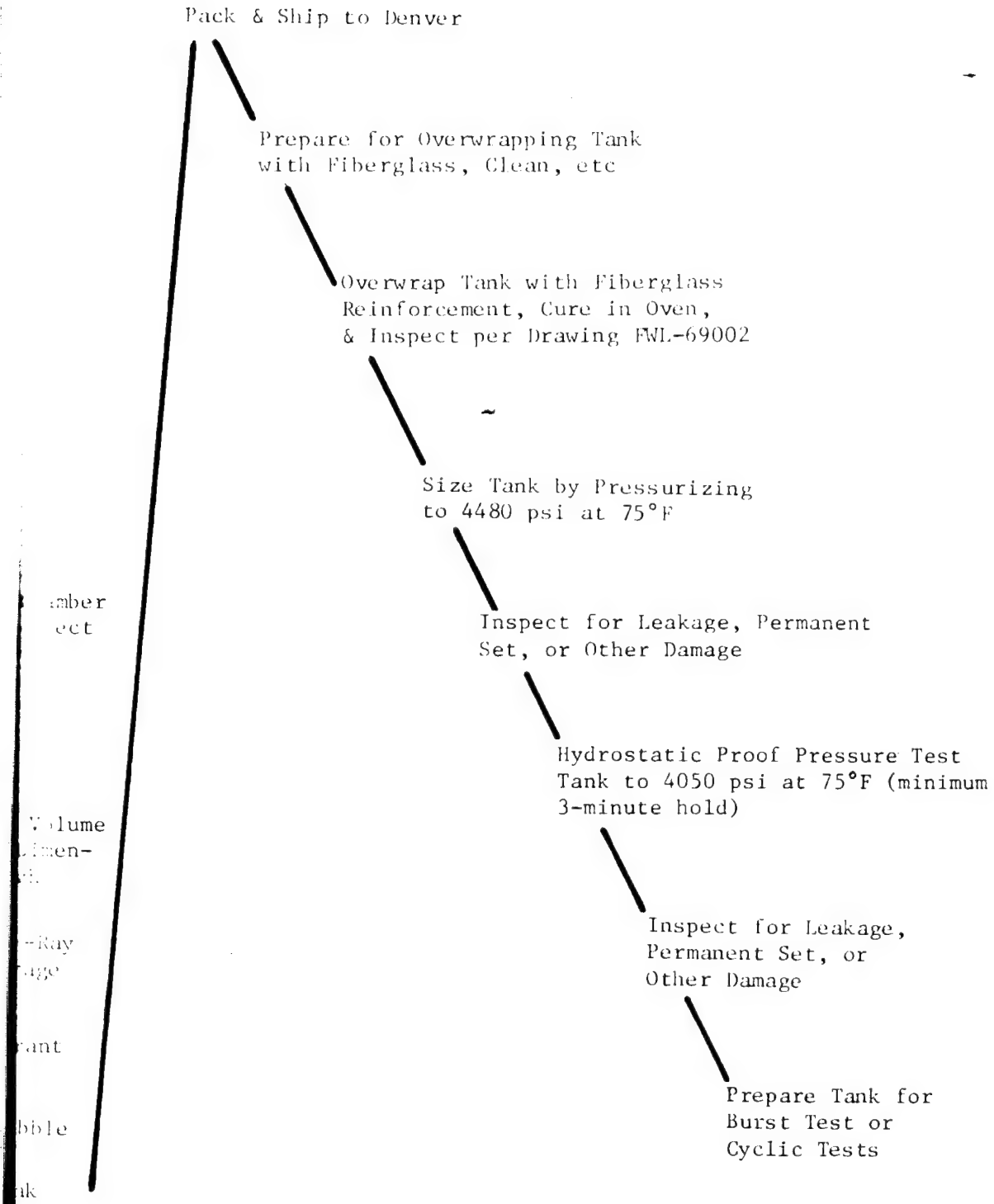

Figure 11 Titanium Tank Overwrap Process Flow Chart (5Aℓ-2.5Sn ELI Grade)

Rework of the explosive-forming die was completed on May 25 and the forming/annealing effort was again accelerated to the highest possible rate. By May 28, eight domes were receiving various steps of the explosive-forming/cleaning/annealing cycle. Again, premature failures occurred. In this instance, three domes cracked on the second shot, two failed during the third anneal cycle after the second shot, and, in an examination of the remaining domes in process, small cracks were noted after the second anneal. These failure conditions were all experienced during a 24-hour time span. Again the program was stopped and the failure causes investigated. The full details of this study may be found in the appendix. In essence, the failures were primarily due to (1) contamination that ultimately allowed a slowly increasing surface case to build up, and (2) stress corrosion resulting from the sensitizing of the material (during the slow cool in the furnace during the first anneal) to chlorinated hydrocarbon cleaner. In the ensuing effort to determine all of the potential causes for failures, the furnace became suspect because surface oxidation caused the failure of one dome while it was receiving its final anneal. After a check of the furnace for leaks using a helium leak detector did not detect any leaks of sufficient magnitude to cause the problem, a second furnace run was made with samples. Once again the contaminated surface condition appeared. Again the helium leak check revealed no leaks so the overall instrumentation system of the furnace was checked out. During this investigation it was noted that when the furnace system vacuum indicator was reading 0.1 micron, a Martin Marietta-calibrated gage, which had been placed in the furnace behind the baffle plates on the opposite side of the furnace from the diffusion pump, was reading 1.25 microns. Further search revealed that the system sensor was connected to a rather small tube just upstream from the diffusion pump. Since there was a question as to the length of time required to relocate the sensor, overhaul the diffusion pump, and recertify the furnace, the vacuum annealing operation was abandoned. It was determined that all annealing operations would be performed in one of two Martin Marietta-owned air furnaces. A protective coating, Turco Pretreat, was evaluated in each furnace so that if one furnace was not available, the other could be used (refer to test evaluation in the appendix).

At this point, metallurgical analysis had identified a number of potential causes of the failures but most all causes centered around the material surface condition. As a result, a complex processing system was developed.

In general, before and after each dome-forming operation, the dome had to be annealed. The dome was prepared for annealing by chem milling 0.005 inch maximum per surface and coating with Turco Pretreat (Fig. 12) to prevent oxidation. After annealing, the Turco Pretreat was removed by again chem milling the dome. This processing sequence proved successful and no further dome cracking was experienced.

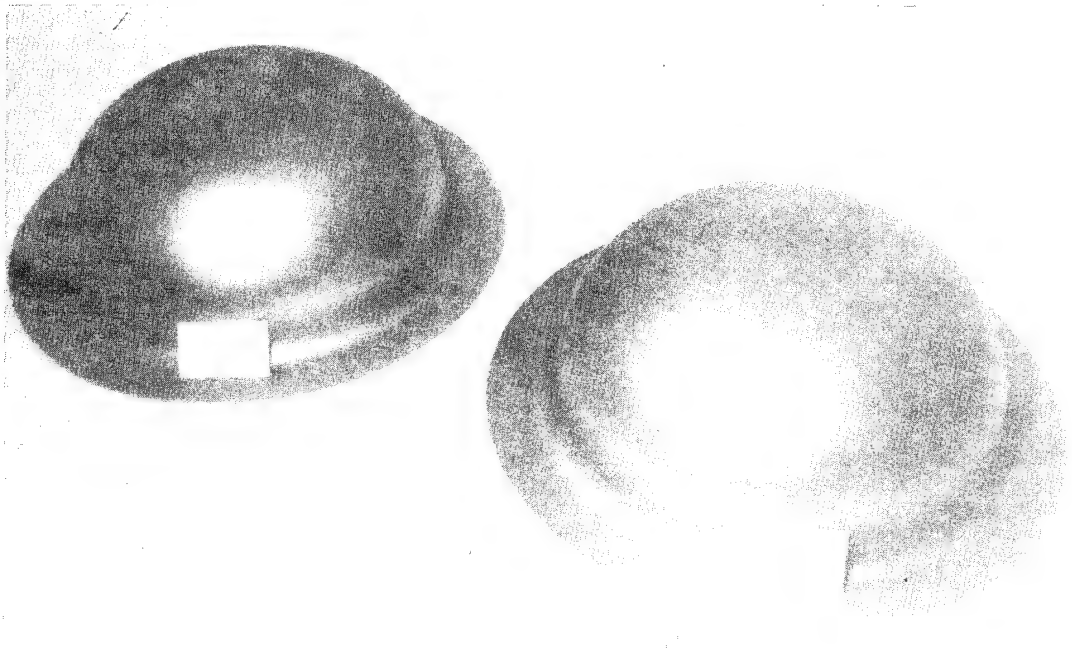

Figure 12 Fully Formed Domes Coated with Turco Pretreat Prior to Annealing in Air Furnace

Explosive forming of domes was then continued, but the in-process time per dome was extended because of the numerous added operations between shots. In addition, several associated facility problems that occurred further stretched the production schedule for domes. Another remaining problem was the lack of forming repeatibility. This resulted in variations from desired contour and close tolerance diameters (Table 4). It was also predictable that the high loss rate would have an effect, not only on the number of tanks that could be made, but also by reducing the option to selectively fit the domes to reduce potential mismatch and other assembly problems.

Figures 13, 14, 15, and 16 illustrate the explosive-forming process in progress.

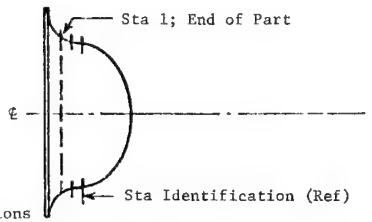

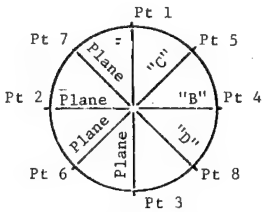

Part Identification U-1

Table 4 Explosive-Forming Data - Typical Contour and Thickness Variations

Station Identification	Plane A Thickness, in.	(cm)	in.	(cm)	Plane B Thickness, in.	(cm)	in.	(cm)	Plane C Thickness, in.	(cm)	in.	(cm)	Plane D Thickness, in.	(cm)	in.	(cm)	Plane A Contour, in.	(cm)	in.	(cm)	Plane B Contour, in.	(cm)	in.	(cm)
	Pt 1		Pt 3		Pt 2		Pt 4		Pt 5		Pt 6		Pt 7		Pt 8		Pt 1		Pt 3		Pt 2		Pt 4	
Dome ℄	--	--	--	--	--	--	--	--	--	--	--	--	--	--	--	--	--	--	--	--				
73	0.196	0.497	0.196	0.497	0.192	0.487	0.197	0.500	0.198	0.502	0.193	0.487	0.194	0.492	0.194	0.492	-0.030	-0.076	-0.080	-0.203	-0.110	-0.279	-0.080	-0.203
66	0.198	0.502	0.198	0.502	0.194	0.492	0.198	0.502	0.201	0.510	0.196	0.497	0.195	0.495	0.198	0.502	-0.090	-0.228	-0.130	-0.330	-0.110	-0.279	-0.090	-0.228
60	0.203	0.515	0.202	0.513	0.202	0.513	0.202	0.513	0.208	0.528	0.205	0.520	0.204	0.518	0.203	0.515	-0.080	-0.203	-0.180	-0.457	-0.100	-0.254	-0.070	-0.177
55	0.210	0.533	0.211	0.535	0.206	0.523	0.208	0.528	0.213	0.541	0.210	0.533	0.211	0.535	0.210	0.533	-0.120	-0.304	-0.270	-0.685	-0.140	-0.355	-0.100	-0.254
48	0.218	0.553	0.222	0.563	0.220	0.558	0.218	0.553	0.228	0.579	0.222	0.563	0.218	0.553	0.217	0.551	-0.120	-0.304	-0.270	-0.685	-0.120	-0.304	-0.090	-0.228
40	0.220	0.558	0.223	0.566	0.223	0.566	0.223	0.563	0.224	0.568	0.225	0.571	0.222	0.563	0.221	0.561	-0.060	-0.152	-0.190	-0.482	-0.040	-0.101	-0.030	-0.076
35	0.220	0.558	0.224	0.568	0.224	0.568	0.220	0.558	0.223	0.566	0.226	0.574	0.222	0.563	0.220	0.558	-0.030	-0.076	-0.120	-0.304	-0.020	-0.050	-0.010	-0.025
30	0.220	0.558	0.224	0.568	0.223	0.566	0.222	0.563	0.223	0.566	0.227	0.576	0.221	0.561	0.221	0.561	-0.020	-0.050	-0.050	-0.127	-0.020	-0.050	0.000	0
25	0.221	0.561	0.222	0.563	0.225	0.571	0.224	0.568	0.225	0.571	0.226	0.574	0.223	0.566	0.223	0.566	+0.010	+0.025	0.000	0	0.000	0	+0.010	+0.025
20	0.218	0.553	0.223	0.566	0.221	0.561	0.222	0.563	0.225	0.571	0.226	0.571	0.223	0.543	0.223	0.568	+0.010	+0.025	+0.040	+0.101	+0.101	+0.025	+0.020	+0.050
15	0.212	0.538	0.212	0.538	0.210	0.533	0.206	0.523	0.216	0.548	0.208	0.528	0.212	0.538	0.210	0.533	0.000	0	+0.040	+0.101	-0.010	-0.025	-0.000	0
10	0.208	0.528	0.208	0.528	0.215	0.546	0.214	0.543	0.214	0.543	0.205	0.520	0.210	0.533	0.208	0.528	-0.030	-0.076	+0.030	+0.076	-0.040	-0.076	-0.020	-0.050
6	0.220	0.558	0.220	0.558	0.224	0.568	0.216	0.548	0.224	0.568	0.218	0.553	0.224	0.568	0.214	0.543	-0.030	-0.076	+0.010	+0.025	-0.050	-0.127	-0.030	-0.076
1	0.230	0.584	0.230	0.584	0.234	0.594	0.233	0.591	0.230	0.584	0.230	0.584	0.233	0.591	0.227	0.576	-0.010	-0.025	+0.030	-0.076	-0.040	-0.101	-0.020	-0.050

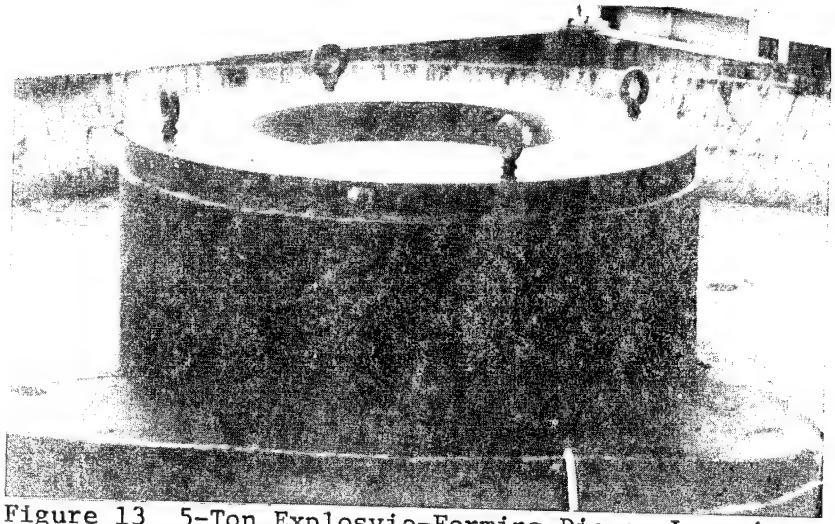

Figure 13 5-Ton Explosvie-Forming Die on Lowering Carriage

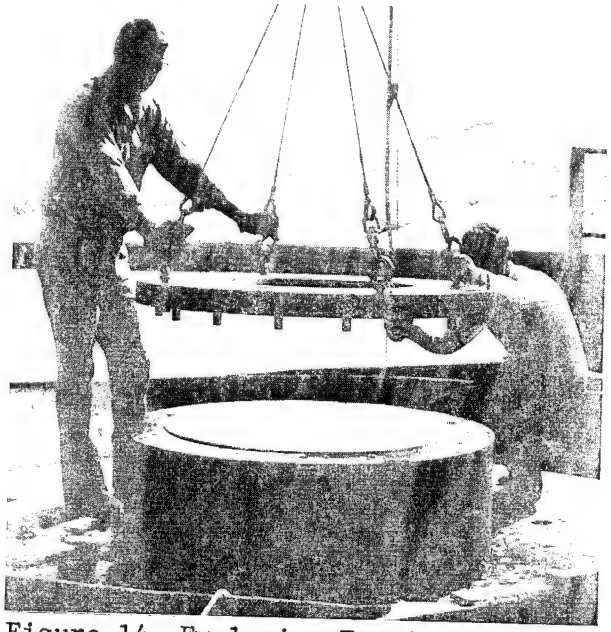

Figure 14 Explosive-Forming Technicians Preparing to Lower and Bolt Down Holding Ring of Forming Die

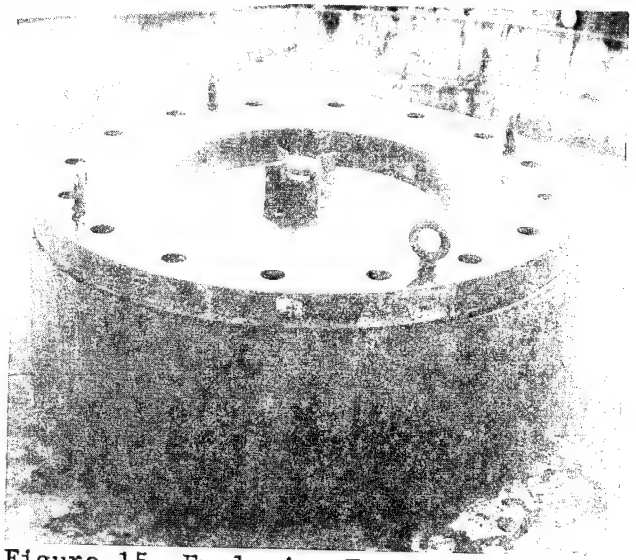

Figure 15 Explosive-Forming Die with Dome Blank and Explosive Charge in Place Prior to Lowering Die Carriage into Explosive-Forming Pool

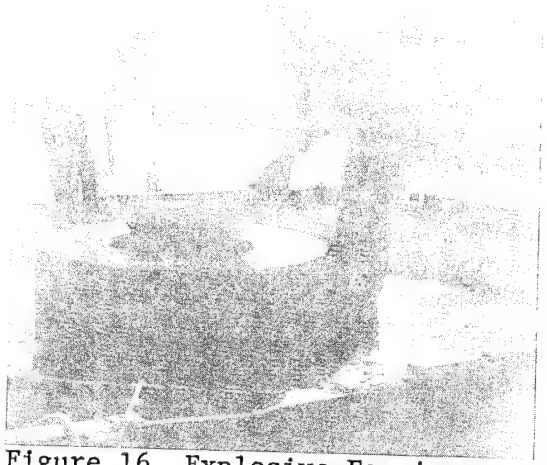

Figure 16 Explosive-Forming Technicians Removing Formed Dome from Forming Die

Figure 17 shows the explosive-forming sequence and contour deviations.

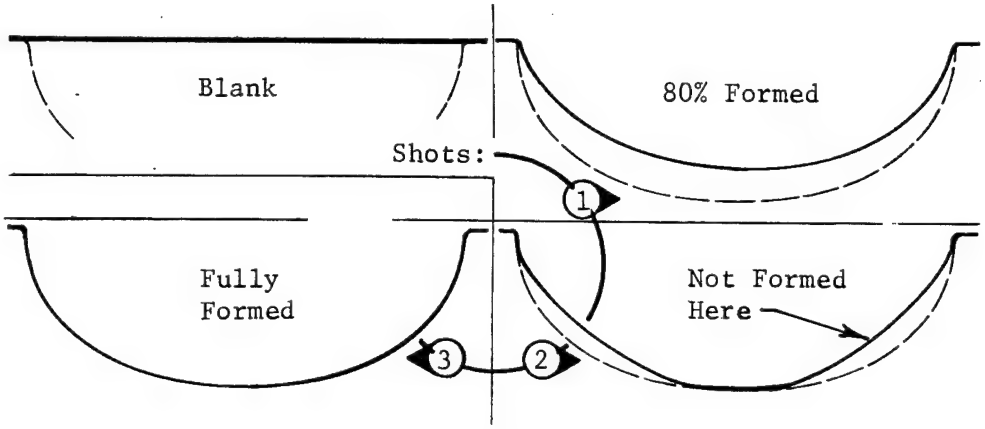

Raw Material Thickness Deviation: $0.220\ ^{+0.046}_{-0.010}$ in.

Best Deviation from Contour (H-2): -0.030, +0.050 in.

Worst Deviation from Contour (P-3): -0.325, + 0.090 in.

Figure 17 Explosive-Forming Sequence

C. CHEMICAL MILLING

The chemical milling process was used in this program for two purposes. Chemical milling, which has been discussed in the previous section on annealing, was used more in the manner of a scale remover and surface conditioner for contamination control. No more than 0.005 inch was removed during any one exposure. The primary ingredient of the etchant solution for this application is a nitric-hydrofluoric acid. The second use for the chemical milling process was for etching the thickness to the final dome configuration. The primary ingredient for this solution is a chromic-hydrofluoric acid. The latter of the two processes was used in place of the originally planned machining because of the thickness and contour tolerances of the explosively formed domes.

The chemical milling procedures and processes for thickness control were never completely optimized during this program, primarily because of the several stops and starts associated with explosive forming and annealing problems.

Early efforts to optimize chem-milling methods began with a fixture designed and fabricated to hold the dome in a horizontal position. Nonuniform etching was experienced whether the flange was up or down. Discussions pointed out that gas entrapment areas along the contour and at the apex were causing preferential etching. The recommended fix was to create a hole at the dome apex to allow gases to flow along the contour and escape through the hole. This apparently solved the problem, but after a manufacturing personnel change and another schedule delay, an alternative method was tried. The fixture was modified to hold the dome in a vertical position and it became necessary to rotate the dome at closely timed intervals to once again prevent preferential etching. This approach met with fairly good success as long as the chem-mill operator closely controlled the rotation intervals. Although some success was experienced, the process was later revised to holding the dome in the horizontal position. This method was more reliable and produced the best results. Figure 2 shows the dome chem-mill pattern desired and Table 5 reflects a typical actual thickness and contour chart for a single dome. Dome E2 reflected the best chem-mill results with 0.109/0.122 inch in the thin area and 0.154/0.164 inch in the thick area. The worst dome was N1, which had 0.109/0.144 inch in the thin area with 0.127/0.188 inch in the thick area. Figure 18 depicts sequential dome positions developed for best chem-milling results. Figures 19, 20, 21, and 22 illustrate the chemical milling process.

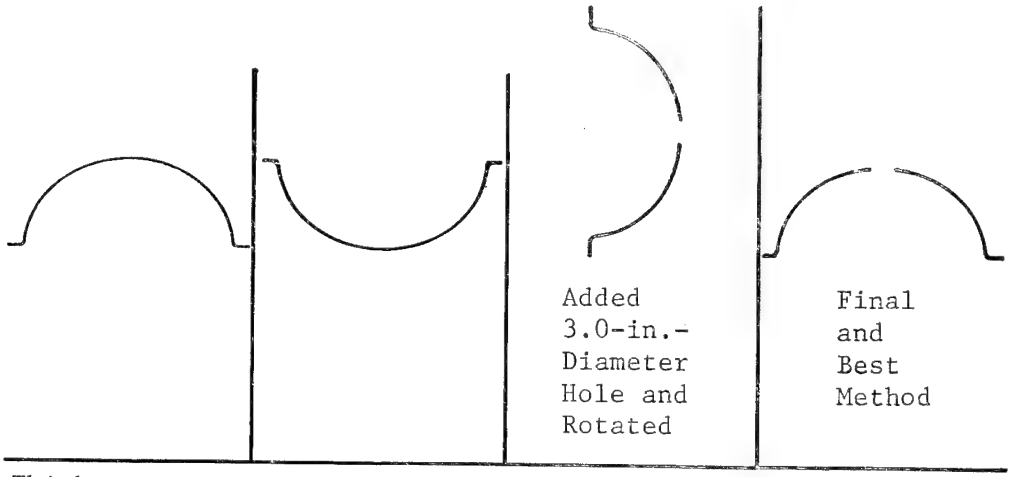

Thickness Deviation after Chem-Mill:

Best (E-2) = $\frac{0.109}{0.122}$ & $\frac{0.154}{0.164}$ Worst (N-1) = $\frac{0.109}{0.144}$ & $\frac{0.127}{0.188}$

Figure 18 Development of Dome Position in Chem-Mill Tank

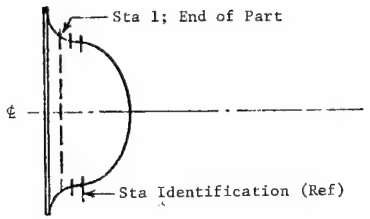

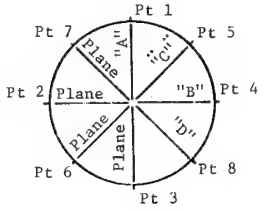

Part Identification

S-1

Table 5 Typical Chem-Milled Dome Thickness and Contour Deviations

Station Identification	Plane A Thickness, in.	(cm)	in.	(cm)	Plane B Thickness, in.	(cm)	in.	(cm)	Plane C Thickness, in.	(cm)	in.	(cm)	Plane D Thickness, in.	(cm)	in.	(cm)
	Pt 1		Pt 3		Pt 2		Pt 4		Pt 5		Pt 6		Pt 7		Pt 8	
Dome ℄	--	--	--	--	--	--	--	--	--	--	--	--	--	--	--	--
73	0.159	0.403	0.161	0.406	0.160	0.406	0.161	0.406	0.156	0.393	0.159	0.403	0.164	0.414	0.160	0.406
66	0.166	0.421	0.162	0.411	0.166	0.421	0.162	0.411	0.158	0.401	0.162	0.411	0.165	0.419	0.162	0.411
60	0.125	0.317	0.166	0.419	0.141	0.358	0.154	0.391	0.128	0.325	0.138	0.350	0.136	0.345	0.131	0.332
55	0.116	0.294	0.128	0.325	0.141	0.358	0.128	0.325	0.123	0.312	0.134	0.340	0.135	0.342	0.122	0.309
48	0.116	0.294	0.129	0.327	0.142	0.360	0.123	0.312	0.118	0.299	0.134	0.340	0.132	0.335	0.122	0.309
40	0.126	0.320	0.132	0.335	0.145	0.368	0.174	0.441	0.112	0.284	0.134	0.340	0.135	0.342	0.125	0.317
35	0.128	0.325	0.133	0.337	0.145	0.368	0.114	0.289	0.112	0.284	0.130	0.330	0.138	0.350	0.124	0.314
30	0.132	0.335	0.136	0.345	0.144	0.365	0.140	0.355	0.110	0.279	0.126	0.320	0.138	0.350	0.125	0.317
25	0.136	0.358	0.141	0.358	0.148	0.375	0.140	0.355	0.114	0.289	0.132	0.335	0.142	0.360	0.129	0.327
20	0.136	0.345	0.132	0.335	0.144	0.365	0.138	0.350	0.112	0.284	0.130	0.330	0.142	0.360	0.120	0.304
15	0.132	0.335	0.134	0.340	0.144	0.365	0.136	0.345	0.109	0.274	0.130	0.330	0.140	0.355	0.124	0.314
10	0.144	0.365	0.144	0.365	0.146	0.370	0.138	0.350	0.112	0.284	0.134	0.340	0.146	0.370	0.138	0.350
6	0.184	0.464	0.174	0.441	0.190	0.482	0.176	0.447	0.170	0.431	0.176	0.447	0.146	0.370	0.180	0.457
1	0.190	0.482	0.156	0.393	0.168	0.426	0.190	0.482	0.180	0.457	0.184	0.467	0.156	0.393	0.156	0.393

Plane A Contour in.	(cm)	in.	(cm)	Plane B Contour in.	(cm)	in.	(cm)
Pt 1		Pt 3		Pt 2		Pt 4	
-0.095	-0.241	-0.055	-0.139	-0.015	-0.038	+0.020	+0.050
-0.110	-0.279	-0.095	-0.241	-0.080	-0.203	-0.065	-0.165
-0.070	-0.177	-0.085	-0.215	-0.065	-0.165	-0.050	-0.127
-0.080	-0.203	-0.090	-0.228	-0.080	-0.203	-0.060	-0.152
-0.080	-0.203	-0.070	-0.177	-0.115	-0.292	-0.090	-0.228
-0.020	-0.050	-0.020	-0.050	-0.060	-0.152	-0.040	-0.101
-0.010	-0.025	-0.010	-0.025	-0.035	-0.088	-0.020	-0.050
0.000	0.000	0.000	0.000	-0.015	-0.038	-0.010	-0.025
+0.020	+0.050	+0.015	+0.038	0.000	0.000	+0.005	+0.012
+0.025	+0.063	+0.020	+0.050	+0.015	+0.038	+0.015	+0.038
+0.010	+0.025	+0.005	+0.012	+0.010	+0.025	+0.005	+0.012
-0.010	-0.025	-0.015	-0.038	-0.010	-0.025	-0.015	-0.038
-0.020	-0.050	-0.020	-0.050	-0.020	-0.050	-0.030	-0.076
+0.003	+0.007	0.000	0.000	-0.010	-0.025	-0.015	-0.038

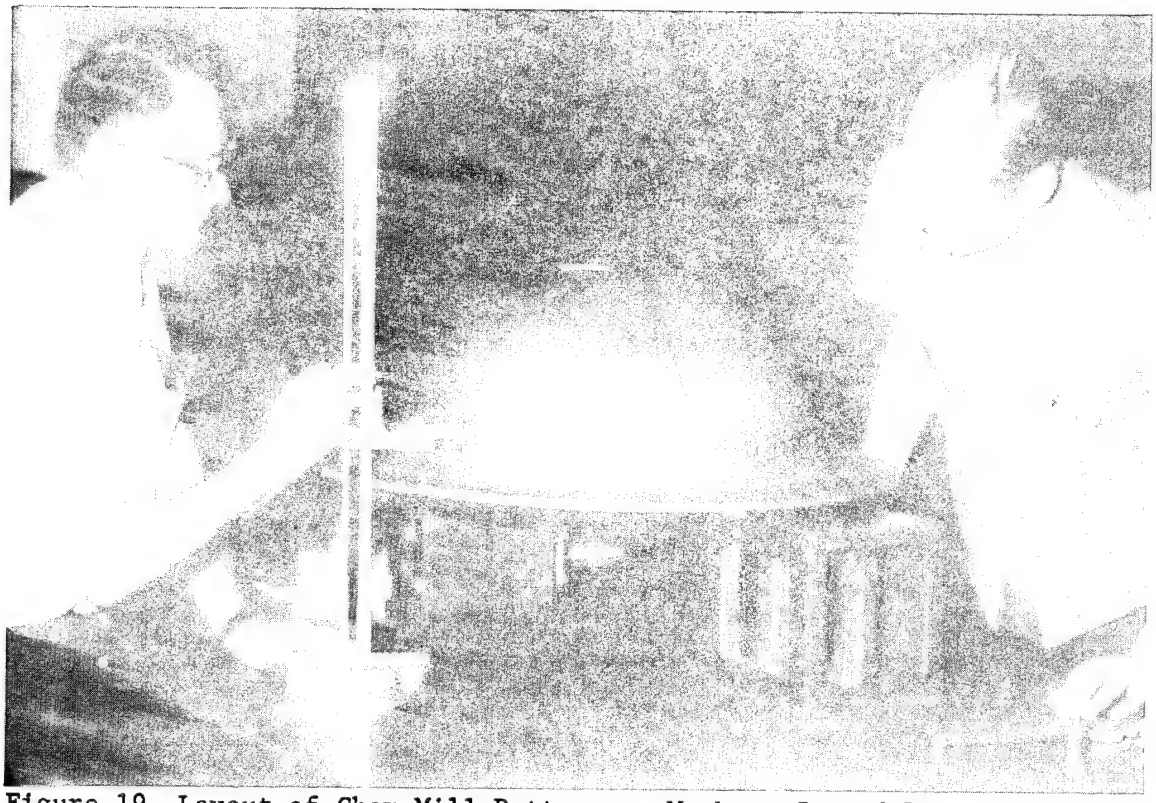

Figure 19 Layout of Chem-Mill Pattern on Maskant-Coated Dome

Figure 20 Chem-Mill Technician Checking Dome Thicknesses with Vidigage Monitor

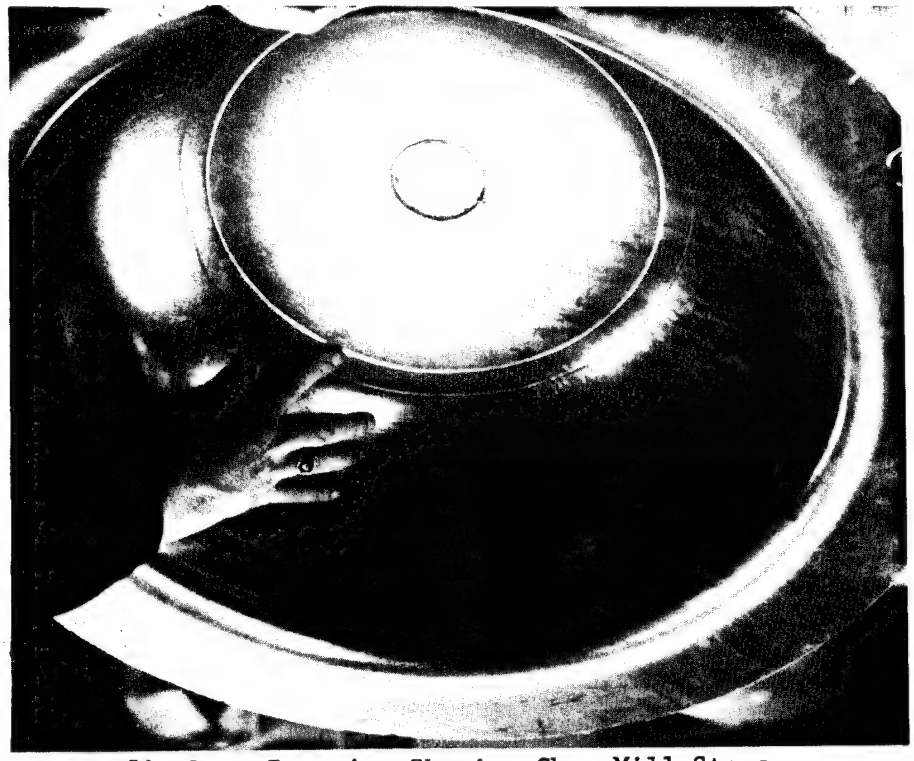

Figure 21 Dome Interior Showing Chem-Mill Steps

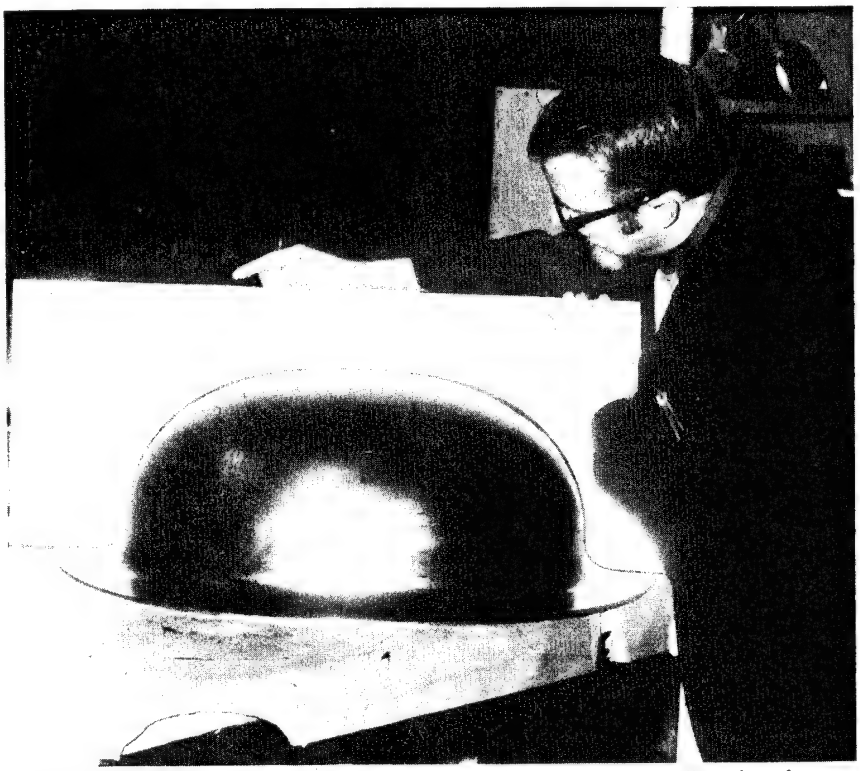

Figure 22 Project Engineer Noting Contour Deviation of Dome with External Contour Template

D. MACHINING AND HOT SIZING

After finding that the variations in diameter of the domes were greater than normally expected for 24-inch-diameter domes, it was determined that the Baltimore Division should perform both machining and electron beam welding. This approach possessed the best opportunity for success since Baltimore personnel could select the best fitup condition that might exist between domes. It also allowed for any small modifications that might facilitate the welding operations.

The machining holding fixtures (Fig. 23, 24, 25, and 26) were devised to allow machining the proper surface interface of the dome-to-barrel section and of the apex hole to the end boss fittings. No machining problems with the end boss fittings were encountered because the boss design utilized tolerances and surface finishes that are normal for that type of hardware. The explosively formed domes, even though annealed following the last forming operation, did experience some movement when the flanges were parted from the domes and when the full-sized hole for the end boss fitting was machined. After several attempts to force the mating surfaces into proper position for machining and subsequent welding, it became obvious that the dome diameters would have to be more nearly uniform than the explosive-forming process had produced. Therefore, a hot creep sizing fixture was designed and fabricated. The dome to be sized was assembled to the fixture, prepared for oxidation prevention by applying Everlube T-50, and placed in an air furnace. The differential coefficient of thermal expansion between titanium and corrosion-resistant steel provided the necessary pressure to perform the sizing operation (Fig. 27, 28, and 29). The hot-sizing operation improved the uniformity of the diameters as may be seen in Table 6.

Another problem that occurred as a result of machining was that after the hole in the dome was machined for the end boss fitting, the dome sprung out of contour when the holding fixture was removed. The machined step-type joint proved to be of some assistance in assembling the fitting to the dome, but the weld fixturing had to be modified to force the dome back into contour to match the fitting.

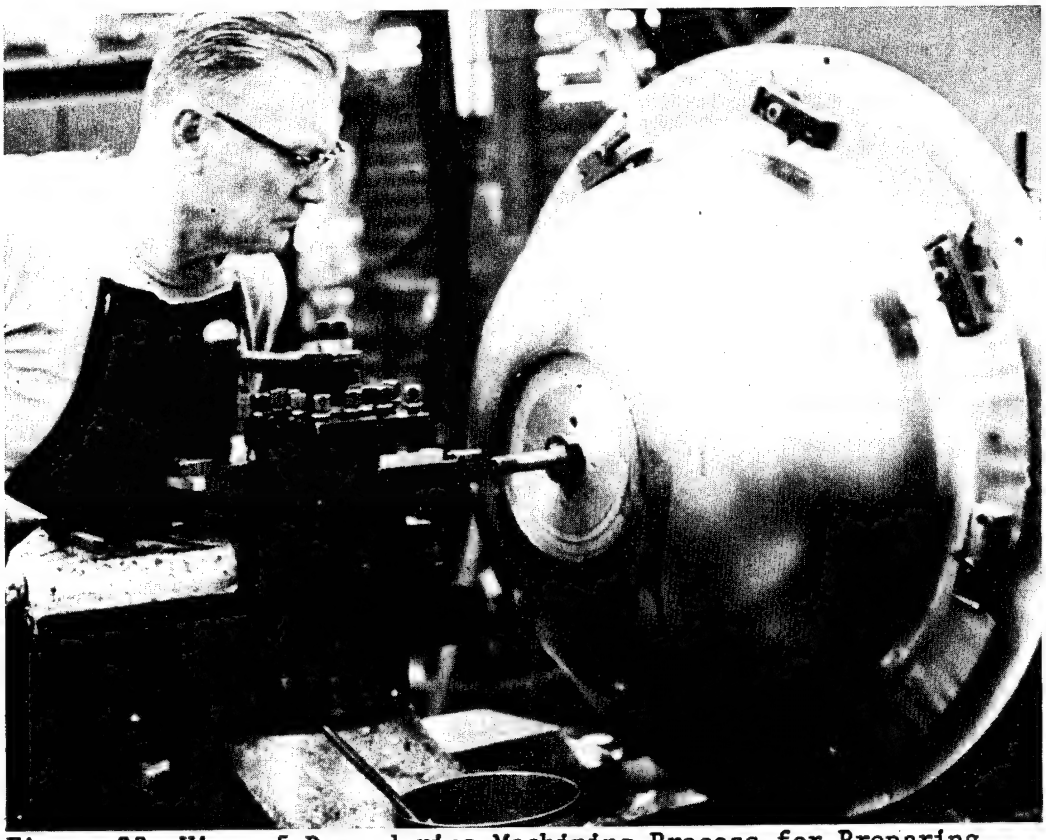

Figure 23 View of Dome during Machining Process for Preparing Dome Cutout at Dome-to-End Fitting Interface

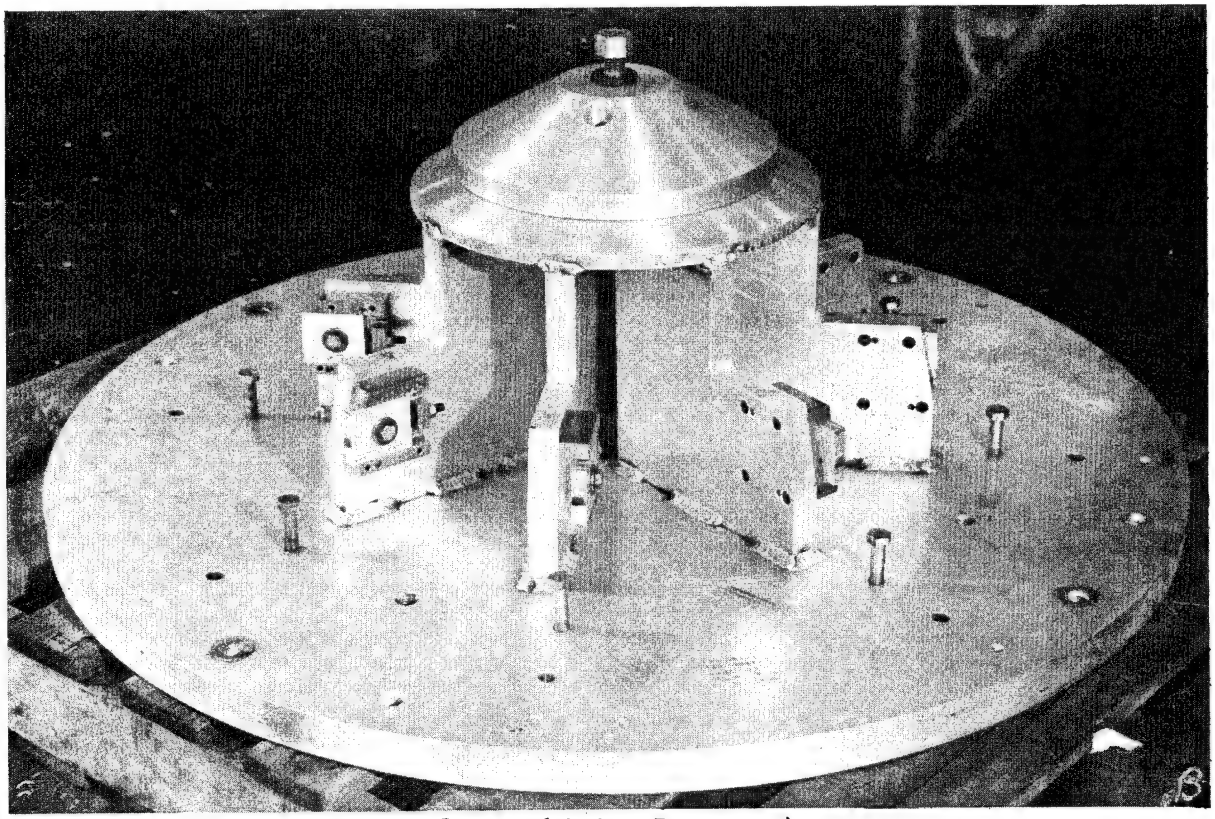

Figure 24 Holding Fixture for Machining Dome at Apex

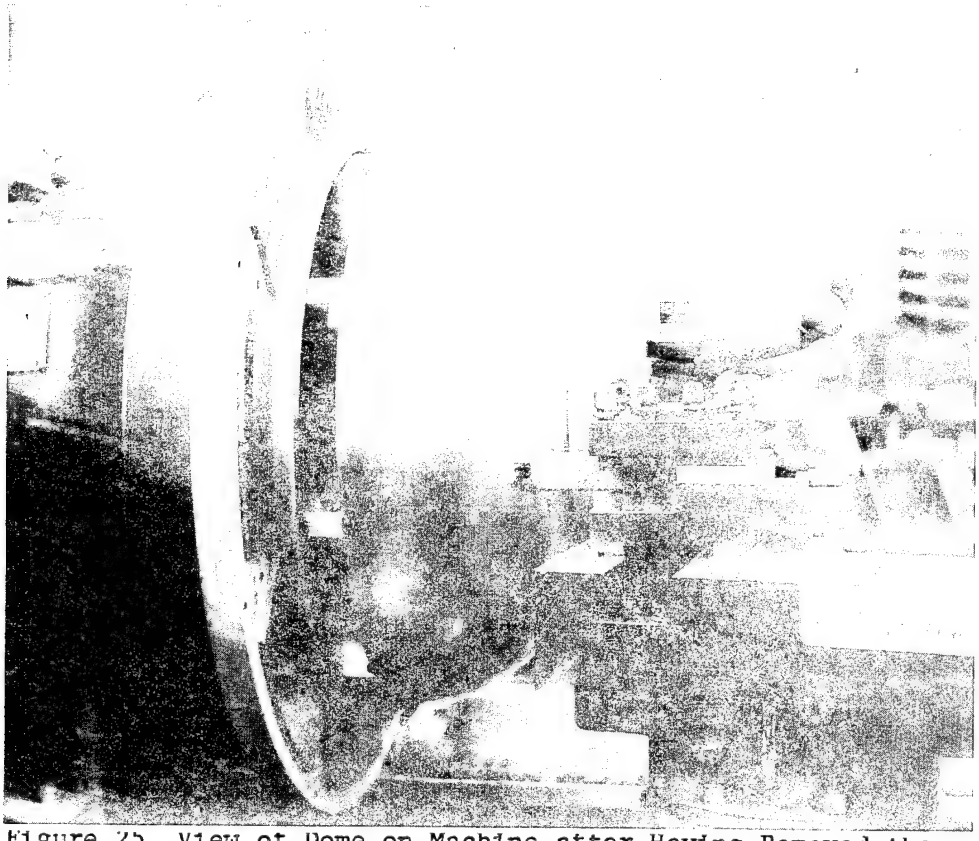

Figure 25 View of Dome on Machine after Having Removed the Flange

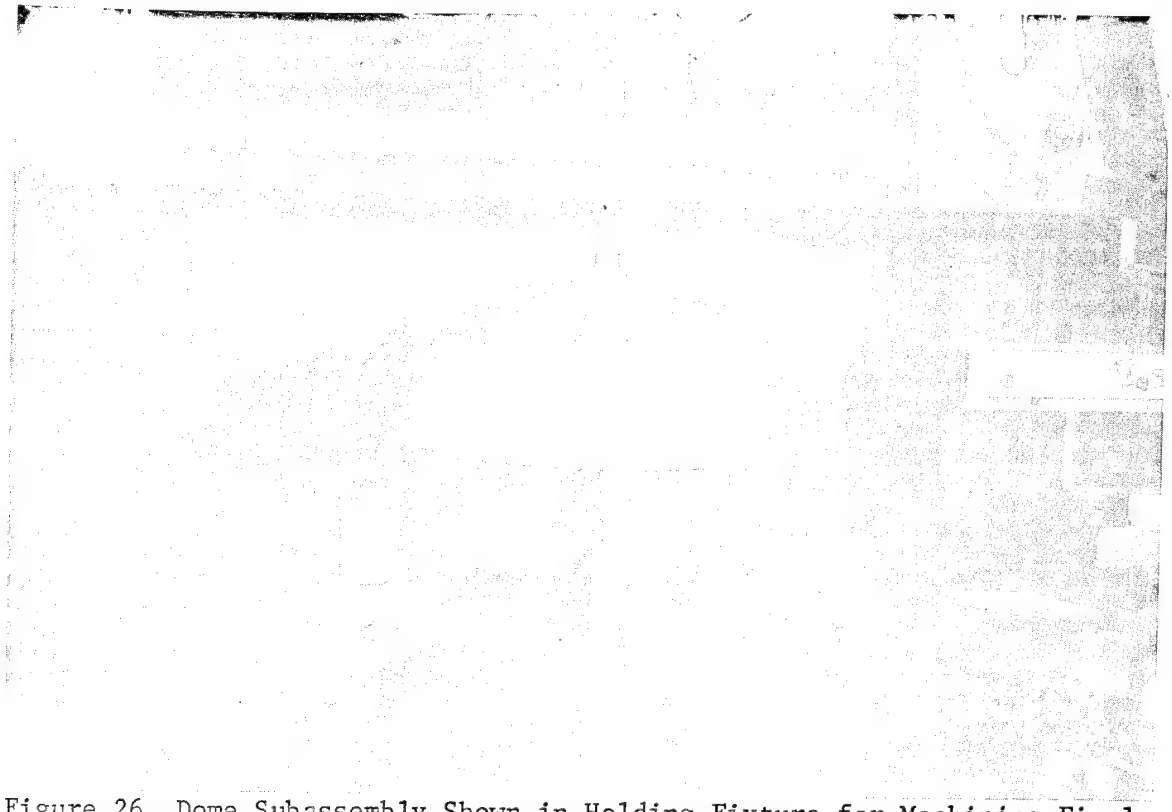

Figure 26 Dome Subassembly Shown in Holding Fixture for Machining Final Outside Diameter to Eliminate "Bell Mouthing"

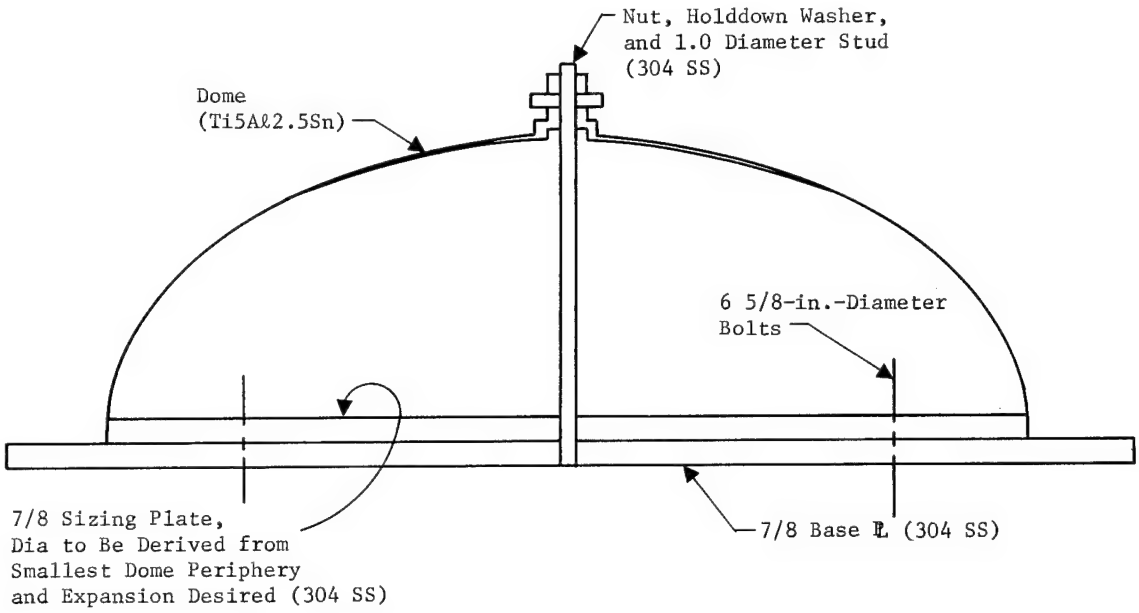

Figure 27 Hot-Sizing Tool Schematic

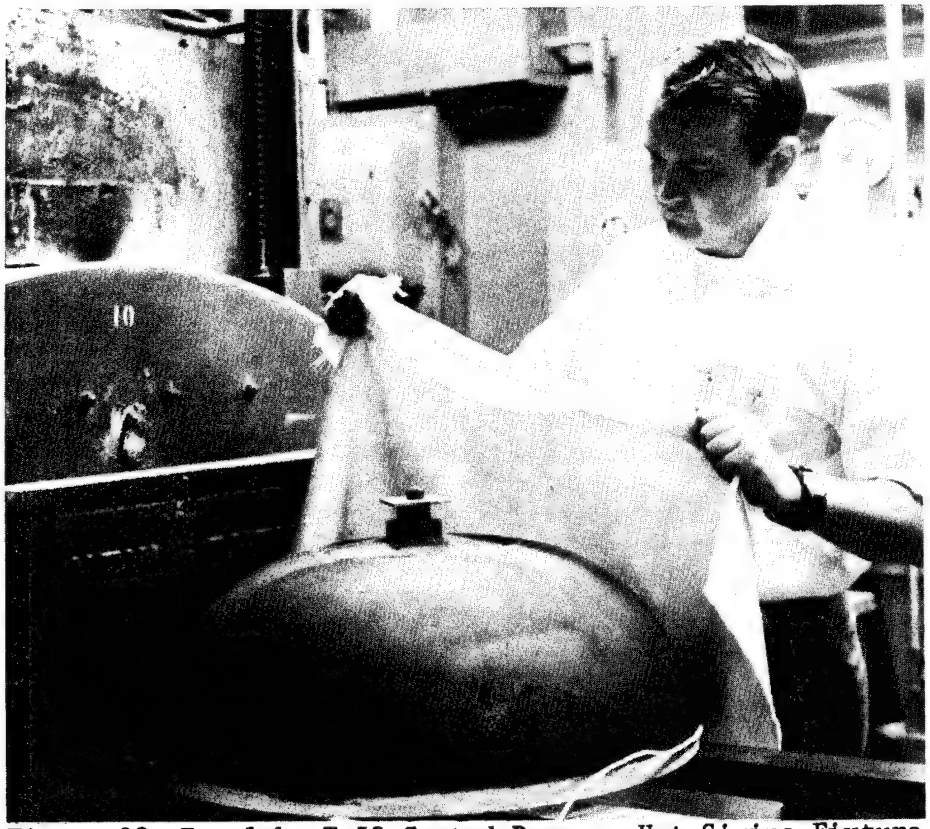

Figure 28 Everlube T-50 Coated Dome on Hot-Sizing Fixture Prior to Air Furnace Sizing Process

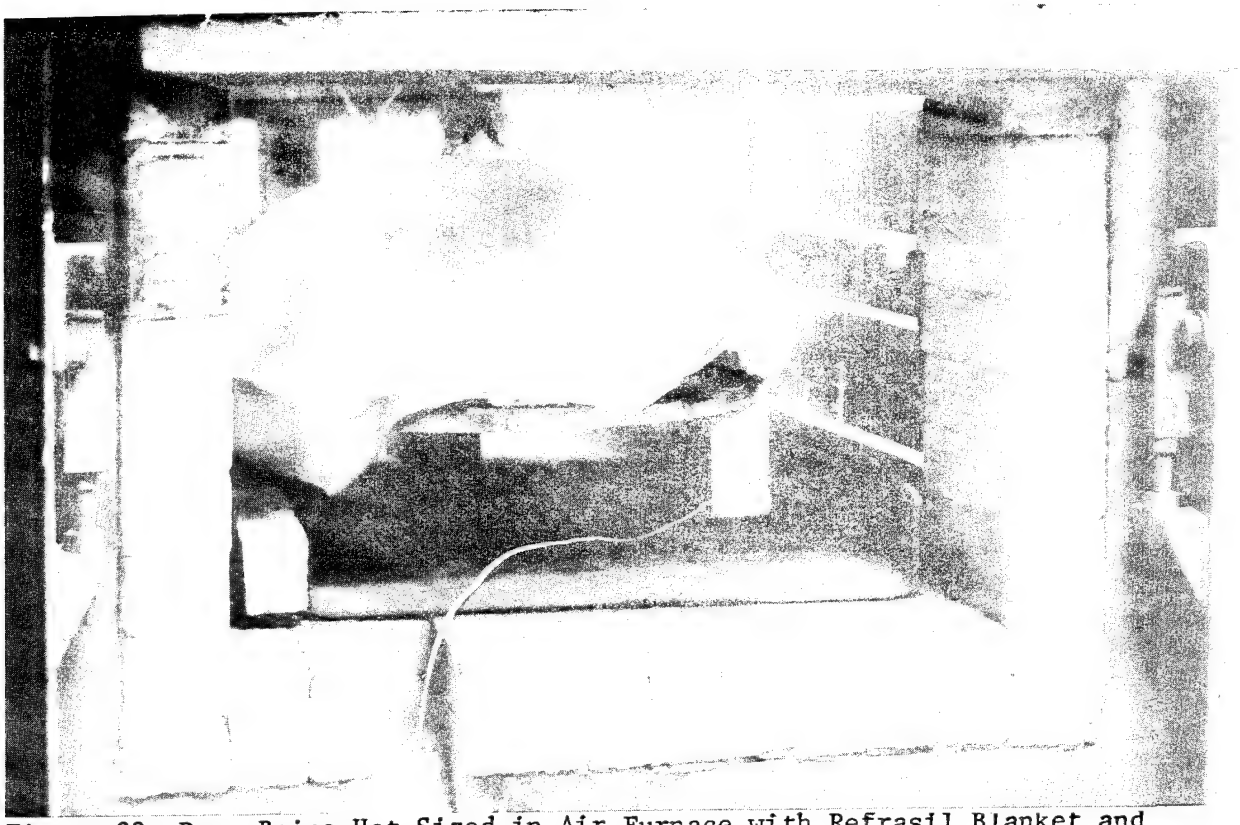

Figure 29 Dome Being Hot-Sized in Air Furnace with Refrasil Blanket and Everlube T-50 Coating to Prevent Oxidation

Table 6 Typical Dome Sizing Dimensions

Dome No.	Before Sizing		After Sizing	
	Diameter, in. (cm)	Out-of-Roundness, in. (cm)	Diameter, in. (cm)	Out-of-Roundness, in. (cm)
A1	23.632 (60.025)	0.180 (0.457)	23.700 (60.198)	0.129 (0.327)
A2	23.603 (59.951)	0.003 (0.007)	23.716 (60.238)	0.012 (0.030)
B1	23.596 (59.933)	0.157 (0.398)	23.699 (60.195)	0.063 (0.160)
B2	23.611 (59.971)	0.043 (0.109)	23.728 (60.269)	0.015 (0.038)

The cylindrical barrel section was rolled into a curved section for annealing because it was longer than the furnace depth. When it was straightened for machining, the edges tended to curl. This made precision machining of the steps to mate with the dome skirt almost impossible. After tank S/N 1 failed prematurely at a girth weld, the step design was changed to a simple butt configuration. Since the step design was used as the means for holding the joint together for welding, it became necessary to TIG-tack the butt joint to hold the dome to the barrel.

As can be seen in Table 6, some ovality and diametric dimensions still do not represent as good a matchup as necessary. It therefore becomes necessary to match two domes that are dimensionally similar. For example, A1 was matched to B1 and A2 to B2. When it became necessary to put two domes together that did not match well, the smaller of the two was resized with some, but not total, success. This situation was avoided where possible.

E. WELDING, INSPECTION, AND ACCEPTANCE TESTING

Electron beam welding was selected as the joining process for this program for two reasons. The major reason was because an electron beam-welded joint has greater as-welded strength properties than a joint that has been affected by the heat of TIG welding. The second reason for selecting the electron beam weld technique was that the final weld pass over the joint is essentially a cosmetic pass that tends to smooth out the contour of the weld bead. This condition was desirable for laying up the fiberglass overwrap over the tank surface. TIG weld beads would necessitate grinding and filling to prevent bridging of the overwrap filaments. The Martin Marietta Baltimore Division was assigned the responsibility for welding in this program because the division has an electron beam facility available and a successful long-term history of electron beam welding of various titanium alloys including 5Aℓ-2.5 Sn.

The electron beam welding was performed in a vacuum chamber. All controls were located and controlled from the outside (see Fig. 30 and 31). The machine used, a Model VK Sciaky electron beam welder, was operated by a qualified technician with over 10 years' experience. Typical weld control parameters included milliamperes, voltage, travel speed, focal setting, and distance of weld head from joint.

Weld tooling for this program was minimal but effective. A detailed description can be found in Martin Marietta manufacturing process 55M61. As shown in MMP55M61, the welded details for the dome-to-fitting joint were rotated under the electron beam gun. The same rotating concept was employed for rotation of the dome-to-barrel weldments. The longitudinal barrel weld was performed just the opposite, with the beam gun traveling across the stationary barrel. It became obvious on examination that precision alignment and extremely close tolerance fitup are very important in performing successful electron beam weldments. The lack of this condition and the associated problems are discussed in the following paragraphs, which are presented in the same sequence as followed in the procedure.

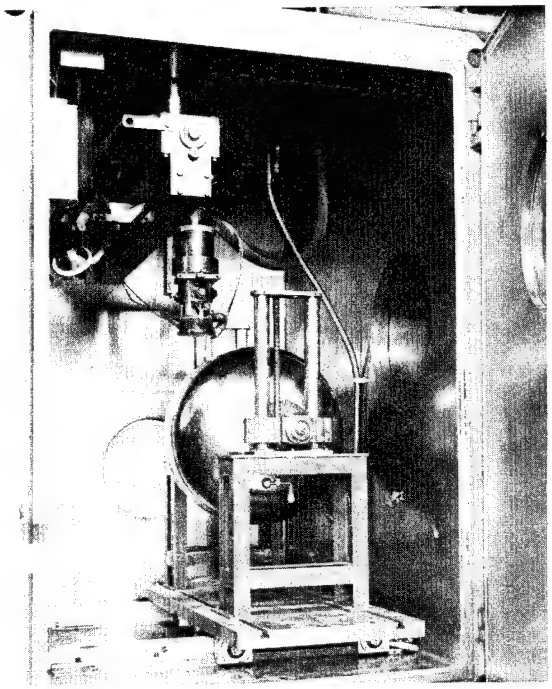

Figure 30 Interior of Electron Beam Vacuum Chamber Showing Titanium Tank Mounted on Rotating Fixture Prior to Welding Dome-to-Barrel Joint (Stationary Weld Head Has Been Adjusted for Proper Elevation and Joint Alignment)

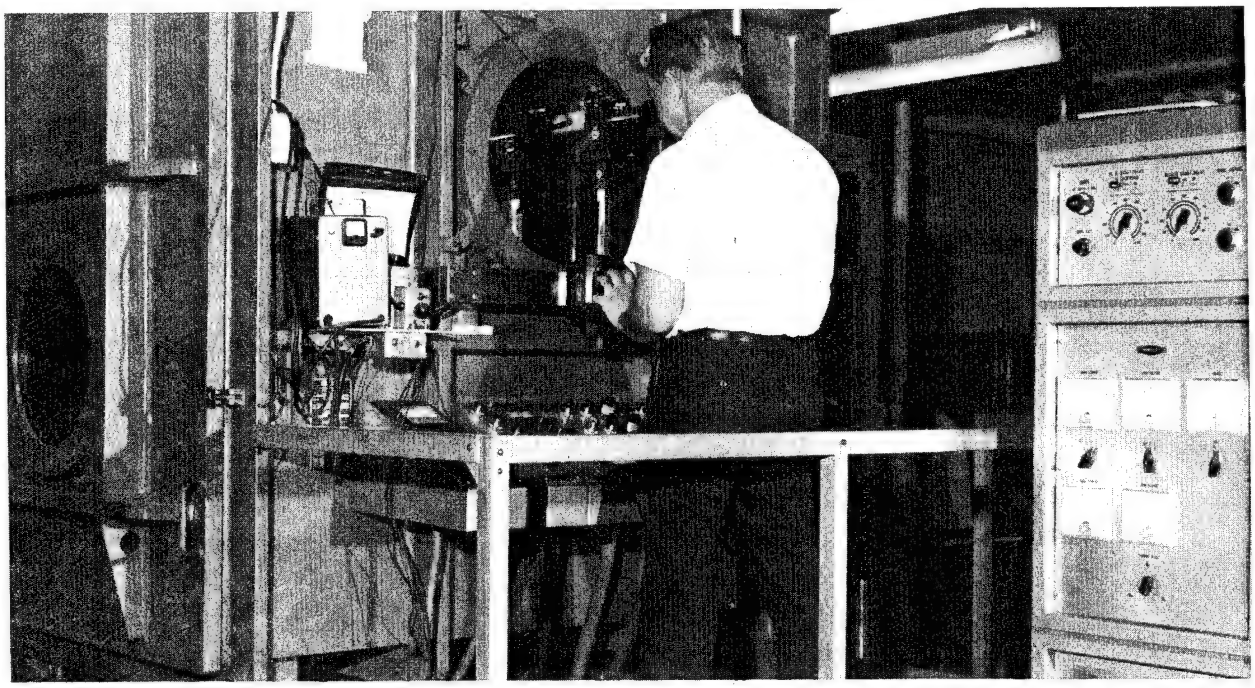

Figure 31 Electron Beam Weld Technician Remotely Aligning EB Weld Head with Dome-to-Barrel Joint Using Optical Scope (After Chamber Has Been Depressurized to Proper Vacuum)

1. Dome-to-Fitting Subassembly, (Two per Tank) (Fig. 32)

The only minor problem in joining this subassembly was caused by the domes springing out of shape after machining the hole from the dome apex. To correct the problem, the weld fixture was reworked to force alignment of the dome contour to the fitting contour prior to welding.

Figure 32 Electron Beam Weld Technician in Weld Chamber Assembling Dome and End Fitting on Fixture for Welding

This weldment was performed prior to trimming the dome flange. The flange stiffened the dome and prevented distortion that might have occurred at the dome-to-barrel interface had the flange been previously removed. As discussed in another section of this report, hot forming of each dome at the dome-to-barrel interface became necessary. The procedure of welding the fitting prior to hot sizing proved to be equally as significant with respect to distortion. The welded-in fitting also served as an alignment feature for the hot-sizing fixture and also for the final dome-to-barrel joint preparation.

Dome subassemblies were mass-produced so selective matching could be utilized. Even though hot sizing improved ovality and diametric continuity, dome subassemblies still varied slightly and were therefore selectively matched when possible.

2. Barrel Subassembly

After selecting two matched dome subassemblies, a barrel was rolled, trimed to fit, and machined for welding. Because there was no provision for access to the final tank closure weld, internal tooling could not be used. The design was therefore engineered to provide an interlocking step joint at the dome-to-barrel interface. This idea was employed to replace the normal weld backup tooling concept. As anticipated, fitup problems occurred (Fig. 33). After S/N 1 failed because of lack of fusion in this joint, a butt joint was determined necessary to eliminate fit and, hopefully, lack of fusion problems. Although the butt joint presented no machining or fit problems, it became necessary to TIG-tack the assembly at about 4-inch intervals around the circumference to hold it together prior to electron beam welding. Slight but acceptable porosity and tungsten inclusion difficulties appeared on X-rays from the TIG tacking (Fig. 34).

3. Dome Subassembly-to-Barrel Subassembly

The first tank liner, S/N 1, was preassembled in the welding chamber so that the barrel section and the two dome subassemblies could be joined during a single vacuum operation. This required that both girth joints be radiographed in the double-wall fashion. After it was determined that the failure of S/N 1 was due to an undetected lack of fusion, we changed the welding sequence so that the barrel was joined to a dome subassembly; that joint was then subjected to single-wall x-ray and dye-penetrant inspections, both inside and out. The final girth weld -- the last weldment, and the most critical -- still required a double-wall x-ray due to the lack of suitable access to the interior of the tank.

After S/N 1 failed during the hydrostatic sizing operation, a failure analysis uncovered lack of fusion in the girth joint. As a result S/N 2, which had been completed, was returned for rework. Rework consisted of removing both interlocking step joints at the girth. Although a new barrel was used for reassembling the tank liner, some volume was lost due to elimination of the old weld area on both domes. The barrel and domes were prepared for final welding by machining a straight butt joint and tack-welding the barrel and dome together.

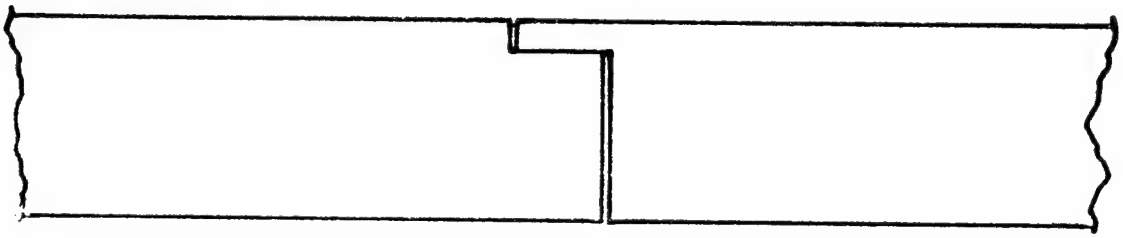

Joint Design

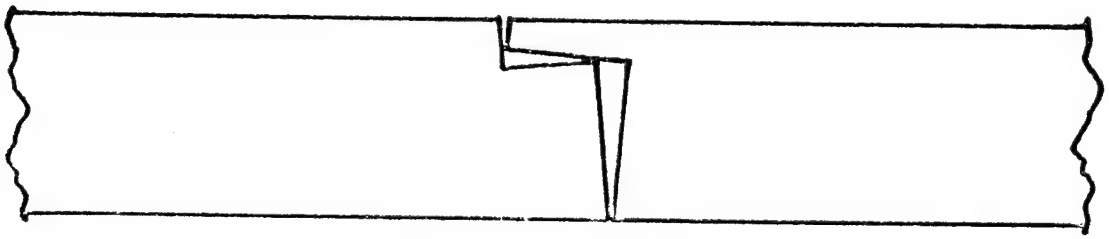

As-Assembled Joint
(Poor Fitup due to Machining Tolerances and Dome Out-of-Roundness)
Figure 33 Interlocking Joint Concept

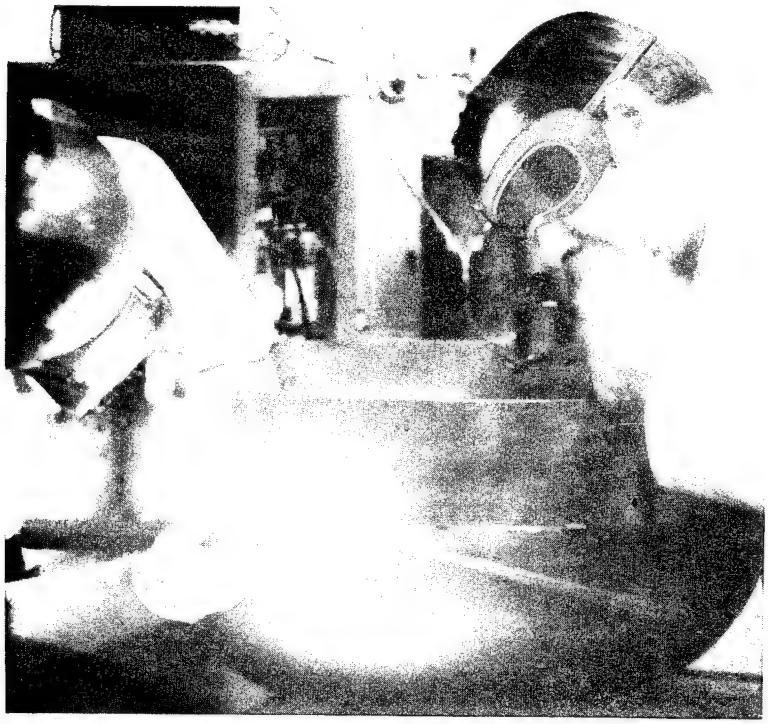

Figure 34 TIG Surface-Tack Weld of Barrel-to-Dome Prior to Performing Electron Beam Weld

Having seemingly solved the lack of fusion problem by going to the better fitting butt joint, S/N 2 was welded and returned from Baltimore to Denver where it was overwrapped and sizing was begun. S/N 2, however, again failed in one of the girth joints and again due to lack of fusion. Three areas of effort were initiated to solve the problem. The holding fixture in the electron beam welder was dismantled and reworked to give a more accurate alignment. The X-ray technique was investigated and several improvements were made to upgrade the confidence level of detecting lack of fusion. To improve the quality of the weld itself, a study of the effect of multiple-pass welds was initiated. This program involved three panels that were welded using a single-pass, a double-pass, and a triple-pass weld bead. Tensile specimens were then removed from each panel and tested to determine the effect, if any, on the strength and quality of the joint. The results are shown in Table 7.

Figure 35 illustrates the lack of fusion on S/N 2 when the single-pass weld technique simply missed the joint. The only thing holding the joint together was the cosmetic pass over the outside for smoothing out the contour. The lower portion of Figure 35 illustrates how the triple-pass weld technique would solve any misalignment encountered. Due to the acceptable results of the tensile tests, the remaining tank liners were joined at the girth with three parallel adjacent welds. No further lack of fusion problems occurred in the girth joints.

Normal inspection and acceptance tests of welded tankage were conducted for this program. Each weld for each subassembly and the final closure weld were dye-checked and X-rayed for quality verification (Fig. 36, 37, and 38). After the X-raying and any weld repairs required were completed, the tank liner was subjected to a proof pressure test of 30 psig. The tank liner was then thoroughly dried and a 24-hour helium leak test was conducted. Every tank liner passed all acceptance tests the first time as recorded in the tank processing logs.

Table 7 Tensile Test Results for Multiple-Pass Electron Beam Weldments

		f_{ty}		f_{tu}	
	Coupon	lb/in.^{2}	(N/cm^2)	lb/in.^{2}	(N/cm^2)
Single Pass	1	103,100	(71,084)	117,800	(81,220)
	2	94,000	(64,810)	118,600	(81,771)
	3	106,000	(73,084)	118,900	(81,978)
	4	108,400	(74,739)	118,200	(81,496)
Double Pass	1	105,700	(72,877)	116,400	(80,254)
	2	105,200	(73,532)	115,600	(79,703)
	3	104,400	(71,981)	116,500	(80,323)
	4	106,000	(73,084)	117,100	(80,737)
Triple Pass	1	104,300	(71,912)	117,300	(80,875)
	2	106,700	(73,567)	117,100	(80,737)
	3	105,600	(72,808)	117,200	(80,806)
	4	106,100	(73,153)	117,600	(81,082)

Note: Parent material design allowables: (5Al-2.5SN titanium),

f_{ty} = 95 ksi - tensile yield,

f_{tu} = 110 ksi - tensile ultimate.

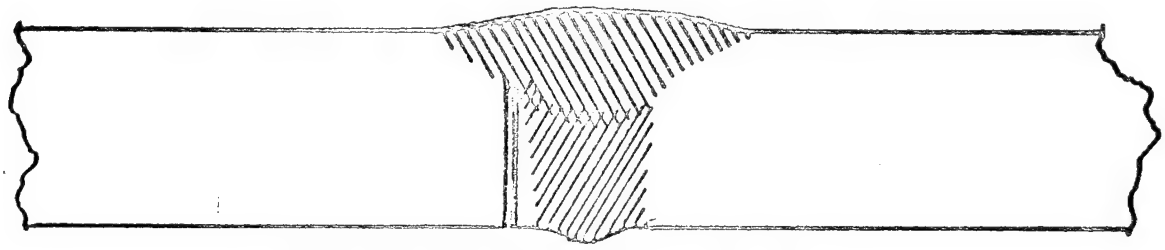

Electron Beam Weld Off ℄ of Joint

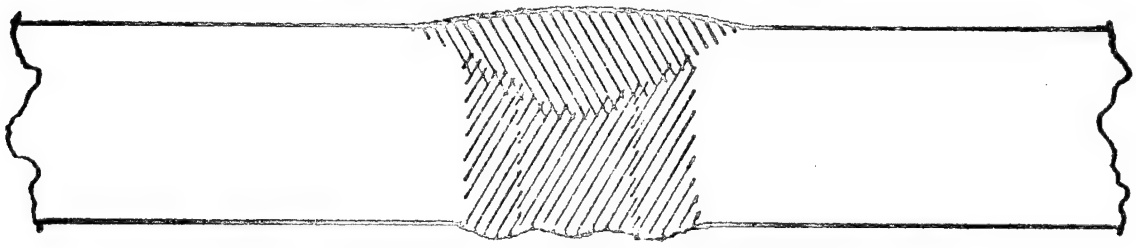

Triple Pass Plus Cosmetic Pass

Figure 35 Defective Single-Pass Electron Beam Weld and Proper Triple-Pass Weld

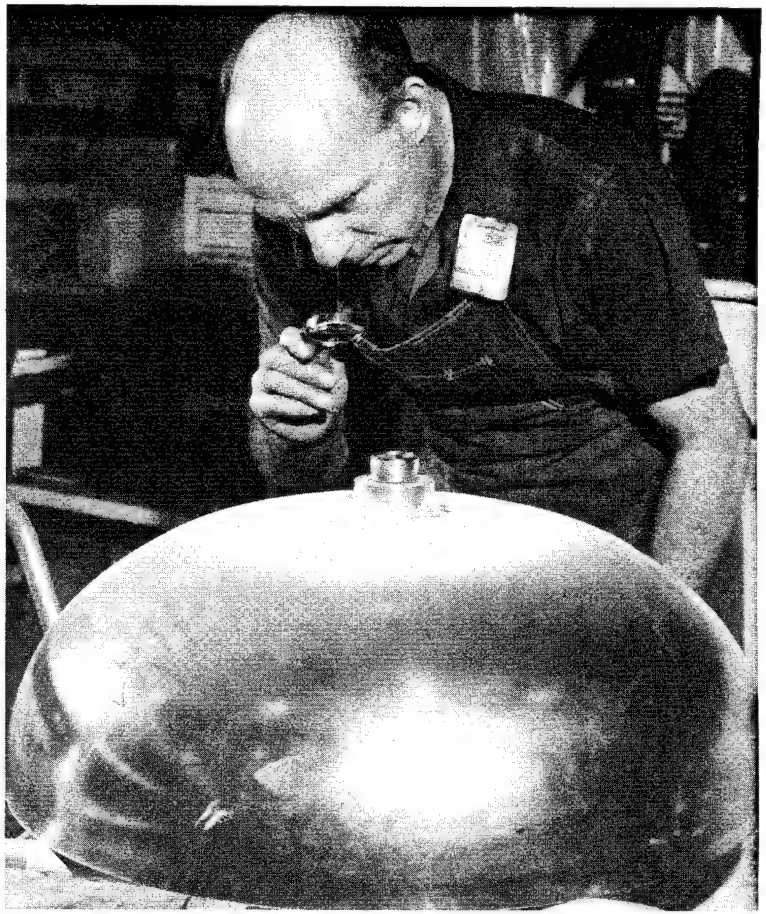

Figure 36 Dye-Penetrant Inspector Checking Dome-to-End Fitting Weld for Quality Acceptance

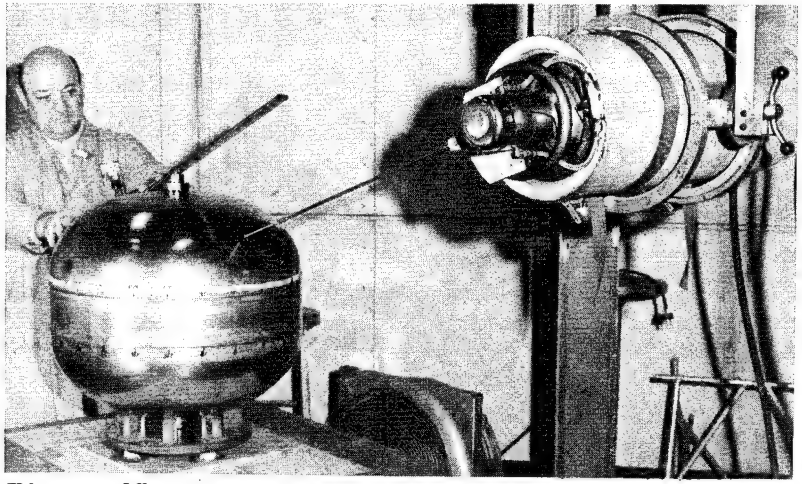

Figure 37 X-ray Technician Aligning X-ray Machine for Shooting Double-Wall X-ray on Section of Dome-to-Barrel Weldment

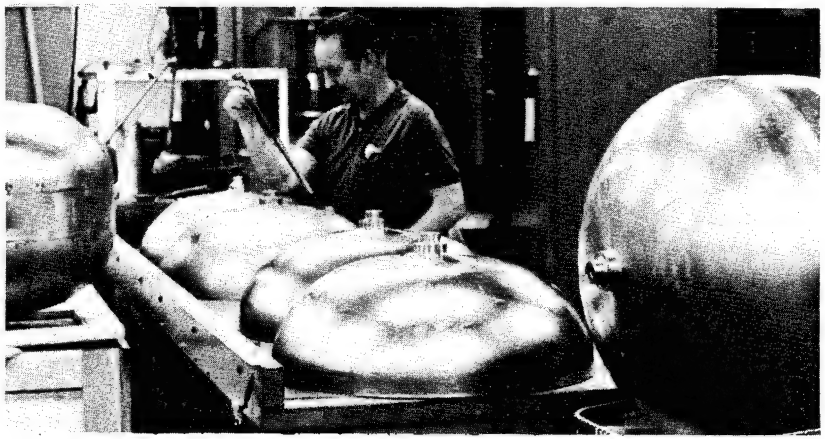

Figure 38 Dome Subassemblies and Completed Tanks Being Visually Inspected by Electron Beam Weld Technician

F. FILAMENT OVERWRAPPING

The vessels were filament-overwrapped in both a lathe winder (Fig. 39) and a polar winder (Fig. 40) using 20 end S/HTS glass roving impregnated with E796 resin under 8 ± 1 pounds tension. Prior to overwrapping, the vessels were cleaned with deionized water and wiped with methyl-ethyl ketone. The first wrap on each vessel consisted of six hoop layers (22 threads/inch each) wound using the lathe winder. The width of the hoop layers covered the cylindrical section of the vessel and was faired approximately 1 inch into each dome to provide a smooth silhouette for subsequent polar wrapping. The distribution of the material in the first six wraps varied from vessel to vessel, depending on the length of the cylindrical section and the girth weld profiles.

The vessel was then transferred to the polar winder. For vessels with welds that caused a profile mismatch, fiberglass cloth doilies, impregnated with the same resin used for winding, were placed over the end boss/dome junctions. Polar wrapping consisted of five complete layer sets. Each layer set comprised a 36-ribbon pattern. Each ribbon was approximately 2.1 inches wide with a roving density within the ribbon of 15 threads/inch. This pattern resulted in 10 polar layers in the cylindrical seciton and required approximately 5600 revolutions of the payoff arm to complete. The vessel was then returned to the lathe winder. Twenty-four 7-mil-thick by ¼-inch-wide by 5-inch-long titanium strips were placed on the cylindrical section, perpendicular to the hoop wrapping, with 3-inch spacing between the strips. The ends of the titanium strips were bent up to prevent migration of the hoop wraps toward the dome. The remaining 14 layers of hoop material were then wound on the vessel, 13 at 22 threads/inch, and one at 24 threads/inch, which completed the winding operation.

After the winding, the vessel was cured in a cam-controlled oven for 2 hours at 150°F and 4 hours at 300°F. Records of the roll numbers of the roving, weights used in the various process steps, and other pertinent fabrication data were maintained on the individual vessel fabrication logs.

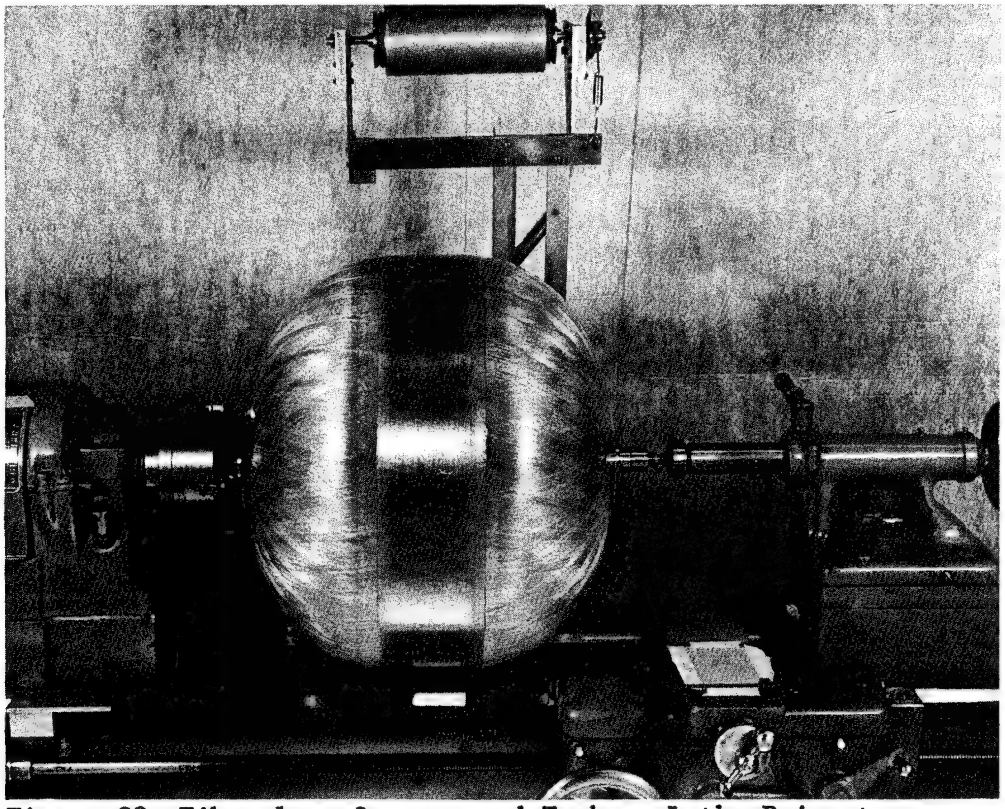

Figure 39 Fiberglass-Overwrapped Tank on Lathe Prior to Adding Hoop Wraps on Cylindrical Section of Tank

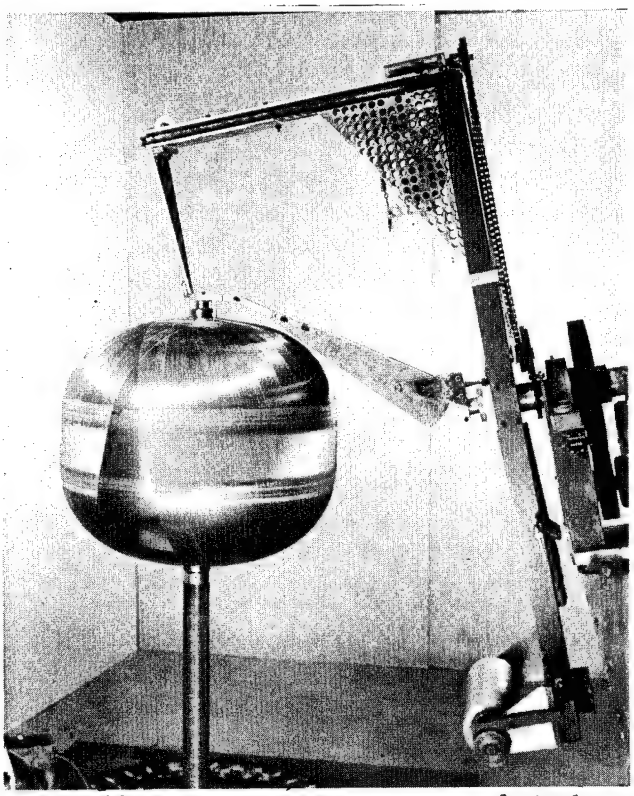

Figure 40 Fiberglass-Overwrapped Tank on Polar Wrap Winding Fixture

IV. SIZING AND TESTING

The planned test program for the fiberglass overwrapped titanium tankage consisted of two types of tests--burst and cycling. The quantity and temperature environment are given in Table 8.

Table 8 Quantity and Environment of Test Tanks

Test Type	Number of Tanks To Be Tested	
	Temperature	
	75° ± 20° F	-423°F ± 20°F
Burst	2	2
Cyclic	2 at 3360 psi	2 at 3360 psi

Prior to conducting the test program, each tank was scheduled for a sizing operation that would place the tank liner in compression and the fiberglass overwrap in tension. This was to be accomplished by hydrostatically pressurizing the tank to 4480 psi at 75°F and then venting the tank to zero psi. The sizing operation was to establish the proper stress relationship between the liner and overwrap to allow optimum performance during operating conditions.

Test plans for sizing and burst tests and cyclic tests can be found in the appendix of this report.

The test program did not develop as planned. Due to performance inadequacies of the manufactured tankage, as previously described, only two tanks completed the sizing procedure without prematurely failing (see Table 9 for the sizing and test performance summation).

Table 9 Sizing and Test Performance Summation

Tank Serial No.	Sizing Pressure		Burst Performance		Number of Cycles at 75°F	Pressure at Failure	
	lb/in.^{2}	N/cm^2 x 10^2	lb/in.^{2}	N/cm^2 x 10^2		lb/in.^{2}	N/cm^2 x 10^2
1						2200	15.16
2						1400	9.65
3						1531	10.55
4						3854	26.56
5						3660	25.23
6	4527	31.20			49	3350	23.09
7	4469	30.80	5062	34.89		5062	34.89
8						3462	23.66

All tanks were instrumented with LVDTs (linear variable displacement transformers) in both the hoop and longitudinal directions on the tank (Fig. 41 and 42). In addition, hoop and longitudinal strain gages were mounted on S/N 5 and 8. This was done as an experiment to determine if the LVDTs mounted on the standoffs on the tank and the strain gages cemented to the fiberglass tank surface would read out comparable strains. In both cases, it was determined that the strain gages transmitted good strain correlation with the predicted strains from the computer but not with the LVDTs (see discussion in following paragraph).

Table 10 summarizes the strain data recorded for all tanks and Figures 43 thru 54 show complete pressure versus strain curves for each tank. Figure 55 illustrates pressure versus strain as predicted by the computer. Figure 56 illustrates the chamber or enclosure in which each tank was first sized and later tested.

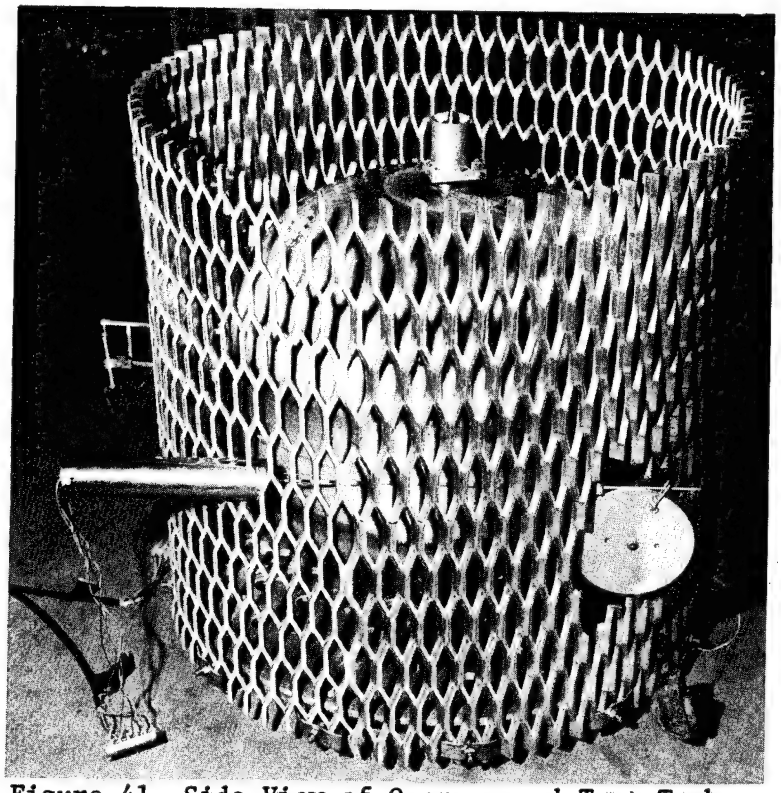

Figure 41 Side View of Overwrapped Test Tank Showing Hoop Strain Displacement Instrumentation

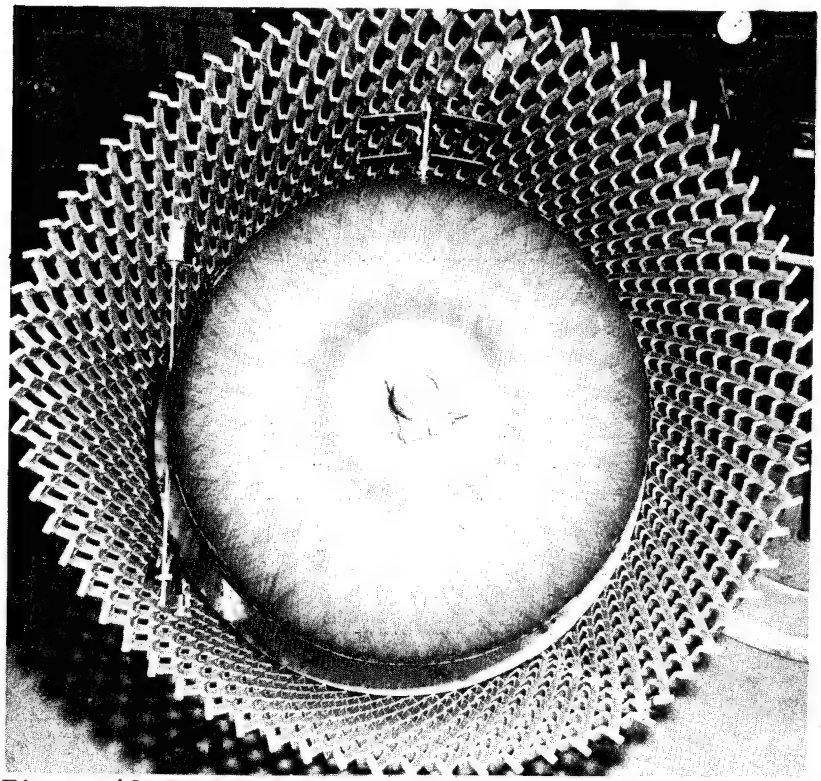

Figure 42 Top View of Instrumented Overwrapped Test Tank Mounted in Fragmentation Shield

Table 10 Strain Data Summary

Serial No.	Failure Pressure lb/in.^{2}	Failure Pressure N/cm^2 x 10^2	STRAIN AT COMPLETION OF TEST (%) Sizing Test LVDT Measurement Longitudinal	Sizing Test LVDT Measurement Hoop	Sizing Test Strain Gage Measurement Longitudinal	Sizing Test Strain Gage Measurement Hoop	Burst Test Longitudinal	Burst Test Hoop	Ambient Cycling Test Longitudinal (First cycle only)	Ambient Cycling Test Hoop (First cycle only)
1	2200	15.16	0.85	0.37						
2	1400	9.65	0.30	0.15						
3	1531	10.55	1.20	0.22						
4	3854	26.56	2.78	0.71						
5	3660	25.23	1.60	0.68	0.65	Gage failed at 1180 psi				
6*	3350	23.09	4.40†	1.03†					2.13	0.49
7	5062	34.89	3.86§	1.20§			4.88	1.40		
8	3432	23.66	1.36	0.59	0.47	Gage failed at 1110 psi				

*S/N 6 failed during 49th cycle.

†Strain at sizing pressure of 4527 psig.

§Strain at sizing pressure of 4469 psig.

Note: See Figures 43 thru 55 for complete curves.

Figures 43 through 47, 49, 51, and 53 illustrate the strain curves generated by plotting LVDT test data during the sizing operation on each tank. Figures 48 and 54 complement Figures 47 and 53, respectively, with regard to data taken from the sizing operation. Strain gages were mounted on S/N 5 and 8 to verify LVDT accuracies. As can be noted, the hoop LVDT and the hoop strain gage data successfully complement each other. However, the longitudinal LVDT and the longitudinal strain gage data do not complement each other. It is concluded that the longitudinal LVDTs on all tanks did not function properly for unexplainable reasons. To support this conclusion, Figure 55, which plots pressure versus strain as predicted by the computer, has been included. This curve shows a generally equal strain condition in both the hoop and longitudinal directions as it should per the design criteria of this program. Figures 48 and 54, the strain curves generated from strain gage data, verify the desired condition and therefore negate all LVDT longitudinal curves as plotted.

Figure 50 is the strain curve generated in the first cycle pressure test of S/N 6. Succeeding cycles are not plotted since they essentially duplicate the first cycle.

Figure 52 is the strain curve generated during ambient burst test of S/N 7. It is interesting as well as predictable to note that there are residual strains in S/N 7 after it was sized and depressurized. No attempt has been initiated to draw any conclusions from these data because S/N 7 was the only tank tested in this manner.

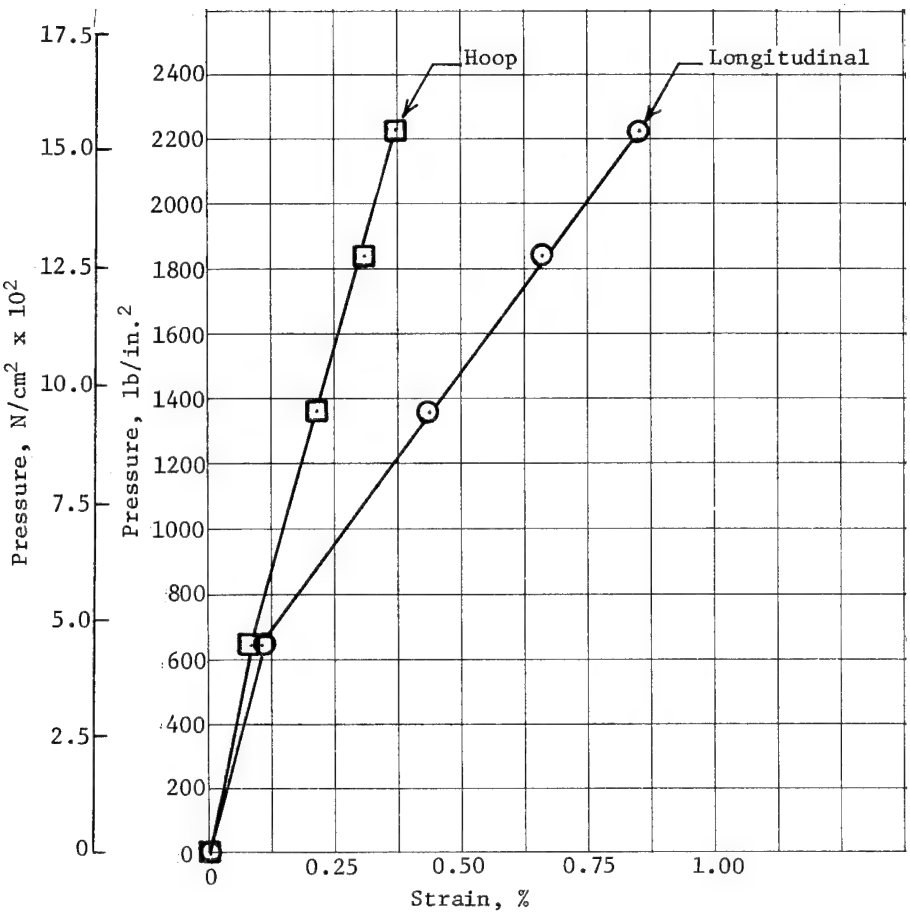

Figure 43 S/N 1 Sizing Test

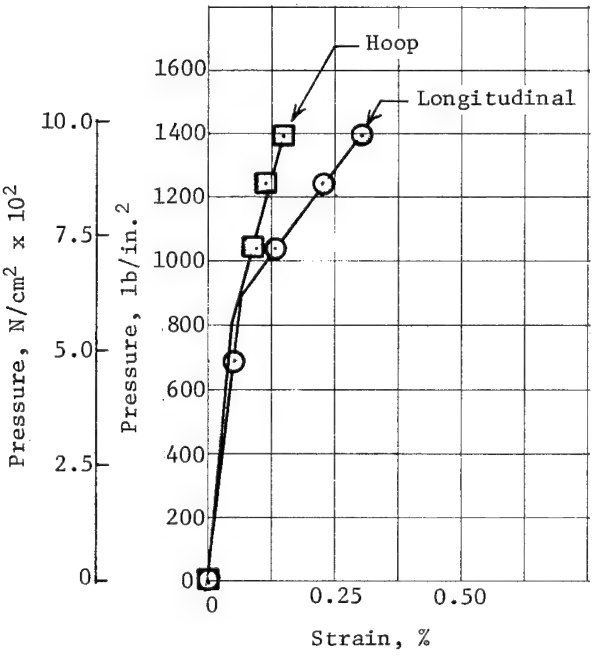

Figure 44 S/N 2 Sizing Test

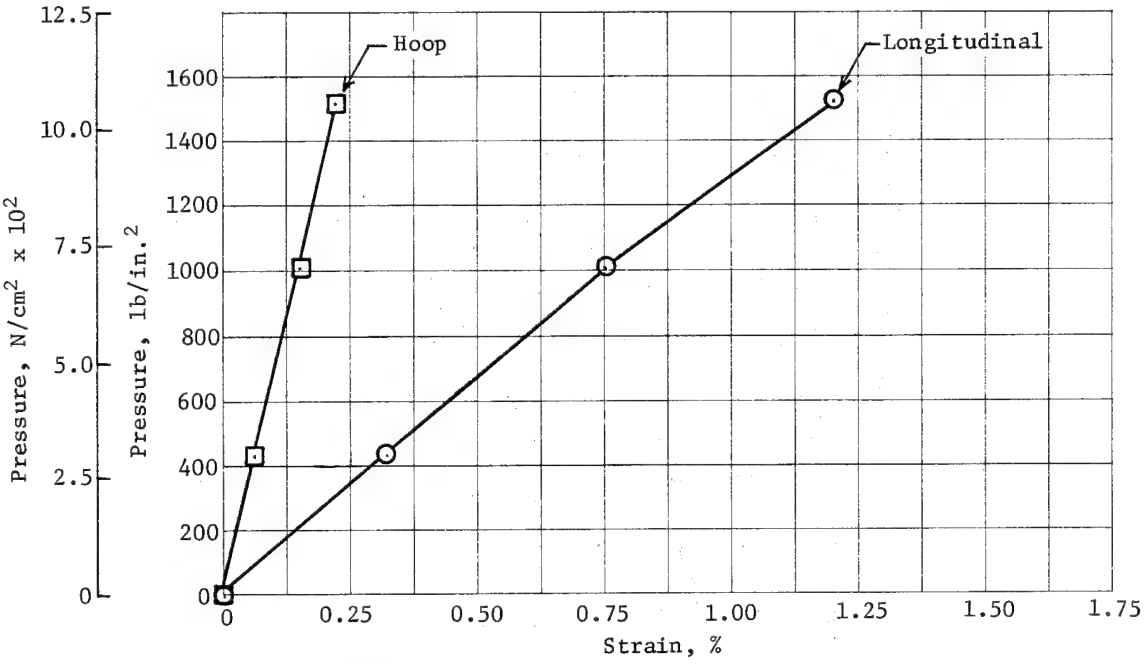

Figure 45 S/N 3 Sizing Test

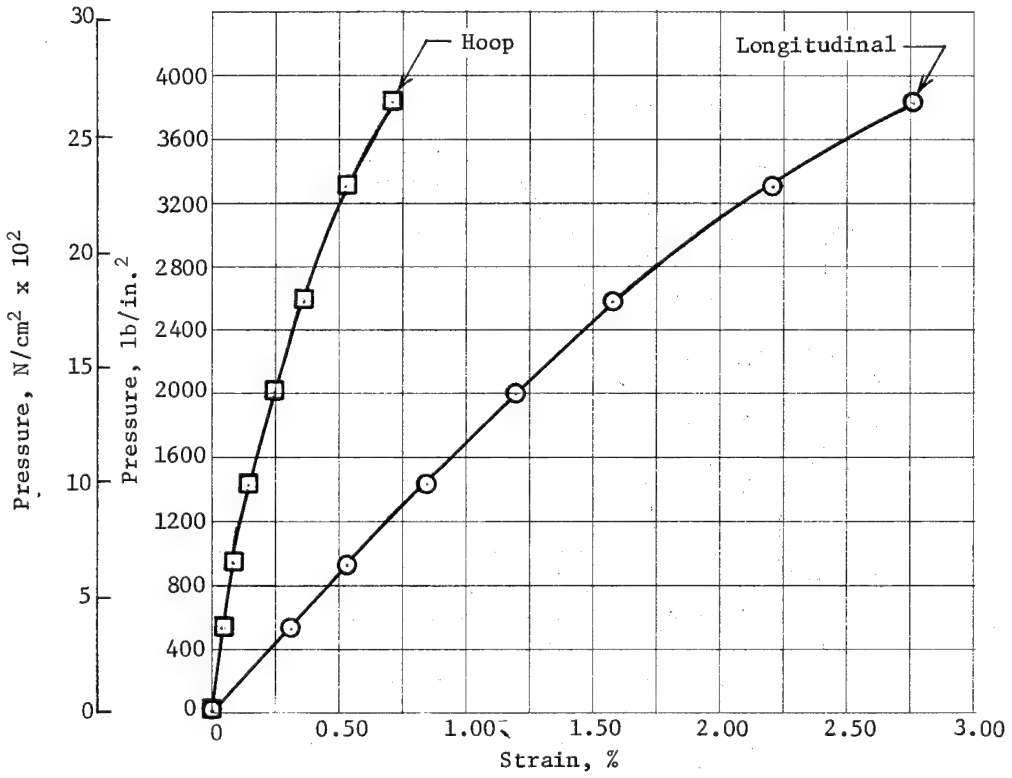

Figure 46 S/N 4 Sizing Test

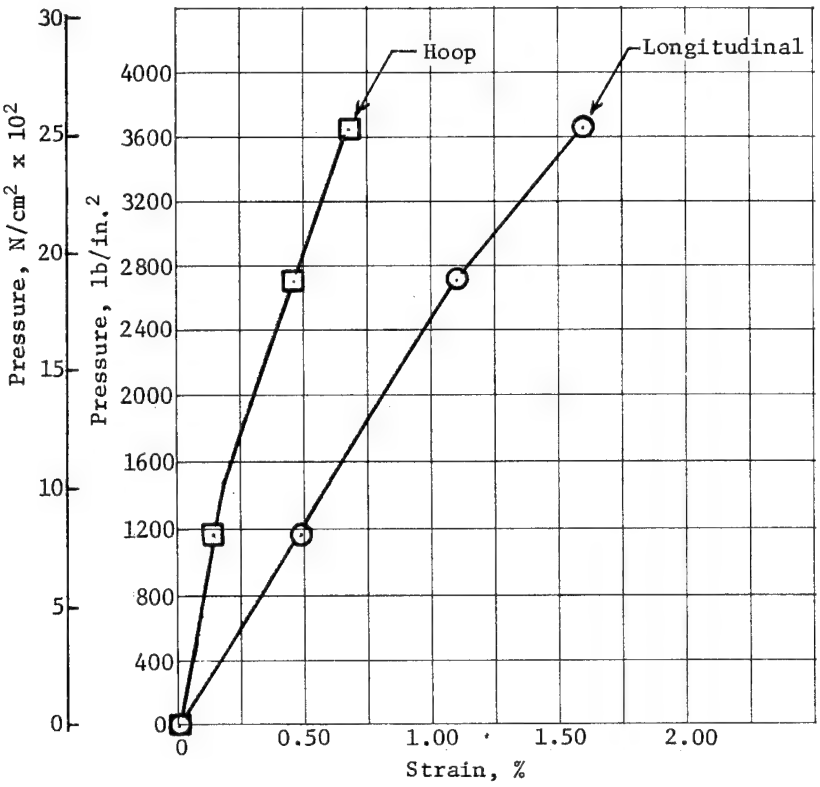

Figure 47 S/N 5 Sizing Test

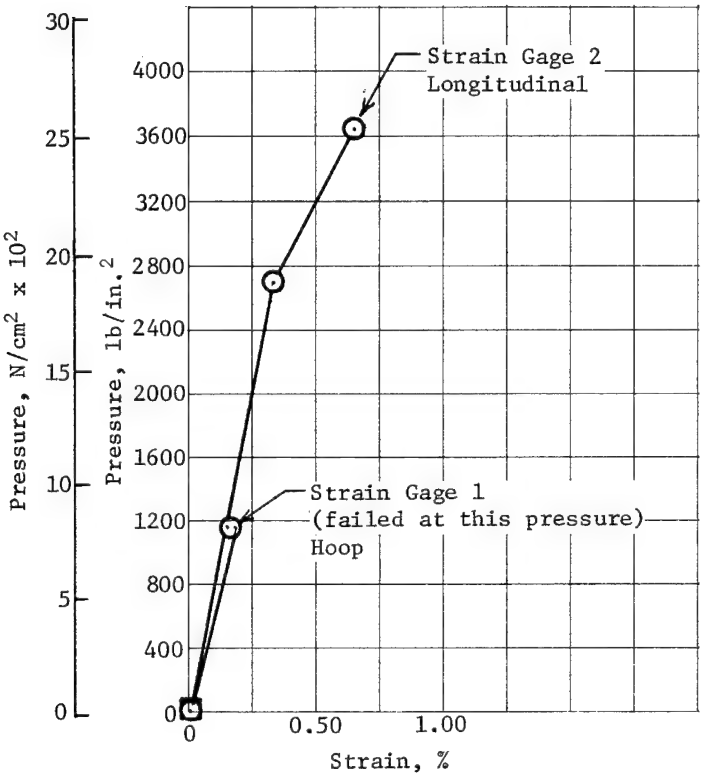

Figure 48 S/N 5 Sizing Test, Strain Gages

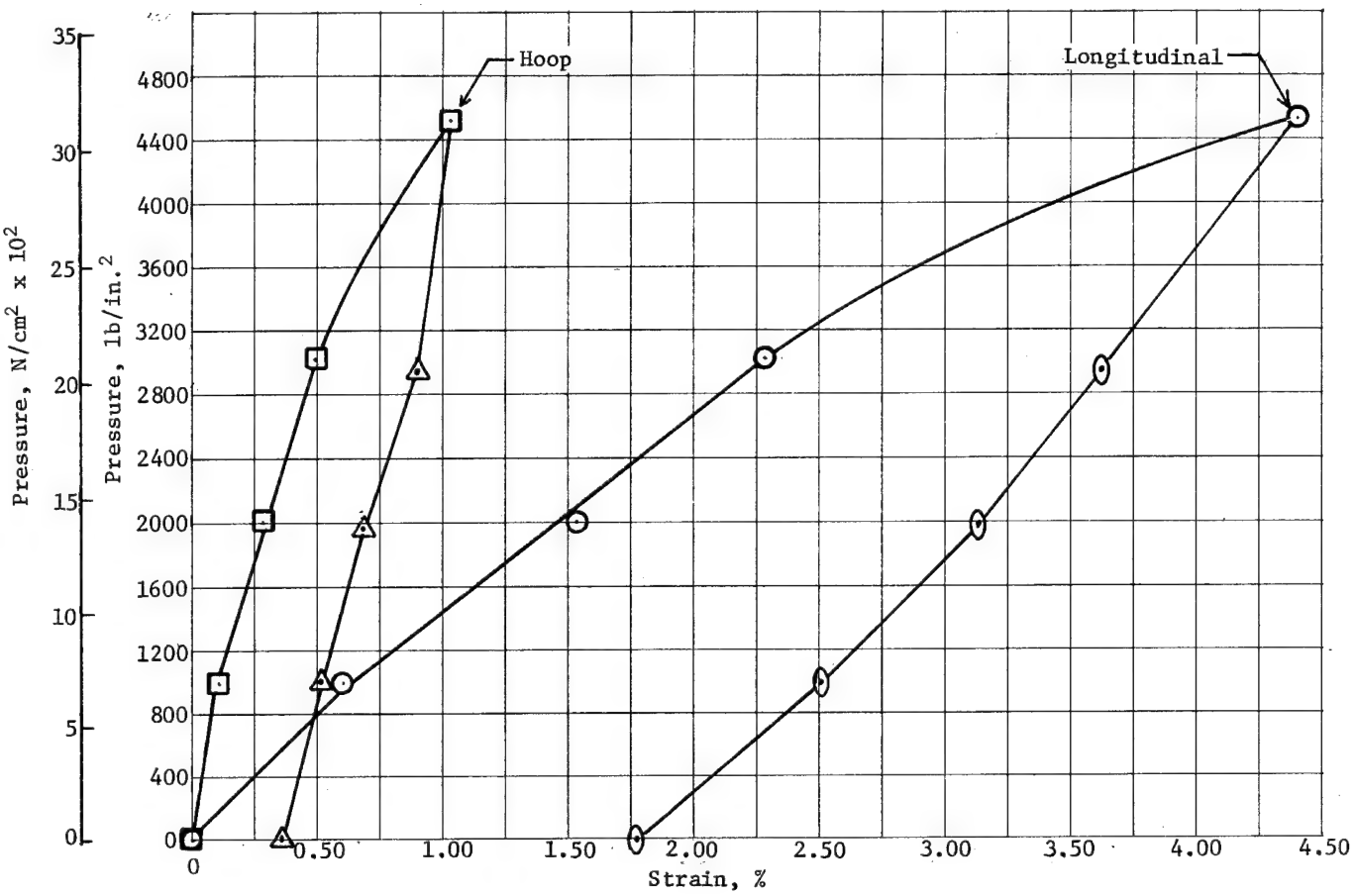

Figure 49 S/N 6 Sizing Test

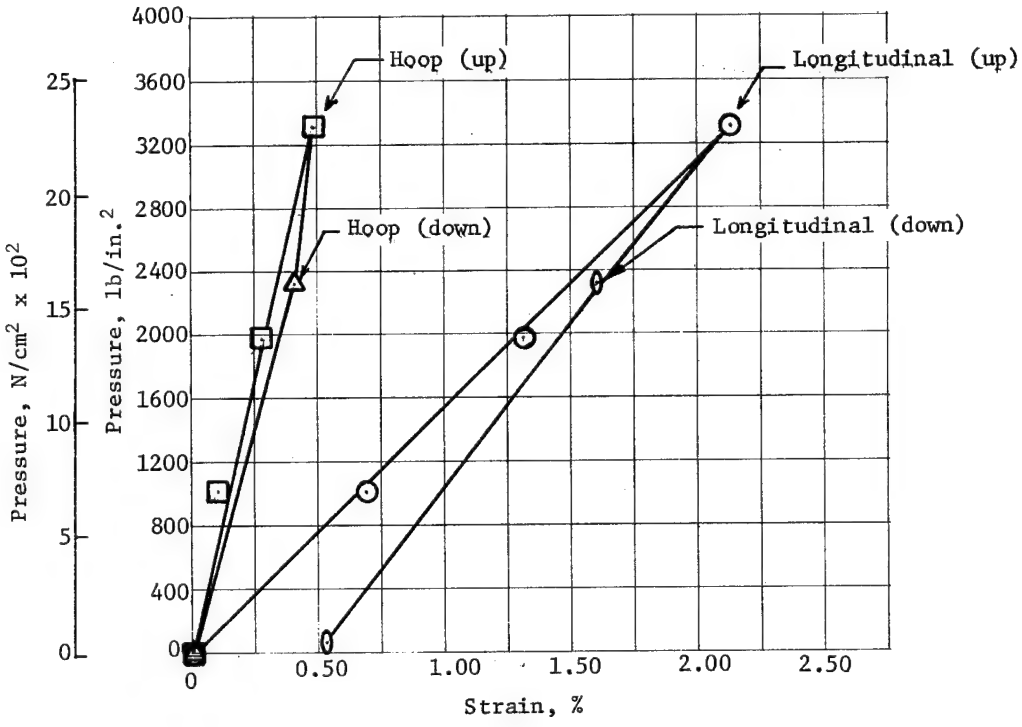

Figure 50 S/N 6 Cycling Test (First Cycle)

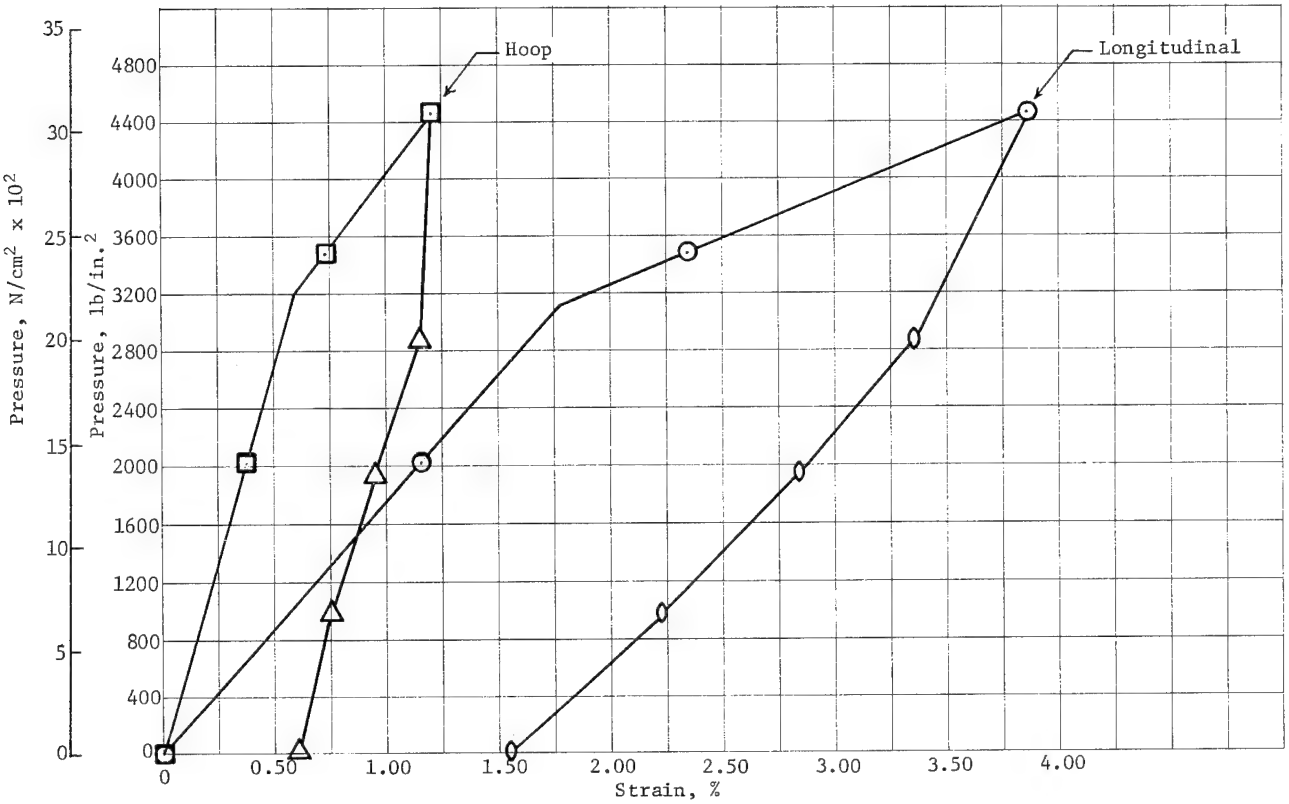

Figure 51 S/N 7 Sizing Test

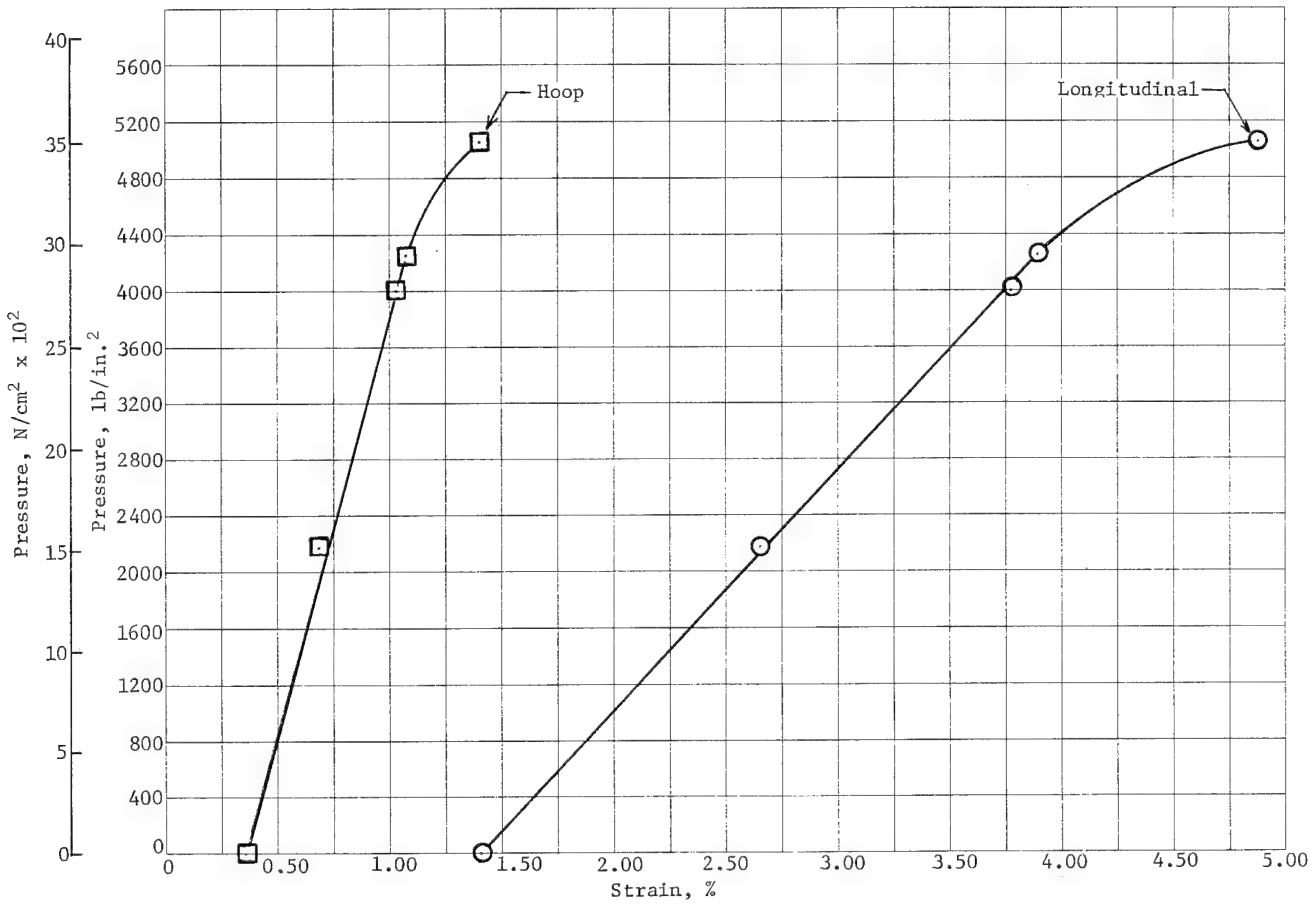

Figure 52 S/N 7 Burst Test

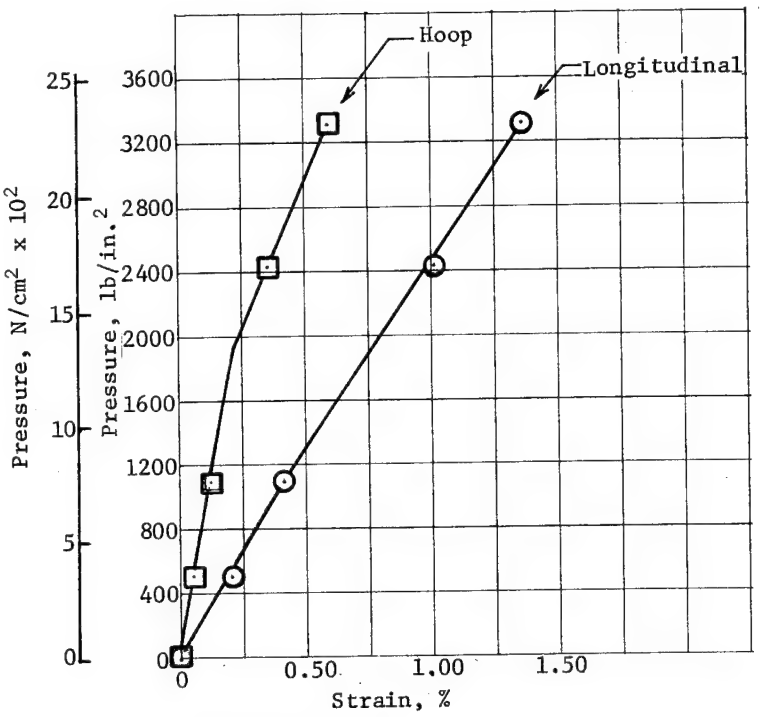

Figure 53 S/N 8 Sizing Test

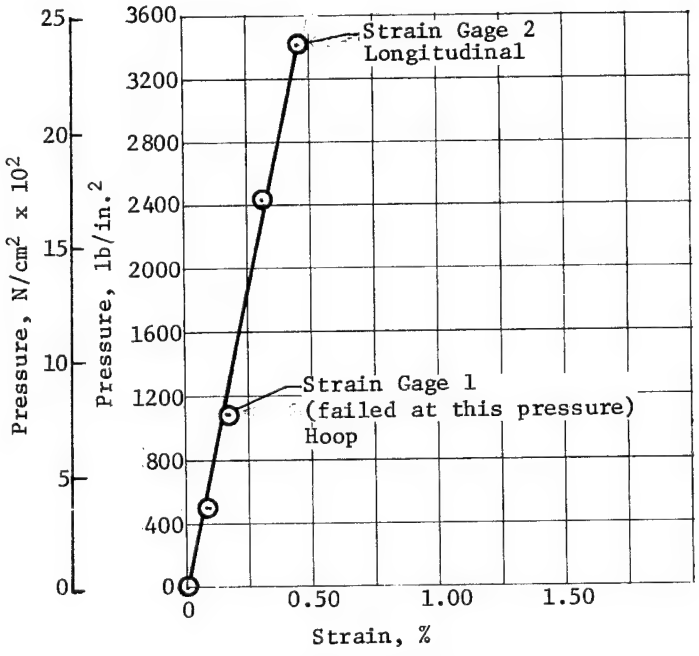

Figure 54 S/N 8 Sizing Test, Strain Gages

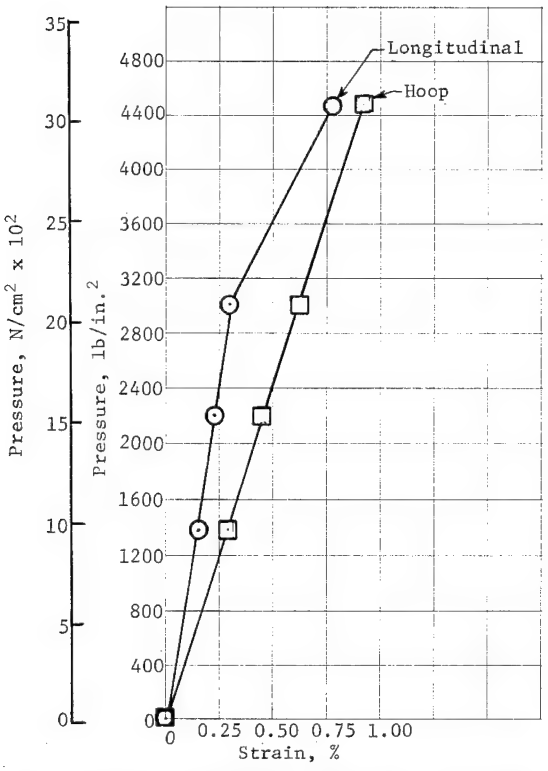

Figure 55 Computer Strain Curves

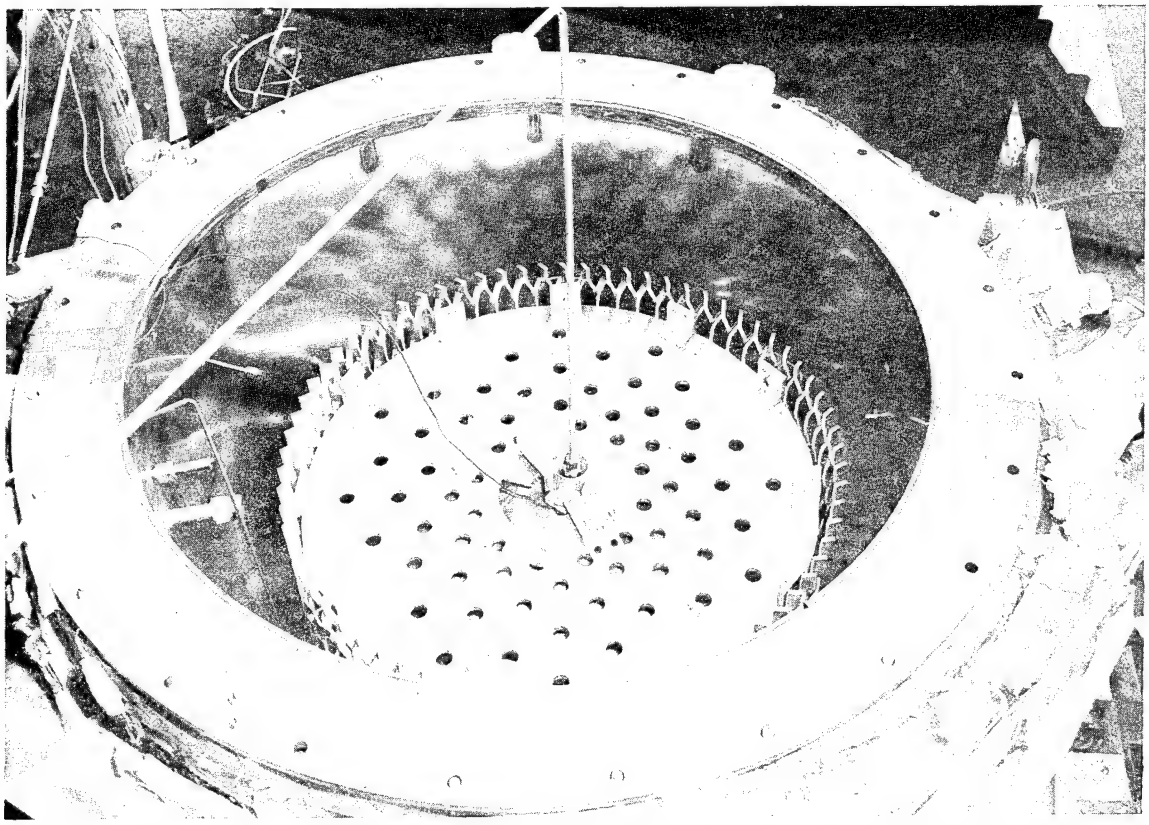

Figure 56 View Looking into Test Chamber with Test Article Installed

V. TEST EVALUATION

A tool-proofing prototype and eight production tanks were fabricated for testing. Premature failures in the hydrostatic sizing operations prevented the full series of tests from being conducted (Table 11). It is worth noting that even though hydrostatic burst pressures exceeded 5000 psi, little or no fragmentation of the titanium liner or of the overwrap material occurred. The first series of failures took place in the girth joints.

Table 11 Overwrapped Tank Performance Summary

Tank Serial No.	Liner Weight, lb (kg)	Overwrap Weight, lb (kg)	Tank Total Weight, lb (kg)	Tank Volume Prior to Sizing, $in.^3$ (m^3)	Tank Volume After Sizing, $in.^3$ (m^3)	Tank Failure Pressure, psi (N/cm^2)
1	45.0 (20.4)	27.0 (12.2)	72.0 (32.6)	7211.0 (0.118)	--	2220.0 (1530.0)
2	42.6 (19.3)	26.2 (16.8)	68.8 (31.2)	6782.0 (0.111)	--	1450.0 (999.0)
3	41.5 (18.8)	26.9 (12.2)	68.4 (31.0)	6871.0 (0.112)	--	1531.0 (1055.0)
4	44.8 (20.3)	27.2 (12.3)	72.0 (32.6)	7129.0 (0.116)	--	3854.0 (2656.0)
5	43.0 (19.5)	30.0 (13.6)	73.0 (33.1)	7231.0 (0.118)	--	3660.0 (2523.0)
6	41.5 (18.8)	27.7 (12.5)	69.2 (31.3)	7058.0 (0.115)	7161.0 (0.117)	3350.0* (2309.0)
7	43.3 (19.6)	27.7 (12.5)	71.0 (32.2)	7266.0 (0.119)	7327.0 (0.120)	5062.0† (3489.0)
8	42.0 (19.0)	28.0 (12.7)	70.0 (31.7)	7038.0 (0.115)	--	3432.0 (2366.0)

*S/N 6 was sized at 4527 psig. Following the sizing operation, the tank was cycled at ambient temperature from 100 psig to 3360 psig. During the 49th cycle, S/N 6 failed at 3350 psig. A pressure decay rate of 21 psig/sec confirmed tank failure during the attempted 50th cycle.

†S/N 7 was sized at 4469 psig. Following the sizing operations, the tank was taken to ambient burst pressure, 5062 psig.

S/N 1 failure analysis indicated that the failure was due to the electron beam partially missing the joint. The defect was camouflaged by the combination of the cosmetic pass and the near diffusion bond created by the close fit and elevated temperature. The welding sequence used on the first two tanks made a double-wall radiograph mandatory. Difficulty in interpreting the double wall X-ray added to the problem of acceptance testing. Ultimately S/N 1 was cut apart at the girth joints, remachined, and joined with a new cylindrical section. Since S/N 1 sustained heavy scratches on the tank liner surface when the overwrap was removed, it became a prototype for liner reworking but was not overwrapped or tested.

S/N 2 failed in the same manner, even though prior to testing it had been reworked as S/N 1 had been. Figure 57 shows the joint indicating a lack of fusion. As indicated in other portions of this report, the holding fixtures were reworked and the entire radiographic process revised. In the process of attempting to rework the girth welds of the remaining tanks, the serial numbers of the tanks no longer reflected the chronological order of fabrication or test.

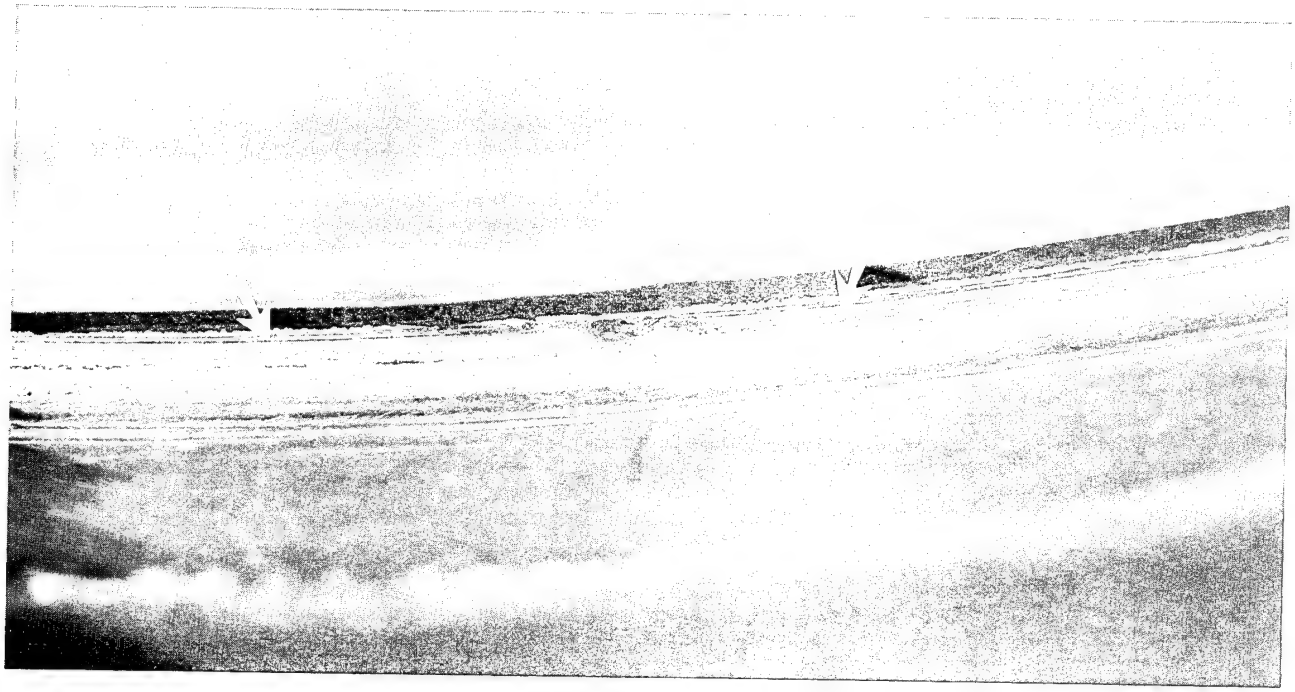

Figure 57 Origin of Failure at Girth Joint; Machining Marks Indicate Lack of Fusion (Typical of S/N 1 and S/N 2)

S/N 2 and S/N 3 (which also failed in the girth prematurely) could not be reworked because not enough cylindrical section of the domes was left for rewelding because they had been machined for the girth joint three times.

After the welding equipment had been reworked and the three-pass weld developed for the girth weld (Fig. 58), S/N 3 was the only tank to fail in the girth weld. Its failure mode, shown in Figure 59, indicates a crack in the area contaminated by mild steel that was melted and splattered from the weld holding fixture while performing the weld.

S/N 4 burst at 3854 psi during the hydrostatic sizing operation. This was the first tank that failed outside the girth weld. In this case, the failure was initiated at the dome-to-fitting joint (Fig. 60). The cause of failure appeared to be a combintation of a lack of ductility (Fig. 61 and 62) and joint mismatch. The mismatch was not a typical joint misalignment, but appeared to be a condition referred to as "sink-in" brought about as the dome-to-fitting joint shrunk under pressure while cooling after the weldment had been completed. A fix for correcting the "sink-in" effect utilizing hot forming is shown in Figure 63. Refer to Table 12 for the forming process.

S/N 5 failed at 3660 psi during the hydrostatic sizing operation (Fig. 64). This is the only tank that failed in the longitudinal joint of the cylindrical band (Fig. 65). The failure area appeared to have been contaminated by an iron inclusion when a portion of the carry-through bolt that was a part of the weld tooling partially melted during welding. This was not detected by X-ray (Fig. 66).

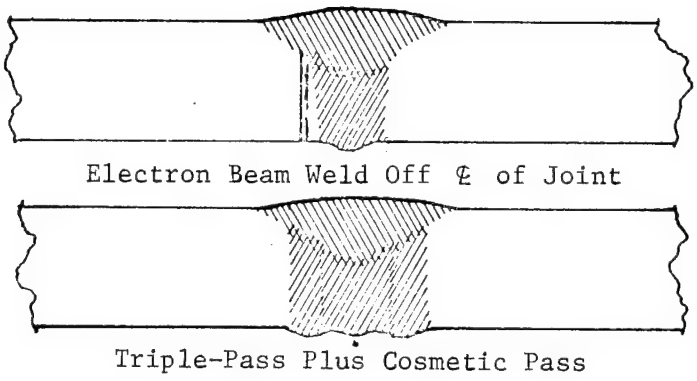

Figure 58 Defective Single Pass Electron Beam Weld and Proper Triple-Pass Weld

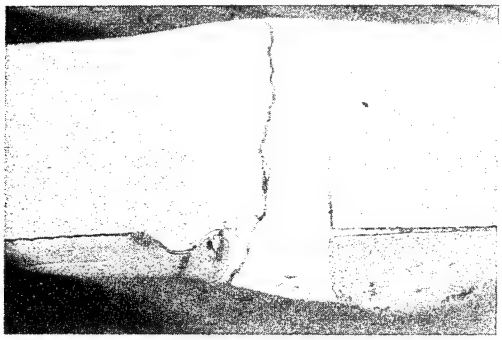

Figure 59 S/N 3 Failure in Girth Joint due to Weld Contamination

Figure 60 Photograph of S/N 4 Tank Showing Fracture After Removal of Fiberglass

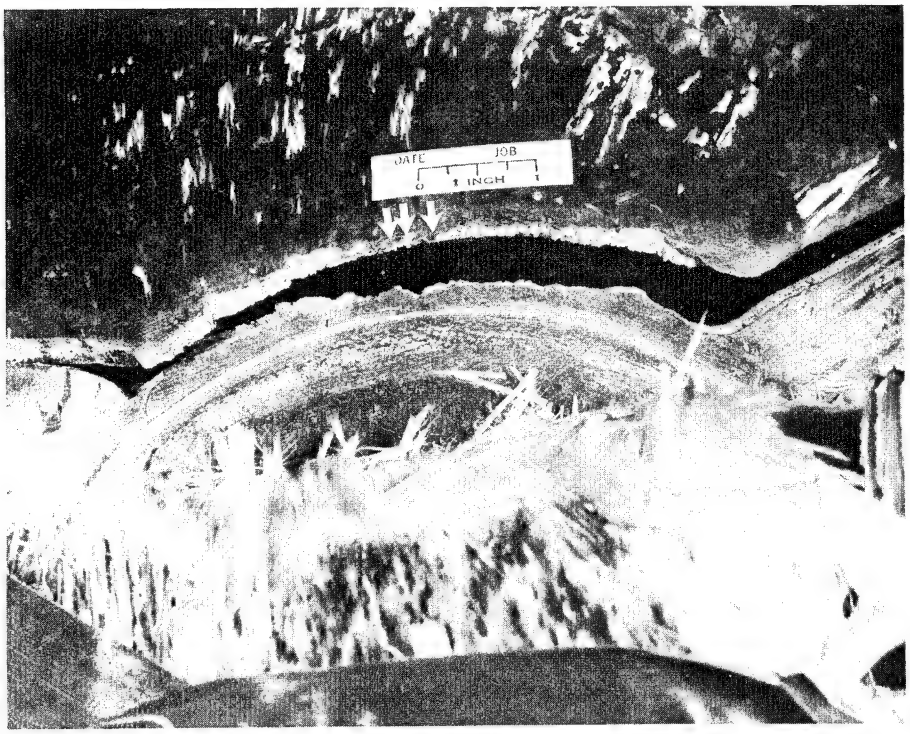

Figure 61 Photograph of S/N 4 Showing Weld Fracture With Arrows Indicating Approximate Origin of Failure

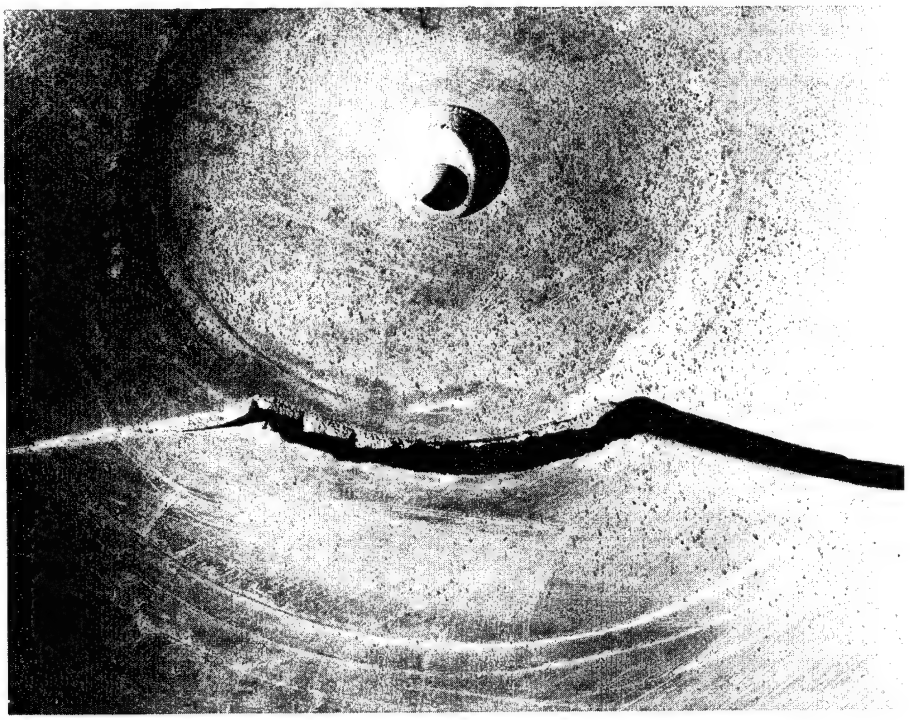

Figure 62 Photograph of S/N 4 Fracture from Inside the Tank

Table 12 Manufacturing Process for Hot-Forming Dome-to-Fitting Contour

- Clean dome and fitting weld assembly, acetone wipe to remove all dirt, grease, and foreign matter from inside and outside surfaces.
- Apply Everlube T-50 to dome and fitting weld assembly. Use spray gun to apply a light even coat to both inside and outside surfaces. Air-dry at room temperature for 1 hour.
- Position dome with fitting down into circular press ring bottom.
- Position inside pressure ring tool to dome and locate assembly in hydraulic press.
- Apply heat (acetylene torch) and pressure (35 to 40 tons) simultaneously to eliminate joggle. Apply heat mainly on tool and do not exceed 1600°F. Monitor with surface pyrometer. Cool while under pressure.
- Inspect assembly. Repeat operation if joggle or offset is not removed.
- Remove assembly from press, remove pressure rings, and clean to remove Everlube T-50 using the following procedure:

  Clean using Method I per MP50063;

  Dye penetrant inspect;

  Radiographic inspect.

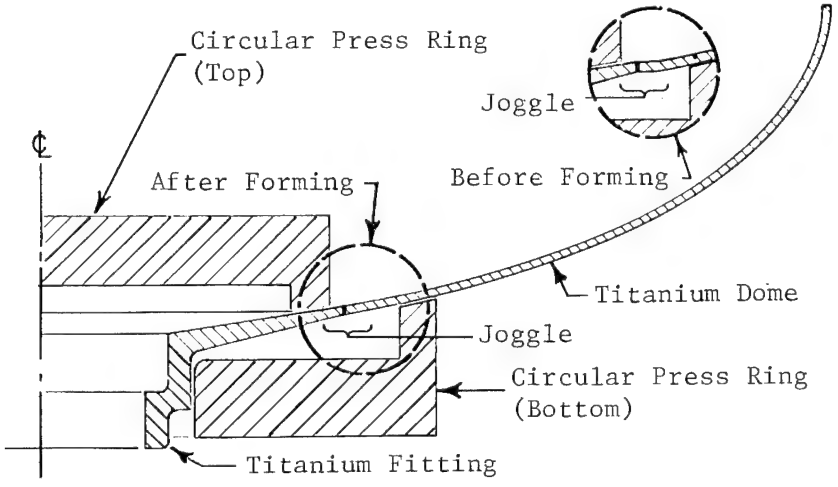

Figure 63 Hot-Forming Schematic

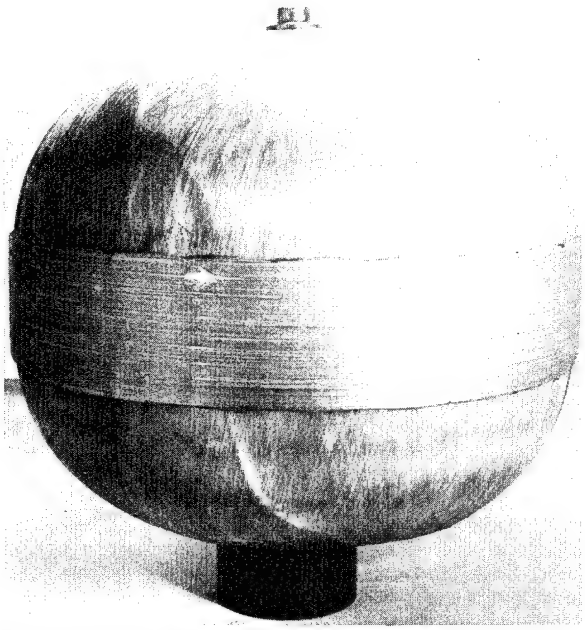

Figure 64 Photograph of S/N 5 Showing the As-Failed Configuration; Arrow Indicates Approximate Origin of Fracture

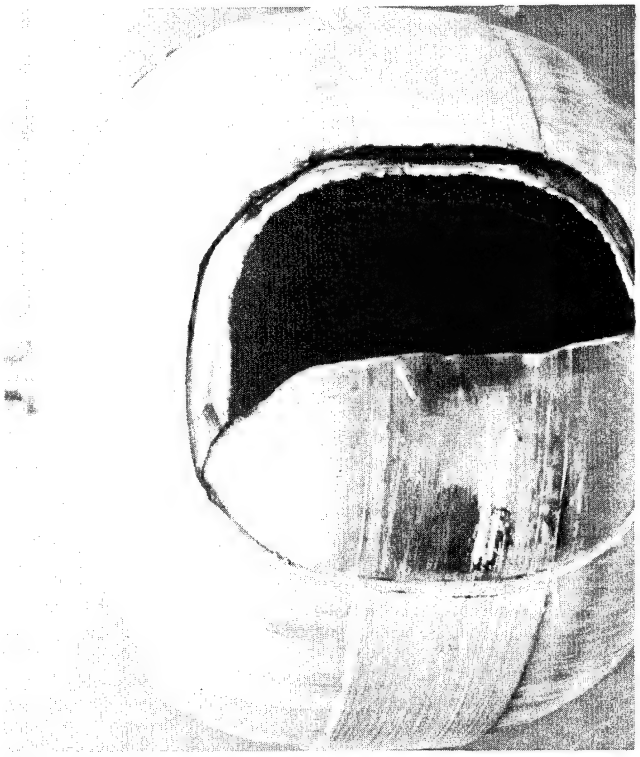

Figure 65 Photograph of S/N 5 Showing Exposed Fracture Surface; Arrow Indicates Failure Origin

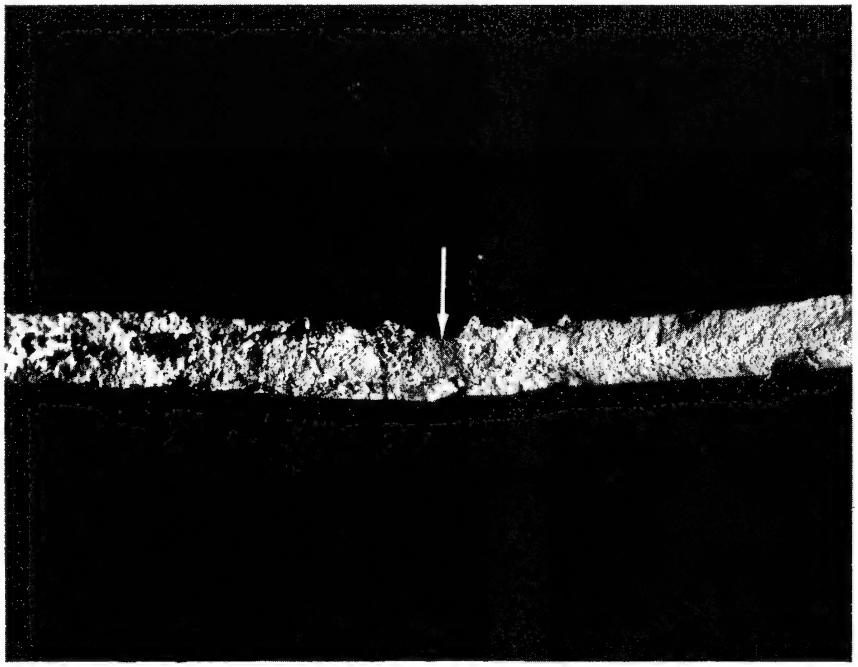

Figure 66 Photomacrograph of Fracture Surface on S/N 5; Arrow Shows Origin of Failure

S/N 6 was successfully sized at 4527 psig. Following the hydrostatic sizing, it was checked for volume increase and then cycled at 75°F between 100 and 3360 psi. On the 49th cycle, there was an indication of a probable failure. On the 50th cycle a pressure decay of 21 psig/sec confirmed the failure and the test was stopped. Figure 67 shows the tank as failed and prior to the failure analysis.

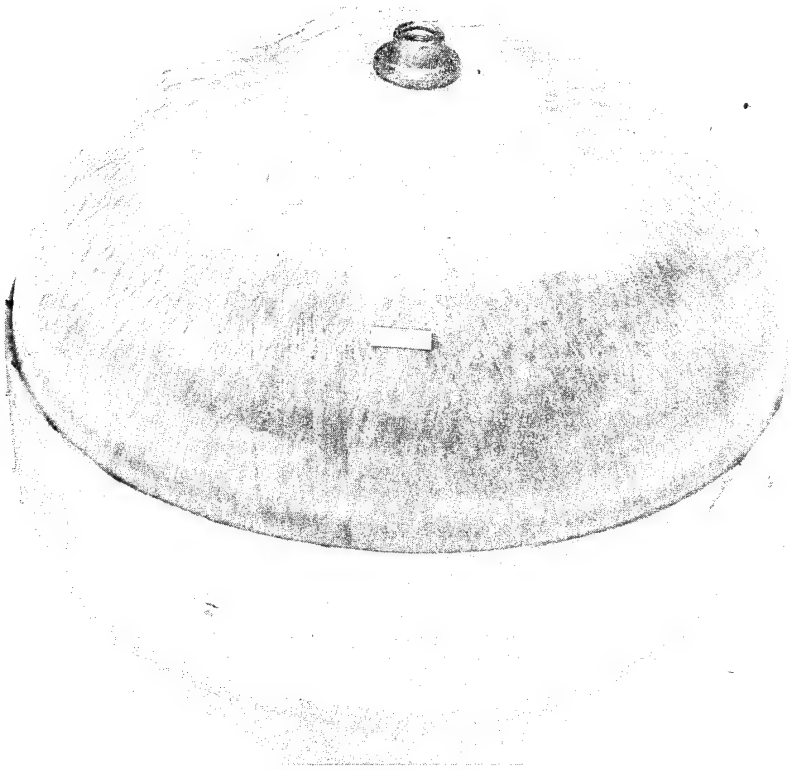

Figure 67 Photograph of S/N 6 Showing As-Failed Configuration

Since the leak on S/N 6 was very small, it was determined that the glass overwrap would have to be completely stripped by hand before the leak area could be determined. After the liner had been stripped, a pressure check at 40 psi did not reveal the leak point. Finally, the liner was baked at 350°F for 1 hr.

A helium leak check revealed the leak to be in the parent material (Fig. 68 and 69). Dissection of the specimen at the failure point indicates the possibility of stress corrosion (Fig. 70 and 71). In addition, the microstructure near the failure point appears to have a grain boundary precipitant typical of overannealing or overheating. Figures 72 and 73 show comparisons of normal "clean" microstructure versus the "dirty" microstructure near the failure point.

S/N 7 was hydrostatically sized at 4469 psig. The volume after sizing was determined to be 7327 $in.^3$ The vessel was then hydrostatically pressurized at 75°F to burst. The tank failed at 5062 psig (Fig. 74). The failure initiation point was in the girth weld. Analysis indicated the failure was due to simple overpressure with no metallurgical cause for failure.

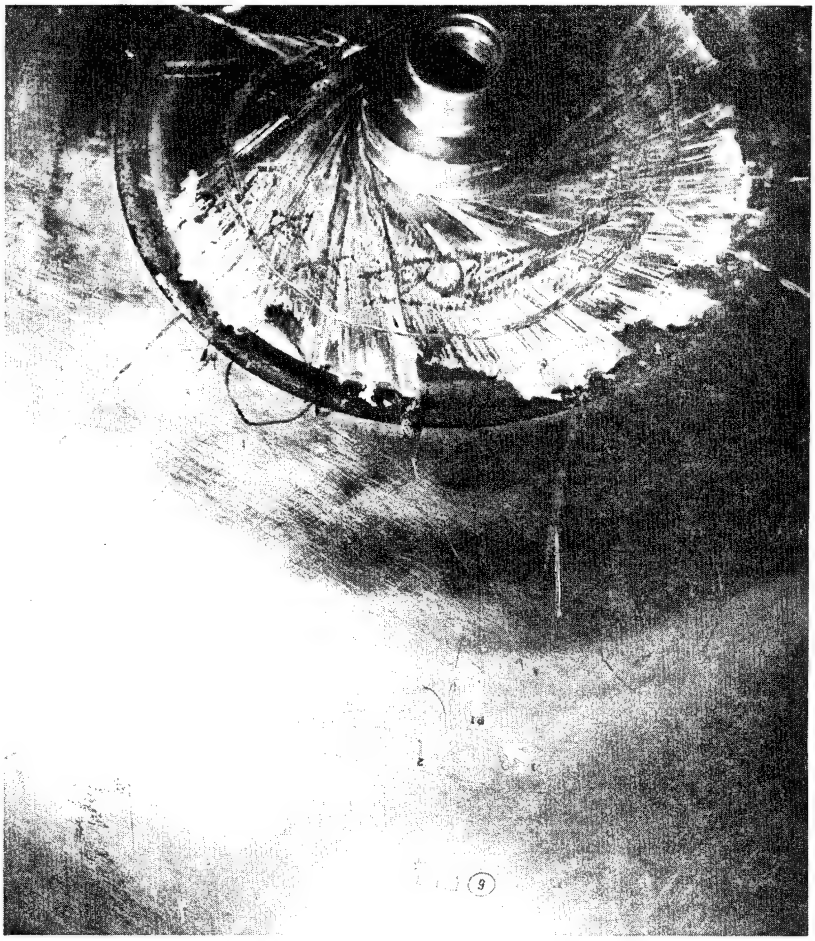

Figure 68 Photograph of S/N 6 Showing Leak Area

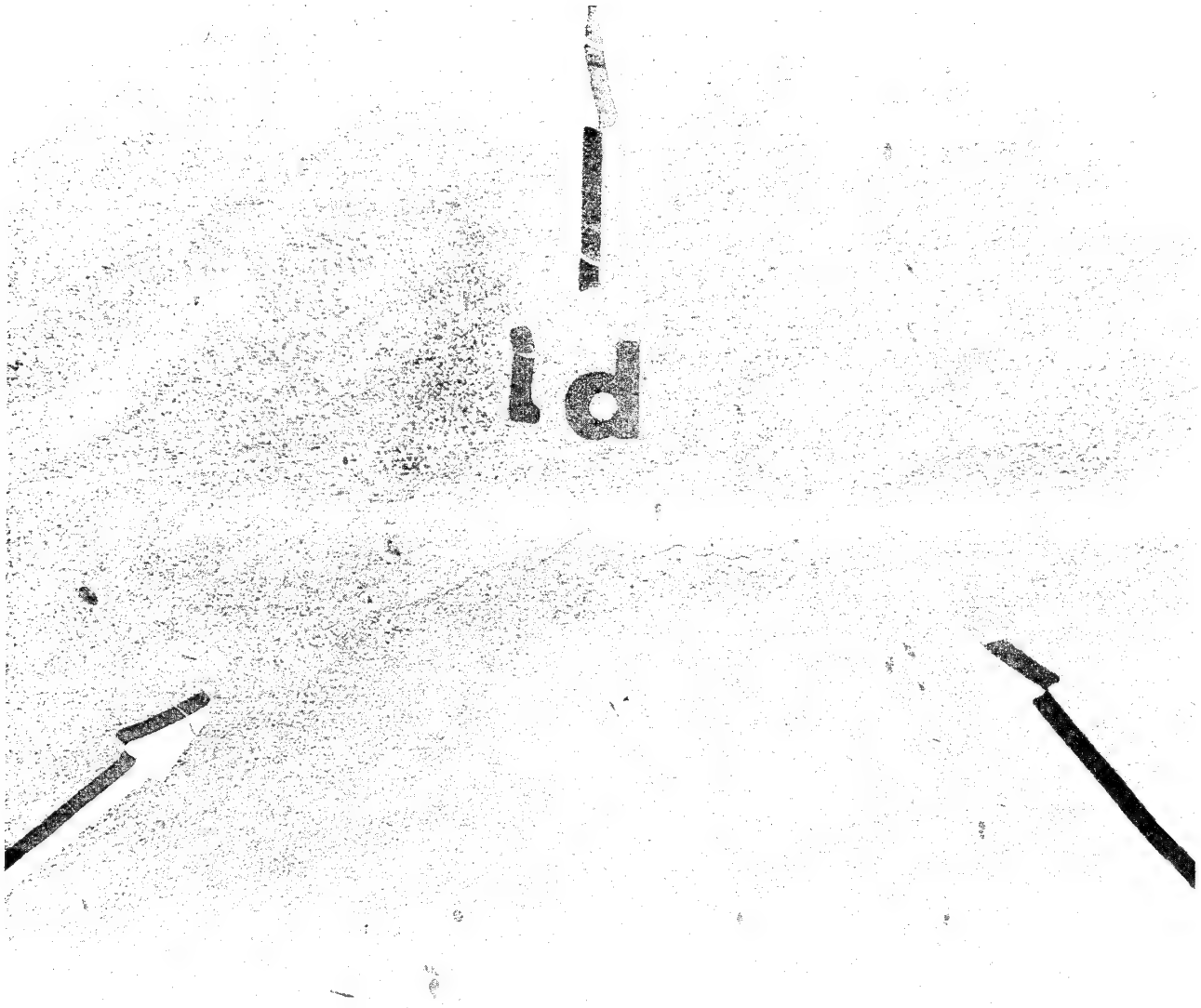

Figure 69 Photomacrograph Showing Fracture of S/N 6 Located on the Exterior of the Dome at Station 59

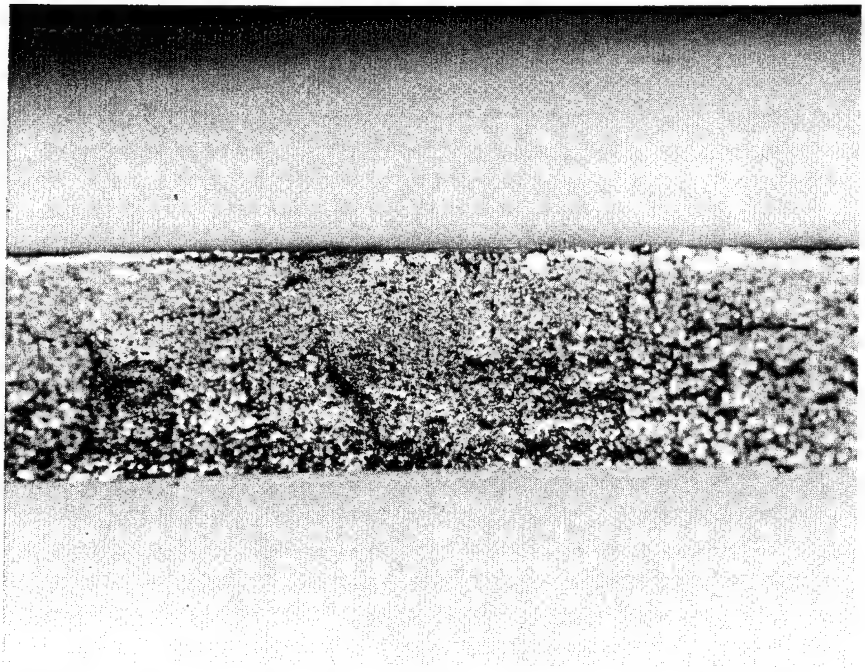

Figure 70 Cross Section of Failure Area on S/N 6 Looking at End of Crack Shown on Figure 67

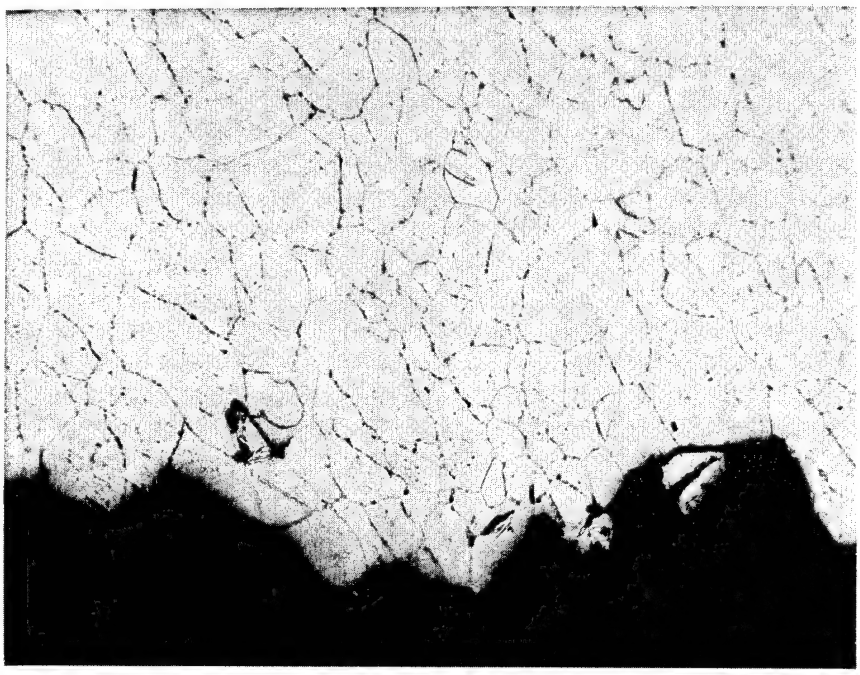

Figure 71 Section of S/N 6 Failure Looking at Edge of Fracture That Follows Grain Boundaries (Magnification, 250X)

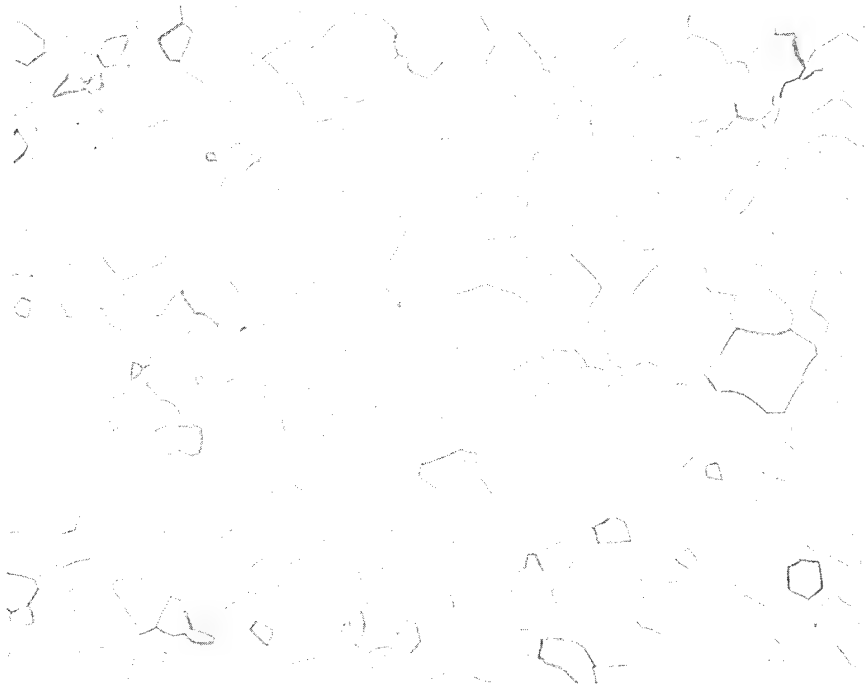

Figure 72 Photomicrograph of Normal "Clean" Microstructure (100X)

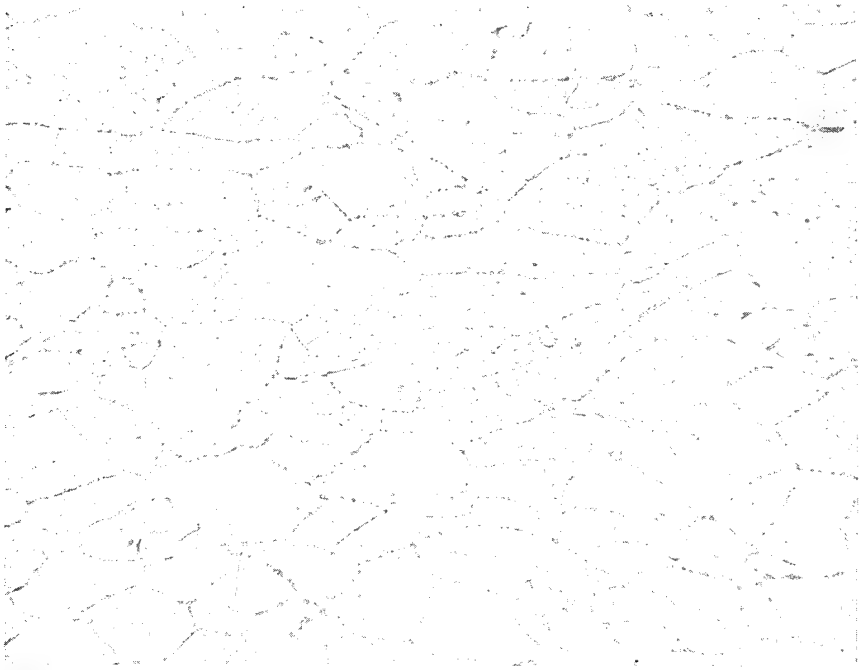

Figure 73 Photomicrograph of the Microstructure Through the Leak Area of S/N 6 (Note the "Dirty" Microstructure and Grain Boundary Precipitant, 250X)

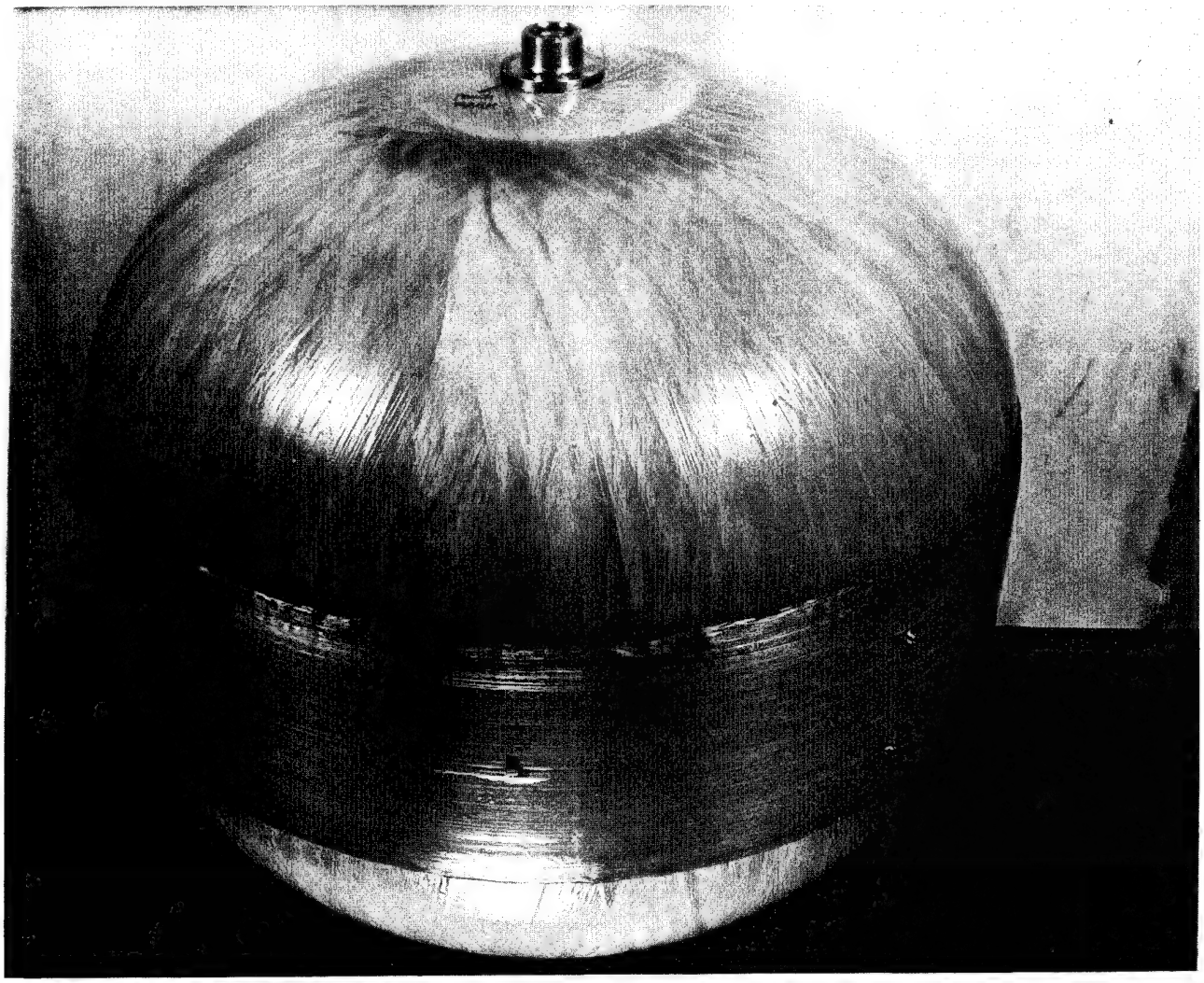

Figure 74 S/N 7 after Failing at 5062 psi (Note the Lack of Fragmentation or Shattering of Overwrap Material)

S/N 8 failed prematurely during hydrostatic sizing at 3432 psig (Fig. 75). The initiation point appeared to be at the dome-to-end fitting joint as indicated in Figure 76 and was due to lack of fusion (Fig. 77).

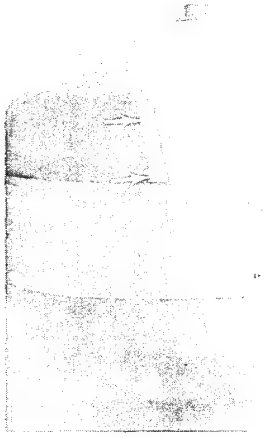

Figure 75 Photograph of Tank S/N 8 Showing the As-Failed Configuration (Arrows Indicate Subsurface Fracture)

Figure 76 Photograph of Tank S/N 8 Showing Exposed Fracture Surface (Arrows Indicate Approximate Origin of Failure)

Figure 77 Photomacrograph of S/N 8 Fracture Surface Showing Lack of Fusion at Dome-to-Fitting Joint

Appendix
Supporting Data

CONTENTS

Engineering Drawings of Tank Liner
and Overwrap

A-5

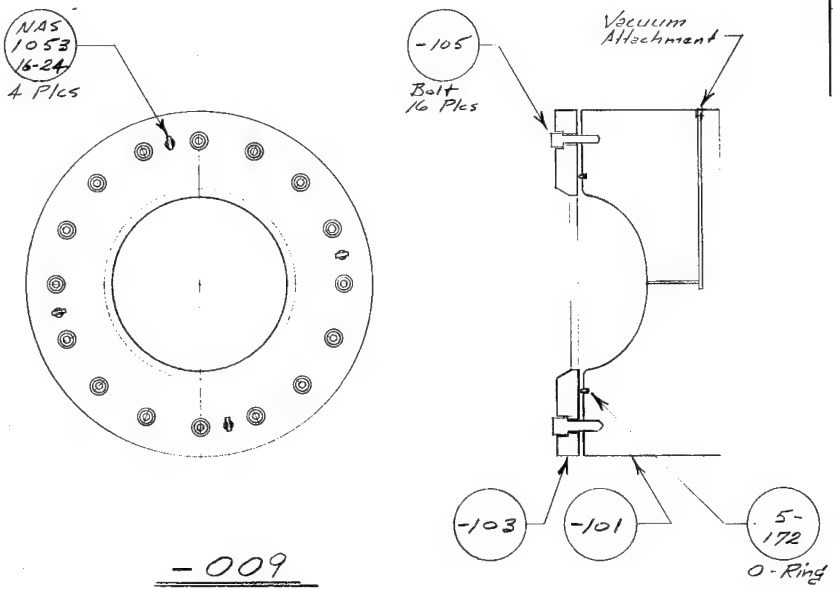

-009

REVISIONS			
SYM	DESCRIPTION	DATE	APPROVED
	Revised w/b	12-22-69	
	Delete Template Reference w/b	1-29-71	

QUANTITY / DASH NO.	PART NO.	ZONE	SER. SYM.	DESCRIPTION	STOCK SIZE	MATERIAL OR VENDOR	ISSUE COND.	MATERIAL SPECIFICATION	FINISH OR MFR. CODE	CHG.
1	5-172			O' Ring	27.485 ID x 0.275					
4	NAS1053-16-24			Eye Bolt						
16	-005			Bolt	1¼-7UNC-2A x 4.00	Steel - Internal Wrench - H.T. 160-180 Min				
	-003			Ring	M/F -03					
	-001			Die	M/F -01					
	-03			Forging - Ring	As Reqd	4340 Steel		A/C Quality		
	-01			Forging - Die	As Reqd	4340 Steel		A/C Quality		
	-009			Die Assy						

LIST OF MATERIAL

EFFECTIVE ON	CALC. WT.	DASH NUMBER	NEXT ASSY	USED ON	FINAL ASSY.	TEST
			APPLICATION		QTY. REQD.	

DIMENSIONING REF. MIL-STD-8
UNLESS OTHERWISE SPECIFIED
DIMENSIONS ARE IN INCHES AND ARE AFTER PLATING
TOLERANCES ON: FRACTIONS ±1/32, DECIMALS X ±1, XX ±.03, XXX ±.010, ANGLES ±1/2°
MACHINED SURFACES 125/
REF. - MIL-STD-10
MIL-1-8500 STATUS
INTERCHANGEABLE
REPLACEABLE
UNCONTROLLED

DRAWN BY w/b DEPT. 1630 DATE 11/20/68
CHECKER R.L.K.
STRESS ENGR.
MFG. ENGR.
MATL. ENGR.
RELIABILITY
QA. ENGR. R.L.K. 2 2 71
PROJECT R.L. Caudill 2/6/71
CONFIGURATION

MARTIN MARIETTA CORPORATION
DENVER DIVISION P.O. BOX 179
DENVER, COLORADO 80201

DIE ASSEMBLY

SIZE	CODE IDENT NO.	
C	04236	FWL-68005
SCALE 1/10		SHEET 1 of 3

FWL-68005-5-1/3

DRAFTING SERVICE GRAPHIC CONTROLS CORPORATION DEN 061808 16-681

RECESS PROFILE COORDINATES

Station	X (+ & -)	Y (-)
1	12.0000	0.0000
2	11.9961	0.1198
3	11.9935	0.2395
4	11.9891	0.3593
5	11.9827	0.4790
6	11.9743	0.5988
7	11.9650	0.7185
8	11.9532	0.8383
9	11.9376	0.9580
10	11.9239	1.0776
11	11.7062	1.1973
12	11.8865	1.3170
13	11.8648	1.4367
14	11.8409	1.5564
15	11.8151	1.6760
16	11.7871	1.7957
17	11.7570	1.9154
18	11.7248	2.0350
19	11.6904	2.1547
20	11.6538	2.2743
21	11.6150	2.3940
22	11.5740	2.5136
23	11.5306	2.6332
24	11.4849	2.7529
25	11.4369	2.8725
26	11.3864	2.9921
27	11.3335	3.1117
28	11.2781	3.2312
29	11.2201	3.3508
30	11.1596	3.4704
35	10.8288	4.0739
40	10.4574	4.6916
48	9.6518	5.6963
* 55	8.6156	6.5629
60	7.5993	7.1800
66	5.9496	7.8312
74	3.5215	8.1968
81	0.0000	8.3945

Origin of X & Y Axes

* Develope Intermediate Station Coordinates Between Sta. 30 and Sta 81 with Automatic Drafting Machine.

Machine Die Cavity to +.030/-.000 Tolerance Meas. Normal to Profile.

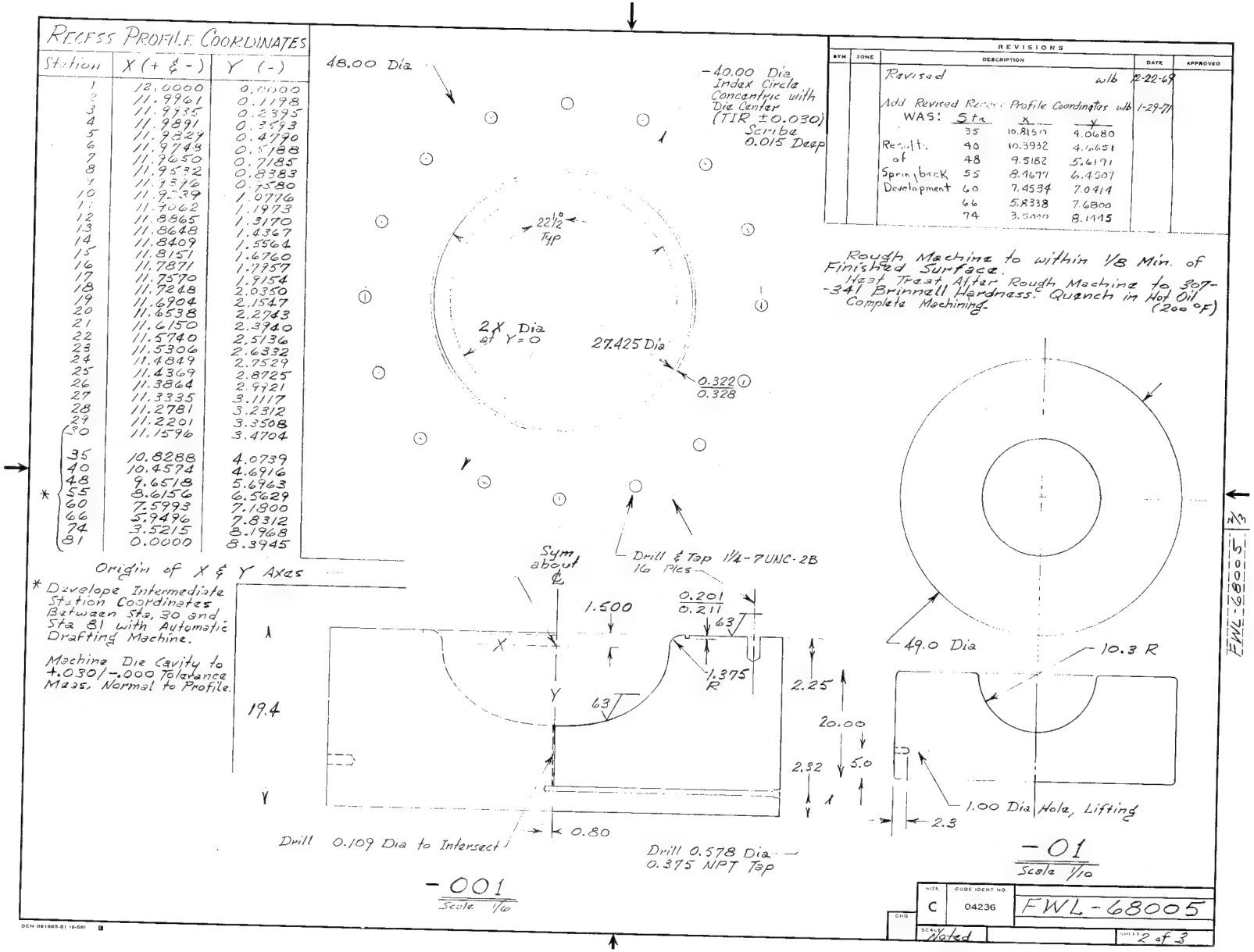

-001
Scale 1/6

-01
Scale 1/10

REVISIONS				
SYM	ZONE	DESCRIPTION	DATE	APPROVED
		Revised wlb	12-22-69	
		Add Revised Recess Profile Coordinates wlb	1-29-71	

WAS:

Sta	X	Y
35	10.8150	4.0680
40	10.3932	4.6651
48	9.5182	5.6191
55	8.4677	6.4507
60	7.4534	7.0914
66	5.8338	7.6800
74	3.5000	8.1115

Rough Machine to within 1/8 Min. of Finished Surface.
Heat Treat After Rough Machine to 307-341 Brinnell Hardness. Quench in Hot Oil (200 °F)
Complete Machining.

FWL-68005 3/3

SIZE	CODE IDENT NO.	
C	04236	FWL-68005
SCALE Noted		SHEET 2 of 3

DCN 081565-01 10-081

A-7

REVISIONS				
SYM	ZONE	DESCRIPTION	DATE	APPROVED

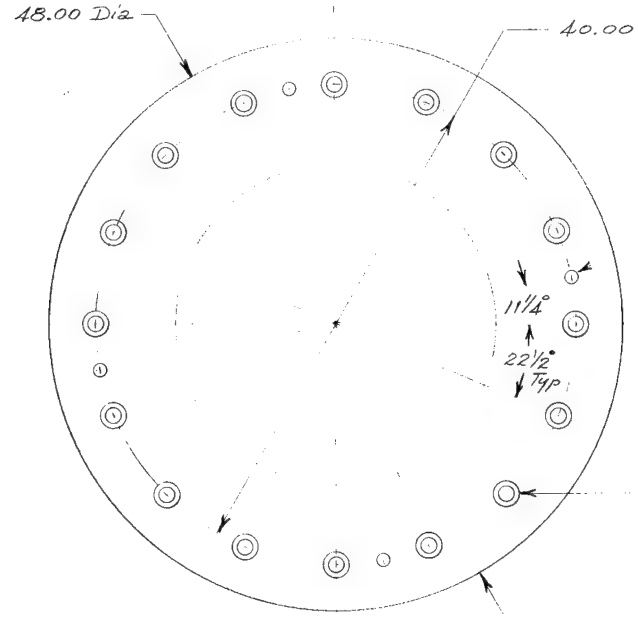

Rough Machine to within ⅛ Min of Finished Surface.
Heat Treat after Rough Machine to 307-341 Brinnell Hardness. Quench in Hot Oil (200°F Min.) Complete Machine.

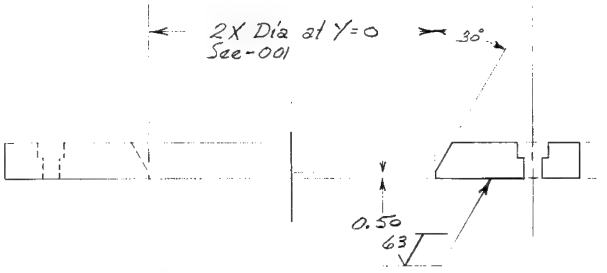

-003
Scale 1/6

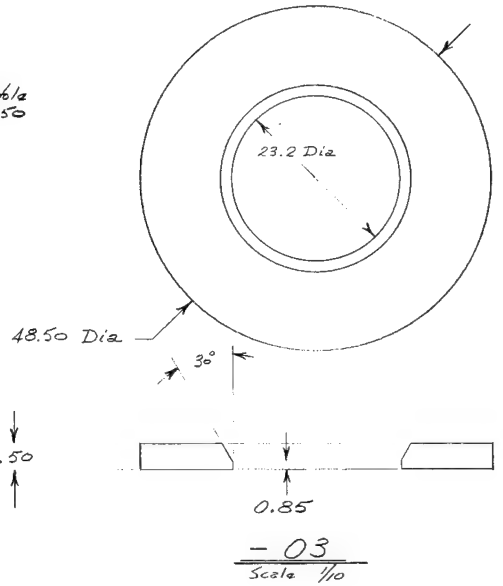

-03
Scale 1/10

FWL-68005 3/3

SIZE	CODE IDENT NO.	
C	04236	FWL-68005
CHG	SCALE Noted	SHEET 3 of 3

DEN 081605-01 10-881

REVISIONS			
SYM	DESCRIPTION	DATE	APPROVED
	Rev Table for 2-Step Liner wlb	11-4-70	
	Revised note 2 and added note 6. Added end item qty. R.K.	1-28-71	

OVERWRAP PROCEDURE

Layer	Hoop Wrap Cyl Length	Polar Wrap No Ribbons	Polar Wrap Ribbon Width	Polar Wrap Wrap Angle	Ends per Inch per Layer	Total Ends per Inch	Weight of Wrap Mat'l, Pounds	Remarks
1 & 2		36	2.1	10° 15'	300	600	3.6	
3 & 4		36	2.1	10° 15'	300	600	3.6	
5 & 6		36	2.1	10° 15'	300	600	3.6	
7 & 8		36	2.1	10° 15'	300	600	3.6	
9 & 10		36	2.1	10° 15'	300	600	3.6	
11-30	5.0				440	8360	6.7	
31	5.0				480	480	0.6	
							25.3	

NOTES:
1. Verify Vessel & Parts Designations and Log. See Marking Note, Sheet 2
2. Weigh Liner (-019) Prior to Wrapping and record in tank log. Weigh vessel (-009) after curing cycle and record in tank log.
3. Overwrapping will be as Specified in above Table and in Accord with NASA-CR-54855
4. Cure Wound Vessel at 150°F for 2 Hours and then at 300°F for 4 Hours in Programer-Controlled Oven, during which Vessel will be Supported in Curing Fixture.
5. Size Vessel by Pressurizing to 4480 psi.
6. Perform internal volume check before and after sizing operation. Record in tank log.

LIST OF MATERIAL

QUANTITY / DASH NO		PART NO	DESCRIPTION	STOCK SIZE	MATERIAL OR VENDOR
X			Roving, Glass, 20 End, S994/HTS Finish Preimpregnated w/ EPON 828/DSA/EMPOL 1040 BDMA (100/115.9/20/1)		
2		-005	End Boss	See Sheet 7	
1		X403, X503	Cylinder Section	M/F X4, X5	
2		X111, X221, X331	Dome	M/F X11, X22, X33	
	1	019	Liner		
019	009	009	Vessel		

DASH NUMBER	NEXT ASSY	USED ON	FINAL ASSY	QTY. REQD.
-009	End Item		8	

DIMENSIONING REF. MIL-STD-8 UNLESS OTHERWISE SPECIFIED. DIMENSIONS ARE IN INCHES AND ARE AFTER PLATING. TOLERANCES ON: FRACTIONS ± 1/32; DECIMALS .X ± .1, .XX ± .03, .XXX ± .010; ANGLES ± 1/2°. MACHINED SURFACES 125 REF. MIL-STD-10. MIL-I-8500 STATUS: INTERCHANGEABLE / REPLACEABLE / UNCONTROLLED

DRAWN BY wlb DEPT. 1630 DATE 1-12-70
CHECKED R.L.K.
STRESS ENGR. [signature] 1630 2/1/71
GR. SUPV. R.L. Kirlin 2-1-71
CUST NMSNTV C.L. Caudill 2/1/71

MARTIN MARIETTA CORPORATION
DENVER DIVISION P.O. BOX 179
DENVER, COLORADO 80201

FIBERGLASS OVERWRAPPED TITANIUM VESSEL

SIZE C | CODE IDENT NO. 04236 | FWL-69002
SCALE — | SHEET 1 of 8

FWL-69002 1/1

DEN 061808 (6-68)

REVISIONS				
SYM	ZONE	DESCRIPTION	DATE	APPROVED

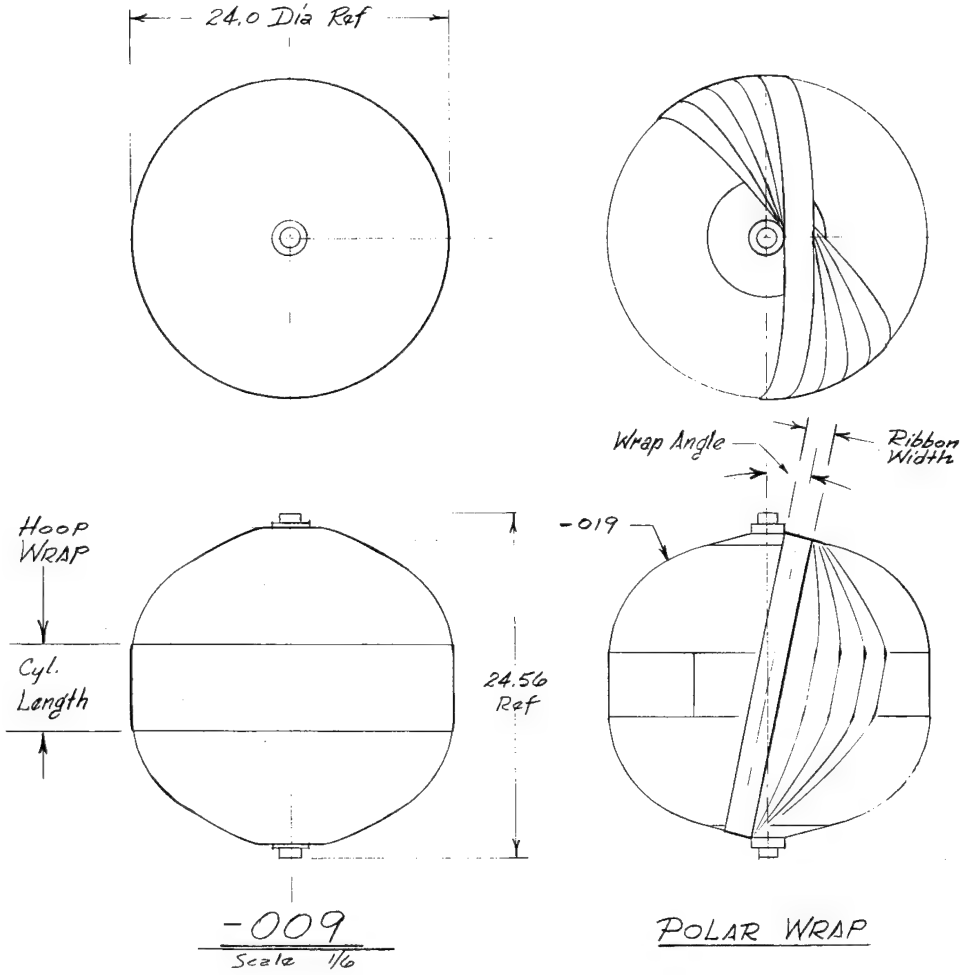

-009
Scale 1/6

POLAR WRAP

GENERAL NOTES:

1. Marking -
Coded Part Numbers are Used to Reflect Material Source and Fabrication Steps of Each Piece of Material.
Piece Tags will be Furnished as Required.
Marking and Remarking of Pieces, Blanks & Parts, and a Log of Fabrication Steps, is Required to Maintain Piece History.

FWL-69002-1 1/2

SIZE	CODE IDENT NO.	
C	04236	FWL-69002
CHG	SCALE Noted	SHEET 2 of 8

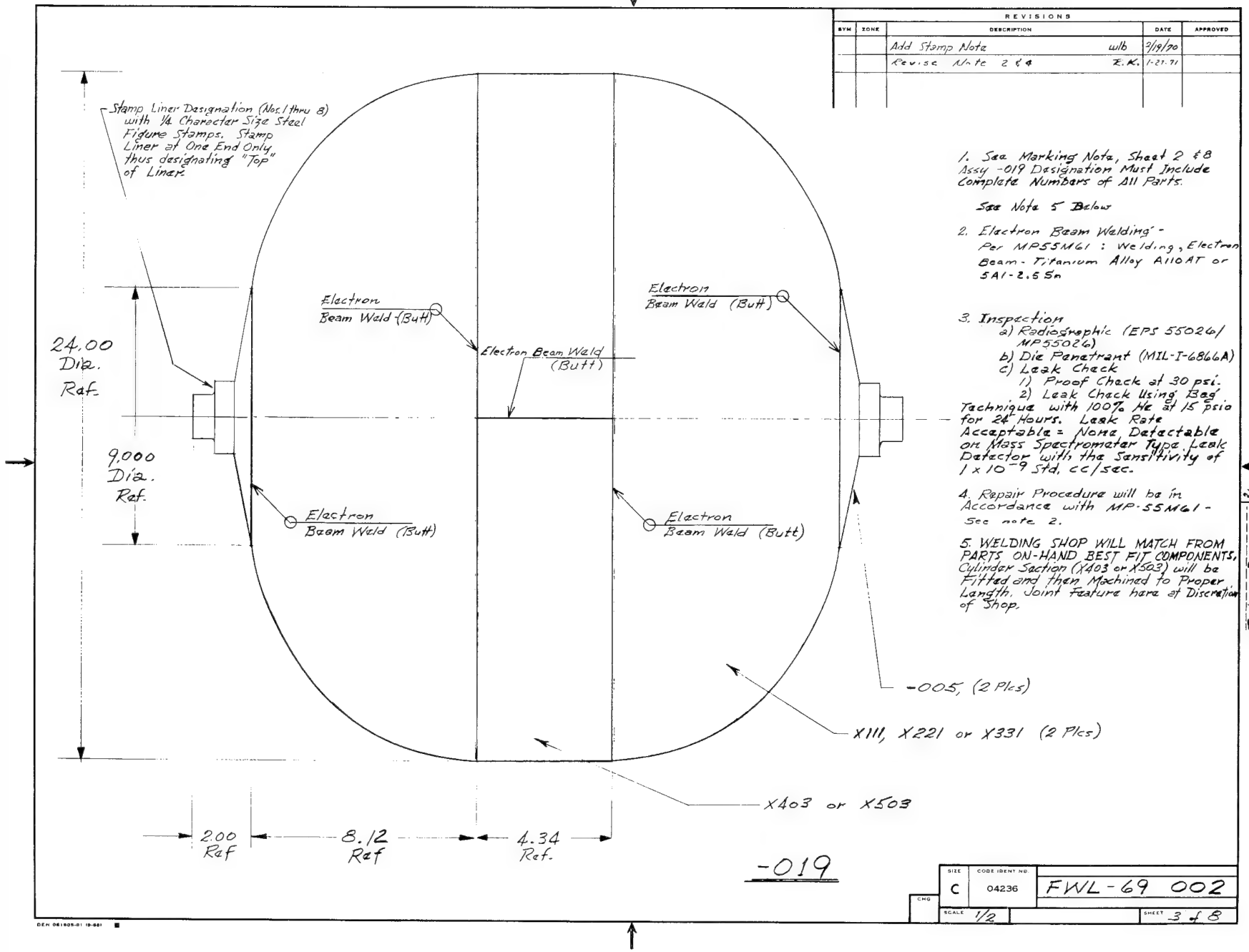

REVISIONS					
SYM	ZONE	DESCRIPTION		DATE	APPROVED
		Add Stamp Note	wlb	2/9/70	
		Revise Note 2 & 4	E.K.	1-27-71	

1. See Marking Note, Sheet 2 & 8 Assy -019 Designation Must Include Complete Numbers of All Parts.

   See Note 5 Below

2. Electron Beam Welding - Per MP55M61 : Welding, Electron Beam - Titanium Alloy A110AT or 5A1-2.5Sn

3. Inspection
   a) Radiographic (EPS 55026/ MP55026)
   b) Die Penetrant (MIL-I-6866A)
   c) Leak Check
      1) Proof Check at 30 psi.
      2) Leak Check Using Bag Technique with 100% He at 15 psia for 24 Hours. Leak Rate Acceptable = None Detectable on Mass Spectrometer Type Leak Detector with the Sensitivity of 1×10^{-9} Std. cc/sec.

4. Repair Procedure will be in Accordance with MP-55M61 - See note 2.

5. WELDING SHOP WILL MATCH FROM PARTS ON-HAND BEST FIT COMPONENTS, Cylinder Section (X403 or X503) will be Fitted and then Machined to Proper Length. Joint Feature here at Discretion of Shop.

FWL-69002 3/9

SIZE	CODE IDENT NO.	FWL-69 002
C	04236	
SCALE 1/2		SHEET 3 of 8

DEN 081805-01 10-681

Upon Delivery of Titanium Dome Mat'l. a Sheet Designation, Represented Here by "X", Will be Marked on Each Sheet. The Fourteen Sheet Designations will be "A, B, C, D, E, F, G, H, K, L, M, N, P, and R."

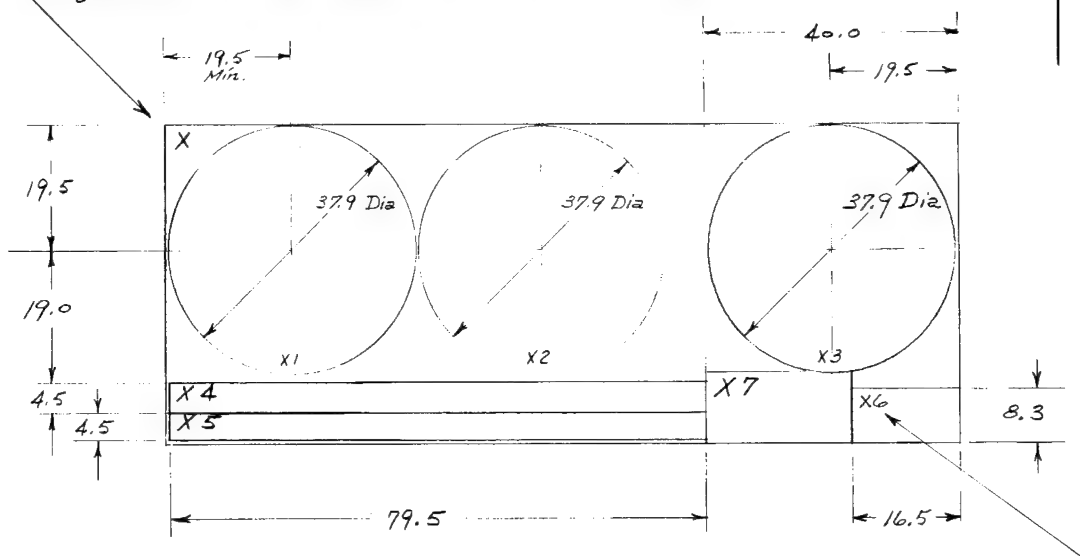

REVISIONS

SYM	DESCRIPTION	DATE	APPROVED
	Revised marking method R.K.	1-27-71	

NOTE:
Prior to Cutting Material Mark Piece Designation on All Resulting Pieces. (Steel Stamp in approx area as shown)

Piece Designation

See FWL-68001 for Parts Using Piece X6.

LIST OF MATERIAL

QUANTITY /	PART NO.	ZONE	SER. SYM	DESCRIPTION	STOCK SIZE	MATERIAL OR VENDOR	ISSUE COND.	MATERIAL SPECIFICATION	FINISH OR MFR. CODE	CHG.
	X			Scrap						
14	X7			Test Mat'l Pc						
14	X6			Test Mat'l						
10	X5			Cyl Sect	48 x 120 x 0.220 +.046 −.010 Stock	5 Al-2.5Sn Ti		(ELI)	Reactive Metals Inc.	
11	X4			Cyl Sect						
14	X3			Dome						
14	X2			Dome						
14	X1			Dome Mat'l Pc						

DIMENSIONING REF. MIL-STD-8
UNLESS OTHERWISE SPECIFIED
DIMENSIONS ARE IN INCHES AND ARE AFTER PLATING
TOLERANCES ON

FRACTIONS	DECIMALS .X	.XX	.XXX	ANGLES
± 1/32	± .1	± .03	± .010	± 1/2°

MACHINED SURFACES REF. MIL-STD-10 125/

MIL-I-8500 STATUS
INTERCHANGEABLE
REPLACEABLE
UNCONTROLLED

DRAWN BY w/b DEPT. 1630 DATE 1-5-70
CHECKER R.L.K.
STRESS ENGR. [signature] 1630 2/1/71
WT. ENGR.
MATL. ENGR.
RELIABILITY
GR. ENGR. R.L. [signature] 2-1-71
PROJECT C.L. Cardell 2/8/71
CUST. APPROVAL

MARTIN MARIETTA CORPORATION
DENVER DIVISION P.O. BOX 179
DENVER, COLORADO 80201

LINER MATERIAL PARTITIONING
FIBERGLASS OVERWRAPPED TITANIUM VESSEL

SIZE C | CODE IDENT NO. 04236 | FWL-69002
SCALE 1/12 | SHEET 4 of 8

EFFECTIVE ON | CALC. WT. | DASH NUMBER | NEXT ASSY | USED ON | APPLICATION | FINAL ASSY. | TEST | QTY. REQD.

FWL-69002 4/4

DEN 081808 (6-68)

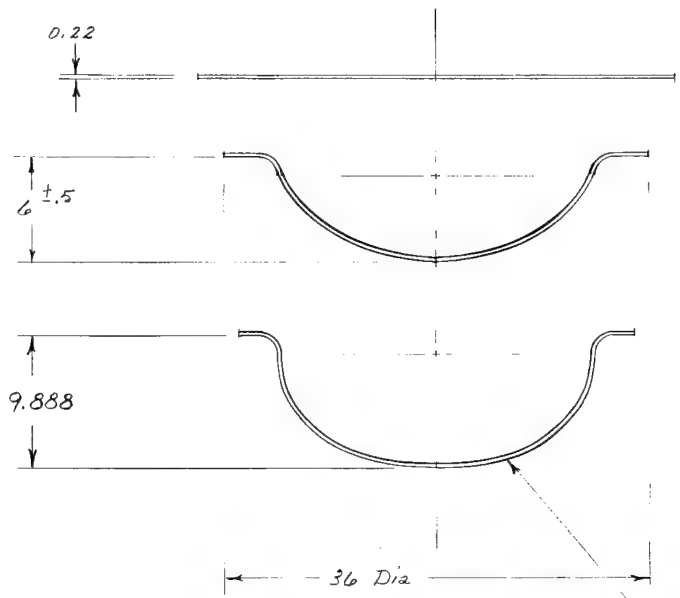

X11, X22, X33

Sequence Steps

Step	No.
Blank, X1, X2, X3 - Start	
Clean per EPS 50063 Method IIA Except No Vapor Degrease Process	1
Chem-mill .005 to .010	2
Explosive Form	3
Clean - Step 1	4
Turco Pretreat	5
Anneal	6
Clean - Step 1	7
Chem-mill .005 to .010	8
Explosive Form	9
Repeat Explosive Forming if Req	10
Clean - Step 1	11
Turco Pretreat	12
Anneal	13
Clean - Step 1	14
Chem-mill .005 to .010	15

Exterior Shape per Template Blank FWL-69005-009
Tolerance: +.030/-.010 from Profile on Template.

REVISIONS

SYM	DESCRIPTION	DATE	APPROVED
	Rev Sequence Steps & Notes wlb	10-6-70	

Die:
Explosive Forming Die per FWL-68005-009

Annealing =
Heat Domes in Air Furnace to 1500 °F ±20° F and Hold Parts at Temperature for One Hour ± 5 Minutes.
Air Cool with All Surfaces Equally Exposed to Air Atmosphere. Provide Copy of Furnace Record For QC verification & enter in dome log.

FWL-69002 5/8

LIST OF MATERIAL

QUANTITY / DASH NO.	PART NO	ZONE	SER SYM	DESCRIPTION	STOCK SIZE	MATERIAL OR VENDOR	ISSUE COND.	MATERIAL SPECIFICATION	FINISH OR MFR. CODE	CHG.
	X33			Annealed Explosive Formed Dome	M/F X3	5Al-2.5Sn Ti		(ELI)		
	X22				M/F X2					
	X11				M/F X1					

DIMENSIONING REF. MIL-STD-8
UNLESS OTHERWISE SPECIFIED
DIMENSIONS ARE IN INCHES AND ARE AFTER PLATING
TOLERANCES ON-

FRACTIONS	DECIMALS .X	.XX	.XXX	ANGLES
± 1/32	± .1	± .03	± .010	± 1/2°

MACHINED SURFACES REF - MIL-STD-10 ✓

MIL-I-8500 STATUS: INTERCHANGEABLE / REPLACEABLE / UNCONTROLLED

		DEPT.	DATE
DRAWN BY	wlb	1630	1-6-70
CHECKER	R.L.K.		
STRESS ENGR.	[illegible] 11 30		1/4/71
WT. ENGR.			
MATL ENGR.			
RELIABILITY			
GR. ENGR.	R L Kihn		2-1-71
PROJECT	C L Candill		2/7/71
CUST. AGENCY			

MARTIN MARIETTA CORPORATION
DENVER DIVISION P.O. BOX 179
DENVER, COLORADO 80201

EXPLOSIVE FORMING & ANNEALING SEQUENCE
FIBERGLASS OVERWRAPPED TITANIUM VESSEL

SIZE C | CODE IDENT NO. 04236 | FWL - 69002
SCALE 1/6 | SHEET 5 of 8

CALC. WT. | DASH NUMBER | NEXT ASSY | USED ON | FINAL ASSY. | TEST | APPLICATION | QTY. REQD. | EFFECTIVE ON

GRAPHIC CONTROLS CORPORATION DEN 061605 (6-68)

REVISIONS				
SYM	ZONE	DESCRIPTION	DATE	APPROVED
A		Revised Dome Thickness with Sta 59 was 60, 6 was 10 (chem-mill sta)	7/14/70 B-14	
B		Added Details B, C, D, E & F		
C		Added Notes 1 thru 5 R.K.	1-28-71	

Notes:
1. Chem mill X11, X22, X33 to thickness as shown in Section A-A
2. Trim domes .125 oversize (Height dimension)
3. Clean domes per EPS 50063, Method II A, and apply Everlube T-50 scale inhibitor.
4. Assemble domes to sizing die and hot size at 1250° ± 25°F for 30 minutes min. & air cool.
5. Remove inhibitor and final machine domes to X11, X221, X331 configuration.

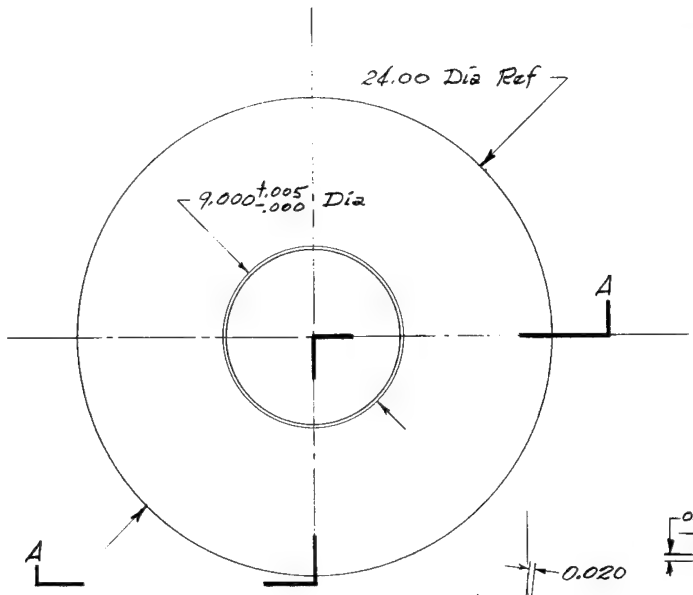

X111, X221, X331
Scale: 1/4

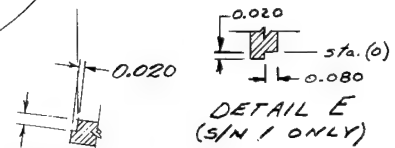

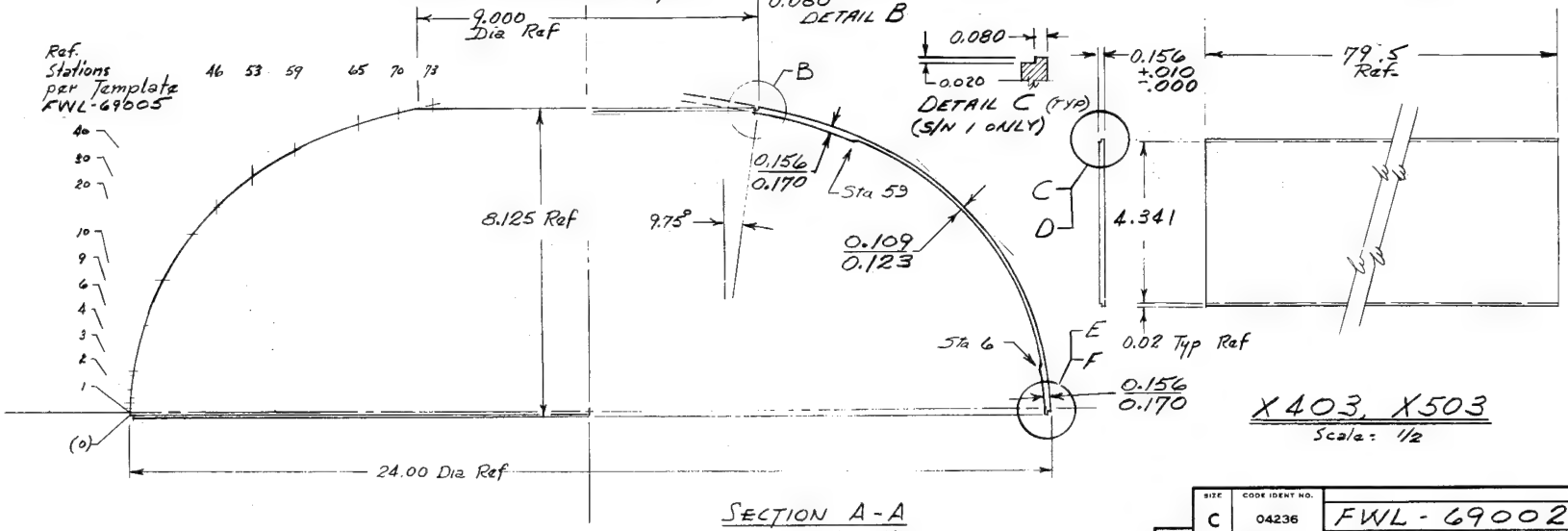

SECTION A-A
Scale: 1/2

X403, X503
Scale: 1/2

FWL-69002 6/4

SIZE	CODE IDENT NO.	
C	04236	FWL - 69002
CHG B	SCALE Noted	SHEET 6 of 8

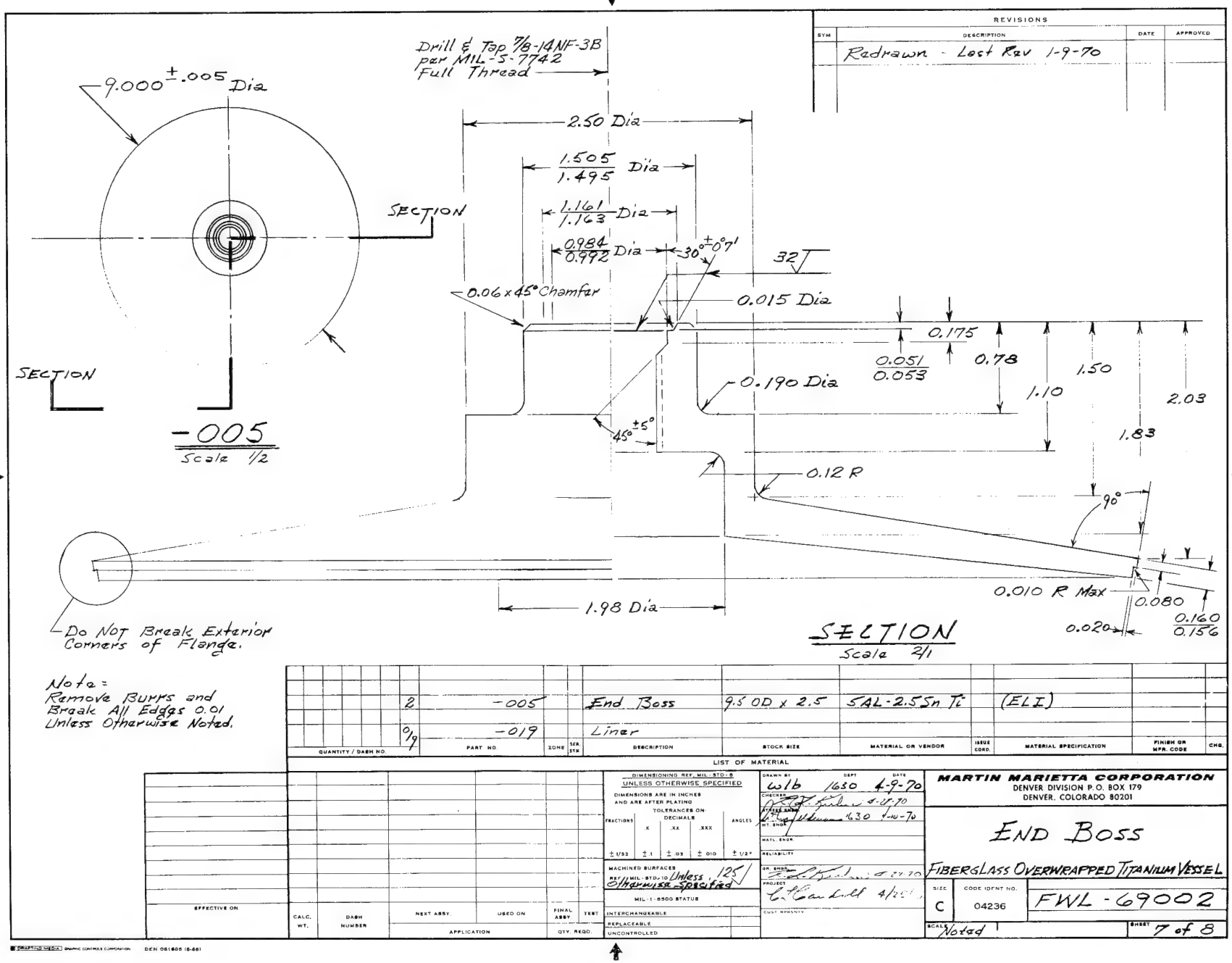

REVISIONS

SYM	DESCRIPTION	DATE	APPROVED
	Redrawn - Last Rev 1-9-70		

Note =
Remove Burrs and Break All Edges 0.01 Unless Otherwise Noted.

LIST OF MATERIAL

QUANTITY / DASH NO.	PART NO.	ZONE	SER. SYM	DESCRIPTION	STOCK SIZE	MATERIAL OR VENDOR	ISSUE COND.	MATERIAL SPECIFICATION	FINISH OR MFR. CODE	CHG.
2	-005			End Boss	9.5 OD x 2.5	5AL-2.5Sn Ti		(ELI)		
0/9	-019			Liner						

EFFECTIVE ON | CALC. WT. | DASH NUMBER | NEXT ASSY. | USED ON | FINAL ASSY. | TEST | APPLICATION | QTY. REQD.

DIMENSIONING REF. MIL-STD-8
UNLESS OTHERWISE SPECIFIED
DIMENSIONS ARE IN INCHES AND ARE AFTER PLATING
TOLERANCES ON DECIMALS: FRACTIONS ±1/32; X ±.1; .XX ±.03; .XXX ±.010; ANGLES ±1/2°
MACHINED SURFACES REF MIL-STD-10 Unless Otherwise Specified 125
MIL-1-8500 STATUS
INTERCHANGEABLE
REPLACEABLE
UNCONTROLLED

DRAWN BY wlb DEPT 1630 DATE 4-9-70
CHECKED 4-17-70
STRESS ANAL. 4-30 4-10-70
WT. ENGR.
MATL. ENGR.
RELIABILITY
QR. ENGR. 4-24-70
PROJECT 4/25
CUST. APPROVAL

MARTIN MARIETTA CORPORATION
DENVER DIVISION P.O. BOX 179
DENVER, COLORADO 80201

END BOSS

FIBERGLASS OVERWRAPPED TITANIUM VESSEL

SIZE C | CODE IDENT NO. 04236 | FWL-69002

SCALE Noted | SHEET 7 of 8

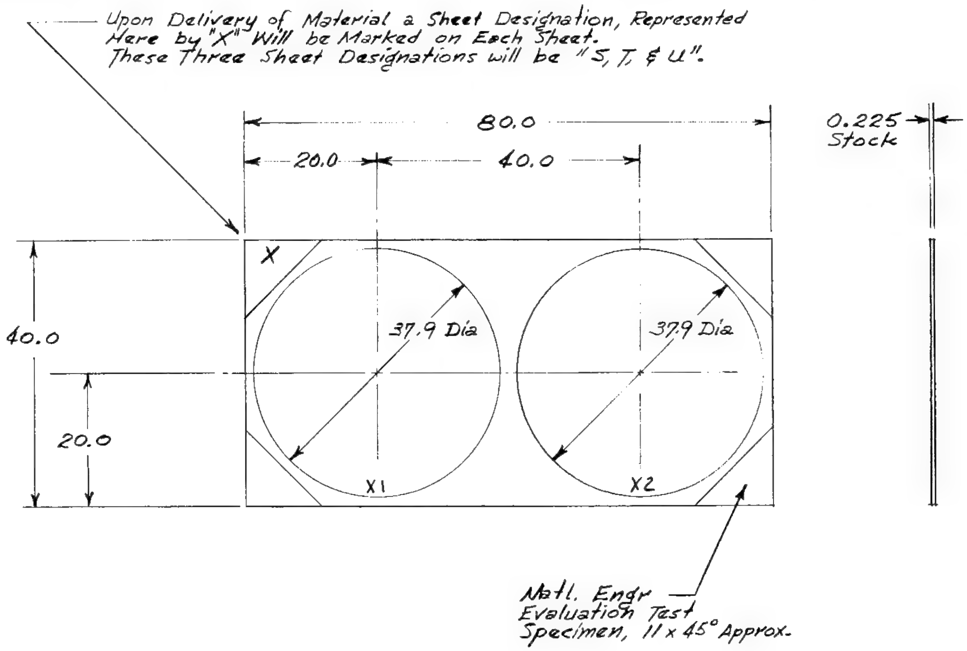

NOTE:
Prior to Cutting Material Mark Piece Designation on All Resulting Pieces - Steel Stamp in approx area as shown.

REVISIONS

SYM	ZONE	DESCRIPTION	DATE	APPROVED

LIST OF MATERIAL

QUANTITY/DASH NO.	PART NO.	ZONE	SER SYM	DESCRIPTION	STOCK SIZE	MATERIAL OR VENDOR	ISSUE COND	MATERIAL SPECIFICATION	FINISH OR MFR CODE	CHG
3	X 2			Dome Matl Pc	40 x 80 x	5 Al-2.5 Sn Ti		ELI Grade		
3	X 1			Dome Matl Pc	.220 +.040 -.010 Stock	5 Al-2.5 Sn Ti		ELI Grade		

ODD DASH NO. SHOWN — EVEN DASH NO. OPP

DIMENSIONING REF MIL-STD-8
UNLESS OTHERWISE SPECIFIED
DIMENSIONS ARE IN INCHES AND ARE AFTER PLATING
TOLERANCES ON:

FRACTIONS	DECIMALS .X	.XX	.XXX	ANGLES
± 1/32	± .1	± .03	± .010	± 1/2°

MACHINED SURFACES 125/
REF: - MIL - STD - 10

MIL - 1 - 8500 STATUS
INTERCHANGEABLE
REPLACEABLE
UNCONTROLLED

CALC WT	DASH NUMBER	NEXT ASSY	USED ON	FINAL ASSY	TEST
		APPLICATION		QTY REQD	

EFFECTIVE ON

DRAWN BY wlb DEPT 1630 DATE 10-7-70
CHECKER R. L. K.
STRESS ENGR [illegible] 1/30 2/1/71
WT ENGR
MATL ENGR
RELIABILITY
ENGINEER [illegible] 2-1-71
PROJECT
CUST APPROVAL C L Caudill 2/1/71

MARTIN MARIETTA CORPORATION
POST OFFICE BOX 179, DENVER, COLORADO

LINER MATERIAL PARTITIONING
FIBERGLASS OVERWRAPPED TITANIUM VESSEL

SIZE C — CODE IDENT NO. 04236 — FWL - 69002
SCALE 1/12 — SHEET 8 of 8

DEN 061008 (6-69)

PROFILE COORDINATES

Sta. Ref.	X (±)	Y (+)	Sta. Ref.	X (±)	Y (+)	Sta. Ref.	X (±)	Y (+)
1	12.0000	0.0	28	11.2781	3.2312	55	8.4677	6.4509
2	11.9961	0.1198	29	11.2201	3.3508	56	8.2869	6.5694
3	11.9935	0.2395	30	11.1596	3.4704	57	8.0963	6.6877
4	11.9891	0.3593	31	11.0963	3.5899	58	7.8947	6.8058
5	11.9829	0.4790	32	11.0303	3.7095	59	7.6809	6.9237
6	11.9748	0.5988	33	10.9614	3.8290	60	7.4534	7.0414
7	11.9650	0.7185	34	10.8897	3.9485	61	7.2101	7.1587
8	11.9532	0.8383	35	10.8150	4.0680	62	6.9487	7.2757
9	11.9396	0.9580	36	10.7372	4.1875	63	6.6659	7.3922
10	11.9239	1.0776	37	10.6562	4.3069	64	6.3577	7.5080
11	11.9062	1.1973	38	10.5720	4.4263	65	6.0180	7.6230
12	11.8865	1.3170	39	10.4844	4.5458	66	5.8338	7.6800
13	11.8648	1.4367	40	10.3932	4.6651	67	5.6383	7.7366
14	11.8409	1.5564	41	10.2984	4.7845	68	5.4297	7.7927
15	11.8151	1.6760	42	10.1999	4.9038	69	5.2055	7.8481
16	11.7871	1.7957	43	10.0973	5.0231	70	4.9629	7.9027
17	11.7570	1.9154	44	9.9906	5.1424	71	4.6973	7.9561
18	11.7248	2.0350	45	9.8796	5.2616	72	4.4028	8.0078
19	11.6904	2.1547	46	9.7640	5.3808	73-a	4.0701	8.0568
20	11.6538	2.2743	47	9.6436	5.5000	b	3.5	8.153
21	11.6150	2.3940	48	9.5182	5.6191	c	3.0	8.208
22	11.5740	2.5136	49	9.3874	5.7382	d	2.5	8.263
23	11.5306	2.6332	50	9.2509	5.8571	e	2.0	8.308
24	11.4849	2.7529	51	9.1083	5.9761	f	1.5	8.343
25	11.4369	2.8725	52	8.9592	6.0949	g	1.0	8.368
26	11.3864	2.9921	53	8.8032	6.2137	h	0.5	8.383
27	11.3335	3.1117	54	8.6395	6.3324	i	0.0	8.388
0	12.000	-0.105						

REVISIONS

SYM	DESCRIPTION		DATE	APPROVED
A	Rev Sta №1	wlb	12-23-69	
	[illegible]			

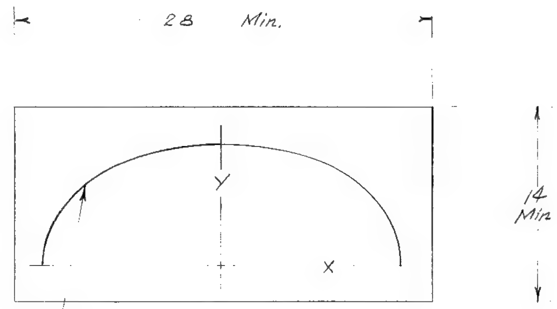

Profile Master to be Produced by Listed Coordinates in Automatic Drafting Machine
Print Profile Photochemically on Blank.

-009
4 Req.

FWL - 69005

QUANTITY / DASH NO	PART NO	ZONE	SER SYM	DESCRIPTION	STOCK SIZE	MATERIAL OR VENDOR	ISSUE COND.	MATERIAL SPECIFICATION	FINISH OR MFR. CODE	CHG.
	-009			Template Blank	1/4 Plate	Alum Alloy				

LIST OF MATERIAL

DIMENSIONING REF. MIL-STD-8
UNLESS OTHERWISE SPECIFIED
DIMENSIONS ARE IN INCHES AND ARE AFTER PLATING
TOLERANCES ON: FRACTIONS ± 1/32; DECIMALS .X ± .1, .XX ± .03, .XXX ± .010; ANGLES ± 1/2°
MACHINED SURFACES REF. MIL-STD-10 ✓
MIL-I-8500 STATUS: INTERCHANGEABLE / REPLACEABLE / UNCONTROLLED

DRAWN BY wlb DEPT 1630 DATE 12-19-69
CHECKER R.L.K. A.11.
STRESS ENGR. [illegible]
GR ENGR [illegible] 2-2-11
PROJECT [illegible]

MARTIN MARIETTA CORPORATION
DENVER DIVISION P.O. BOX 179
DENVER, COLORADO 80201

TEMPLATE BLANK
EXPLOSIVE FORMING DIE
FIBERGLASS OVERWRAPPED TITANIUM VESSEL

SIZE C | CODE IDENT NO 04236 | FWL - 69005
SCALE None | SHEET 1 of 1

EFFECTIVE ON | CALC. WT. | DASH NUMBER | NEXT ASSY. | USED ON | APPLICATION | FINAL ASSY. | TEST | QTY. REQD.

DEN 061605 (6-68)

Analysis to Support Design
Revision to Employ Chemical Milling

ANALYSIS TO SUPPORT DESIGN REVISION TO EMPLOY CHEMICAL MILLING

Figures showing head shapes, thicknesses, and stresses for two liner thickness variation schemes are included here. The method of analysis and computer program used to obtain these results are given in the interim report.* The major difference in the schemes is in the smaller thickness value and the locations at which thicknesses are changed. These results are plotted like those of the interim report and are directly comparable.

A third head shape is included for comparison. It was taken from the interim report and is labeled "continuously varying liner thickness." It shows that the three head shapes are only slightly different. Weights, volumes, and some critical stresses are given in the attached table for the three schemes. It shows that the two-step 0.156, 0.120 inch scheme is only 2.73 pounds heavier than the continuously varying scheme of the interim report.

SUMMARY

	Continuously Varying Liner Thickness*	2-Step 0.156 - 0.109	2-Step 0.156 - 0.120
Liner Thickness in Cylinder, in.	0.156	0.156	0.156
Design Pressure, psi	5,600.0	5,600.0	5,600.0
Vessel Contained Volume, $in.^3$	7,223.0	7,232.0	7,142.0
Vessel Weight, lb	62.43	61.82	65.16
Maximum Filament Stress, psi	375,000.0	367,000.0	345,000.0
Maximum Liner Stress in Head after Sizing, psi	-89,200.0	-116,000.0	-81,000.0
Liner Stress in Cylinder after Sizing, psi	-89,000.0	-89,000.0	-89,000.0

Composite Overwrapped Metallic Tanks, Interim Report, NASA CR-72756, October 1971.

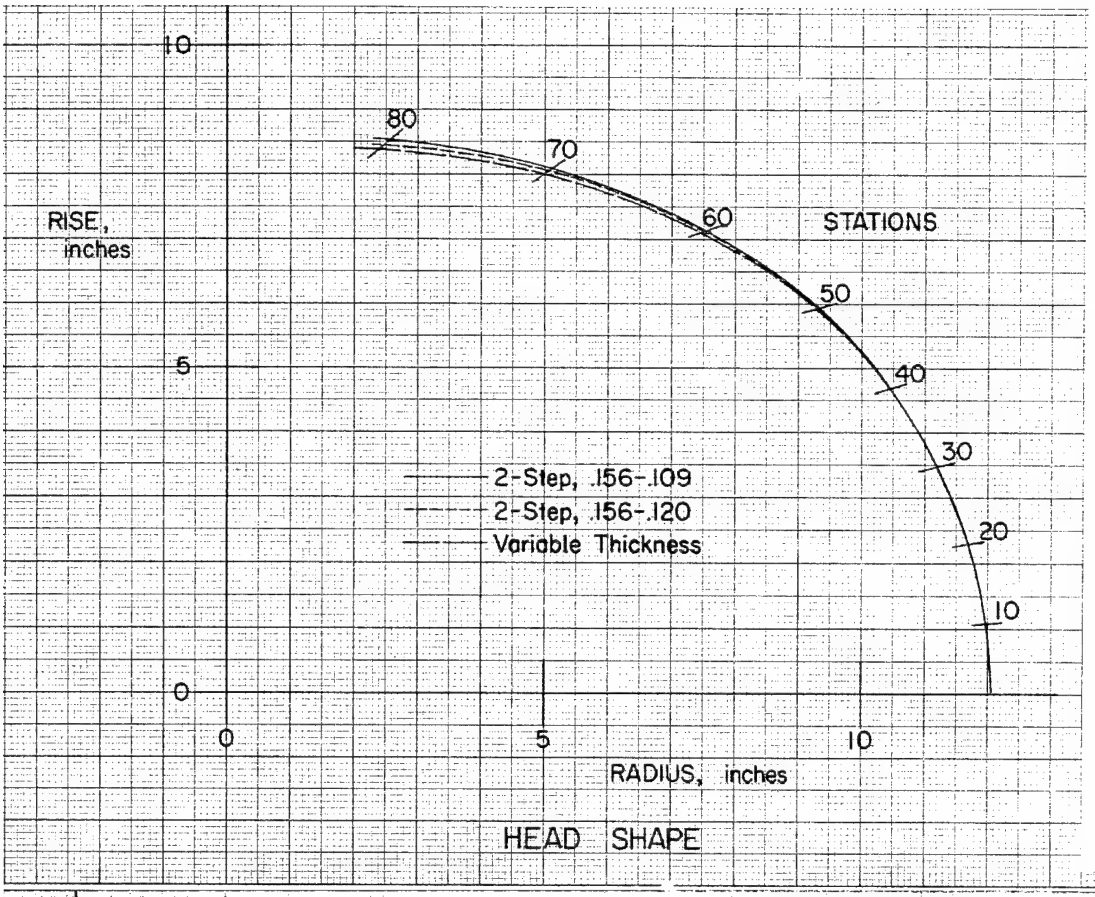

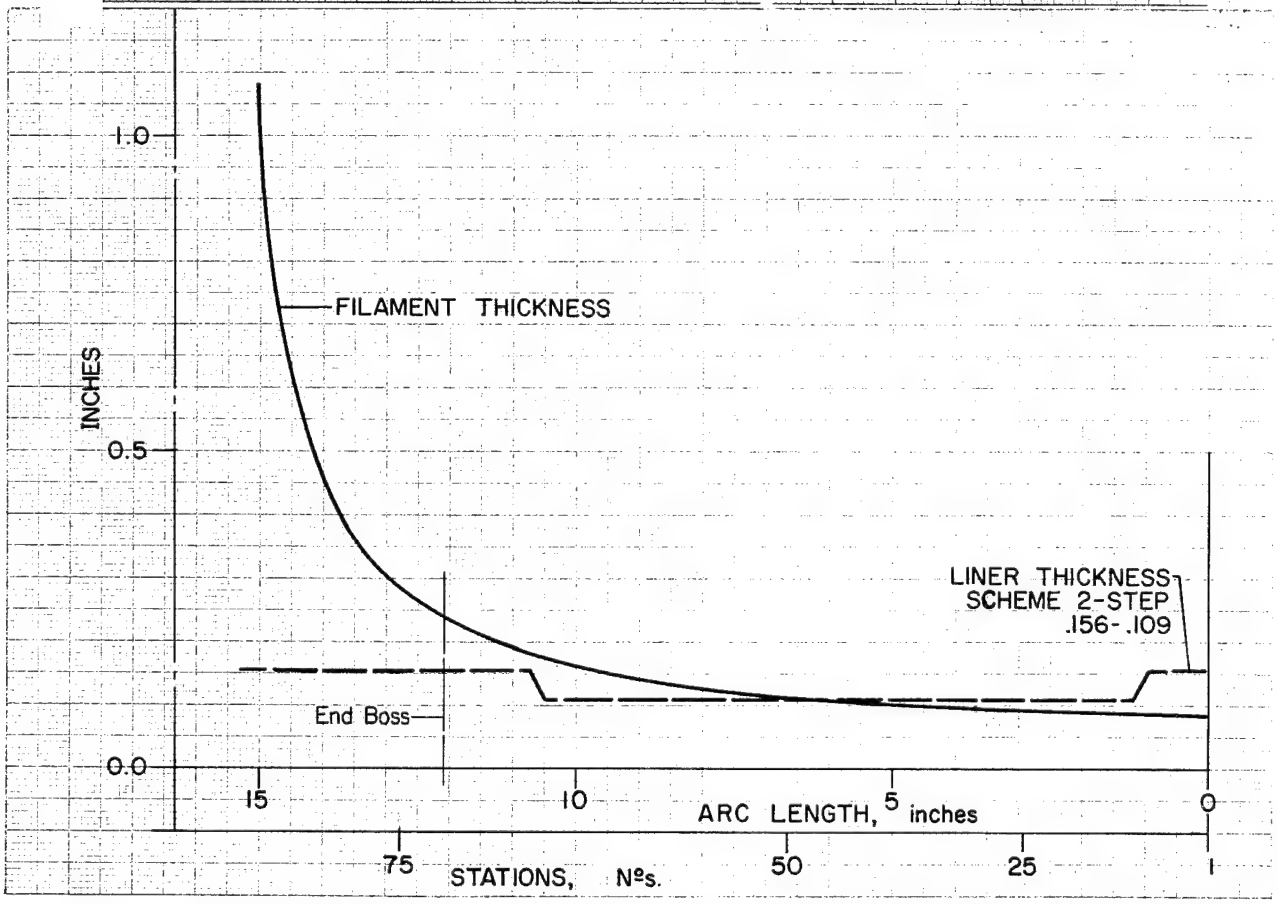

Liner and Filament Thickness

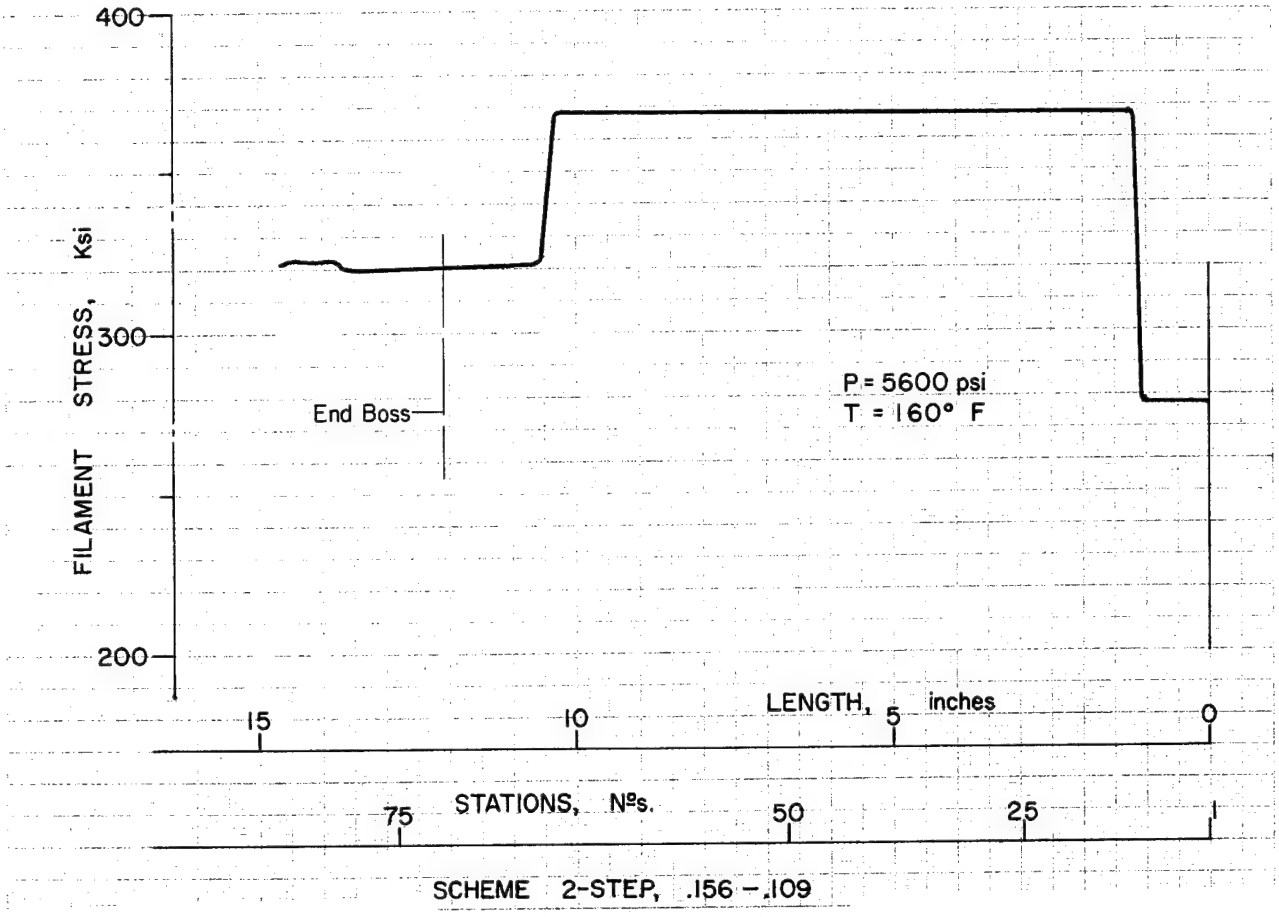

SCHEME 2-STEP, .156 – .109

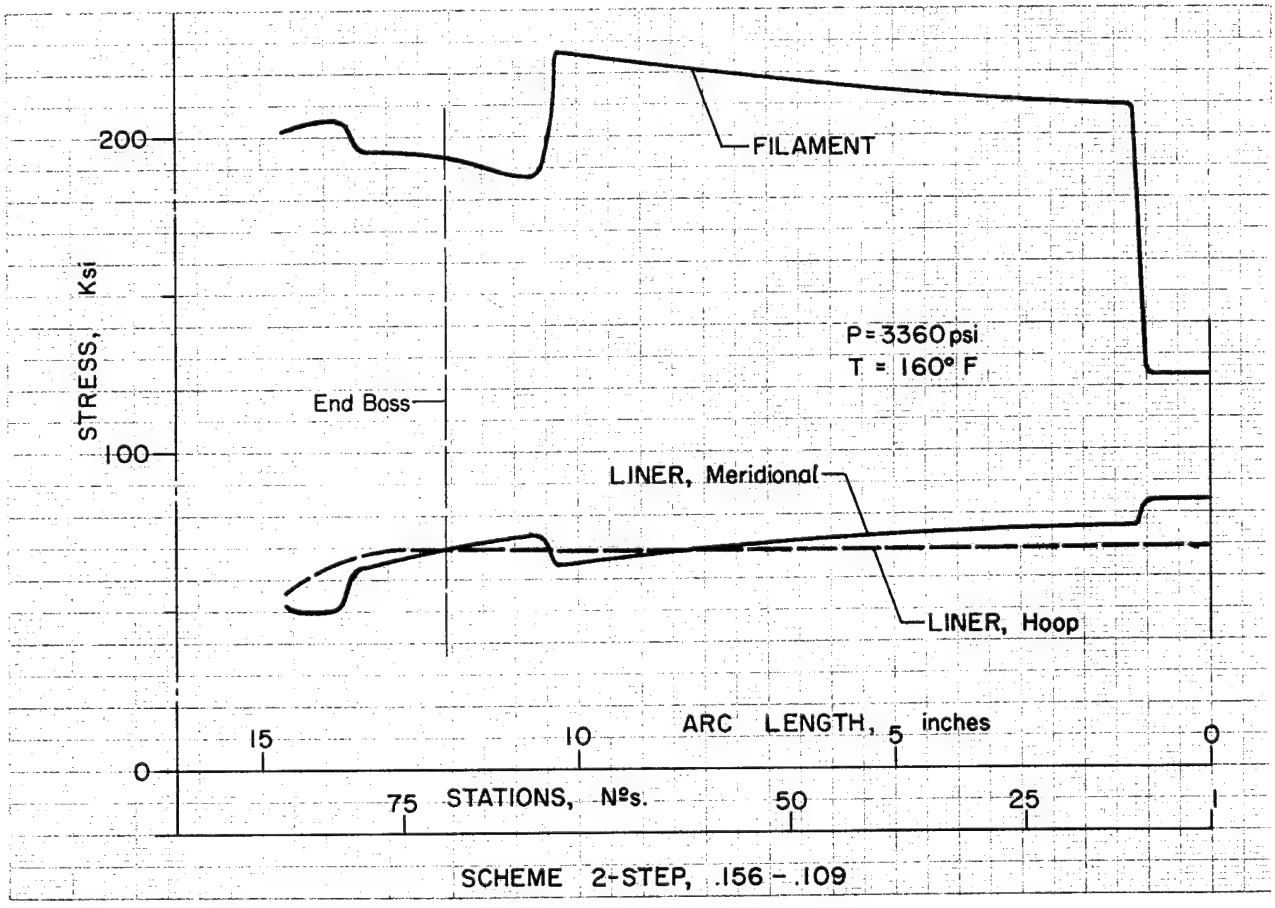

SCHEME 2-STEP, .156 – .109

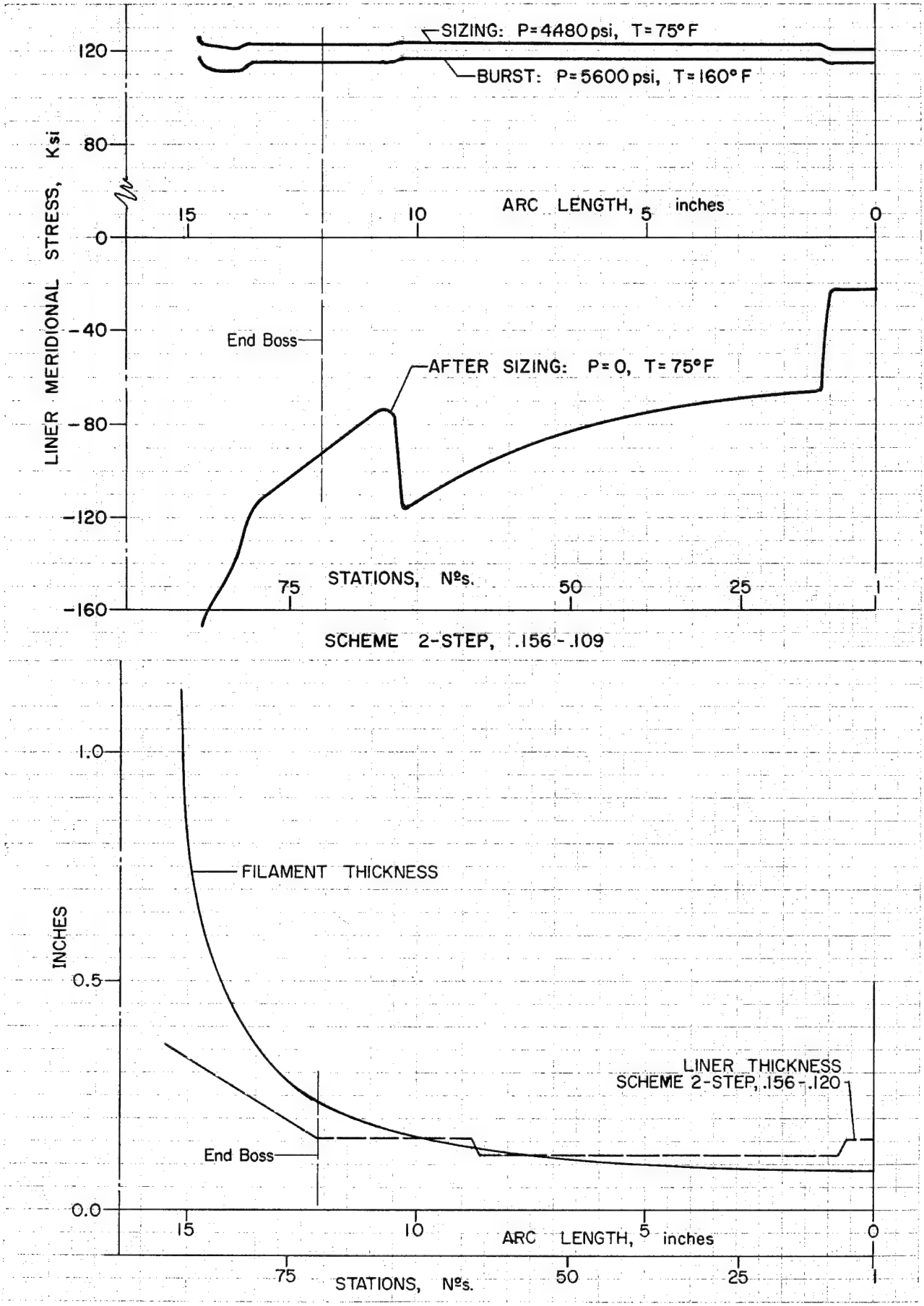

Liner and Filament Thickness

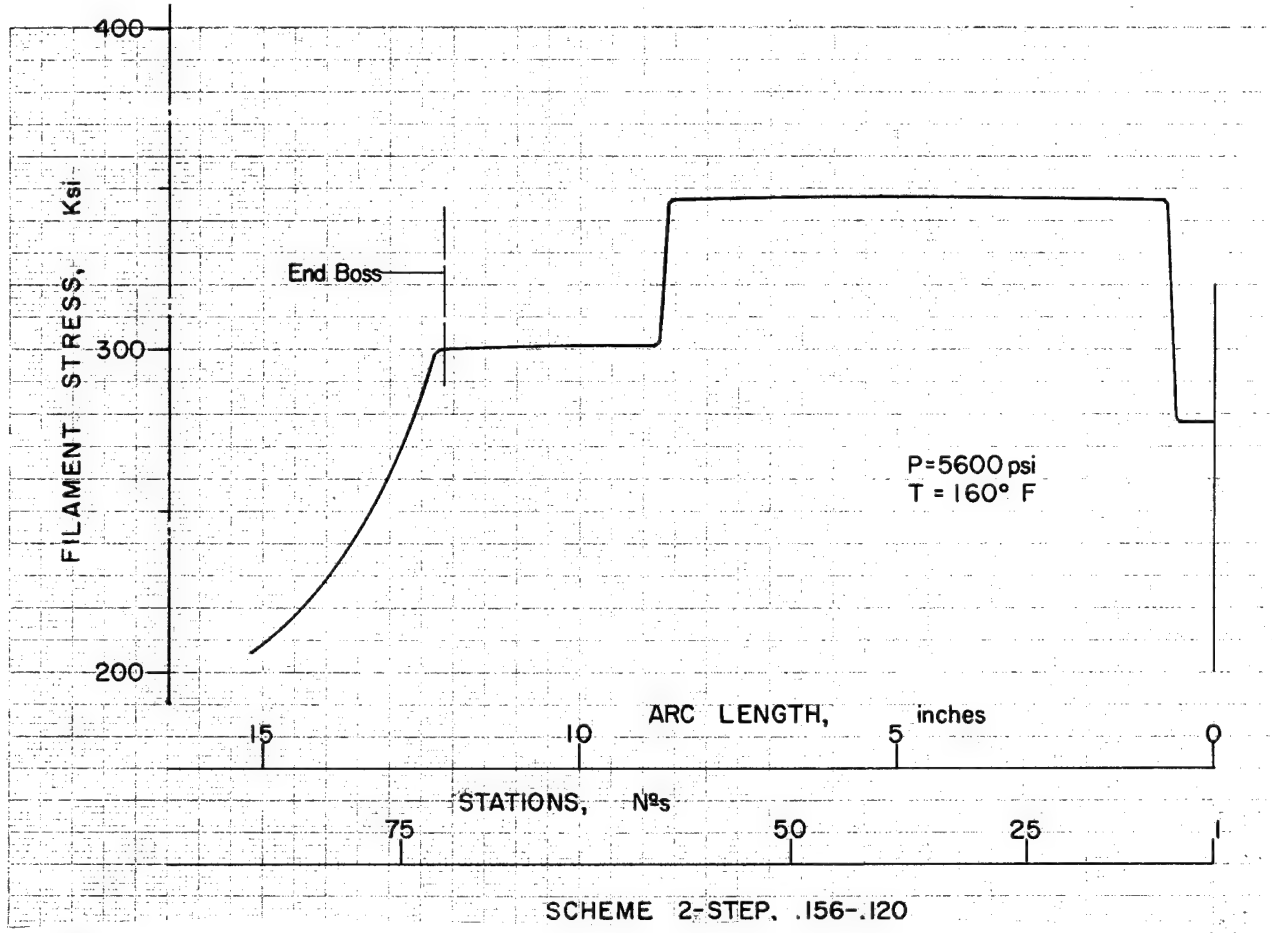

SCHEME 2-STEP, .156-.120

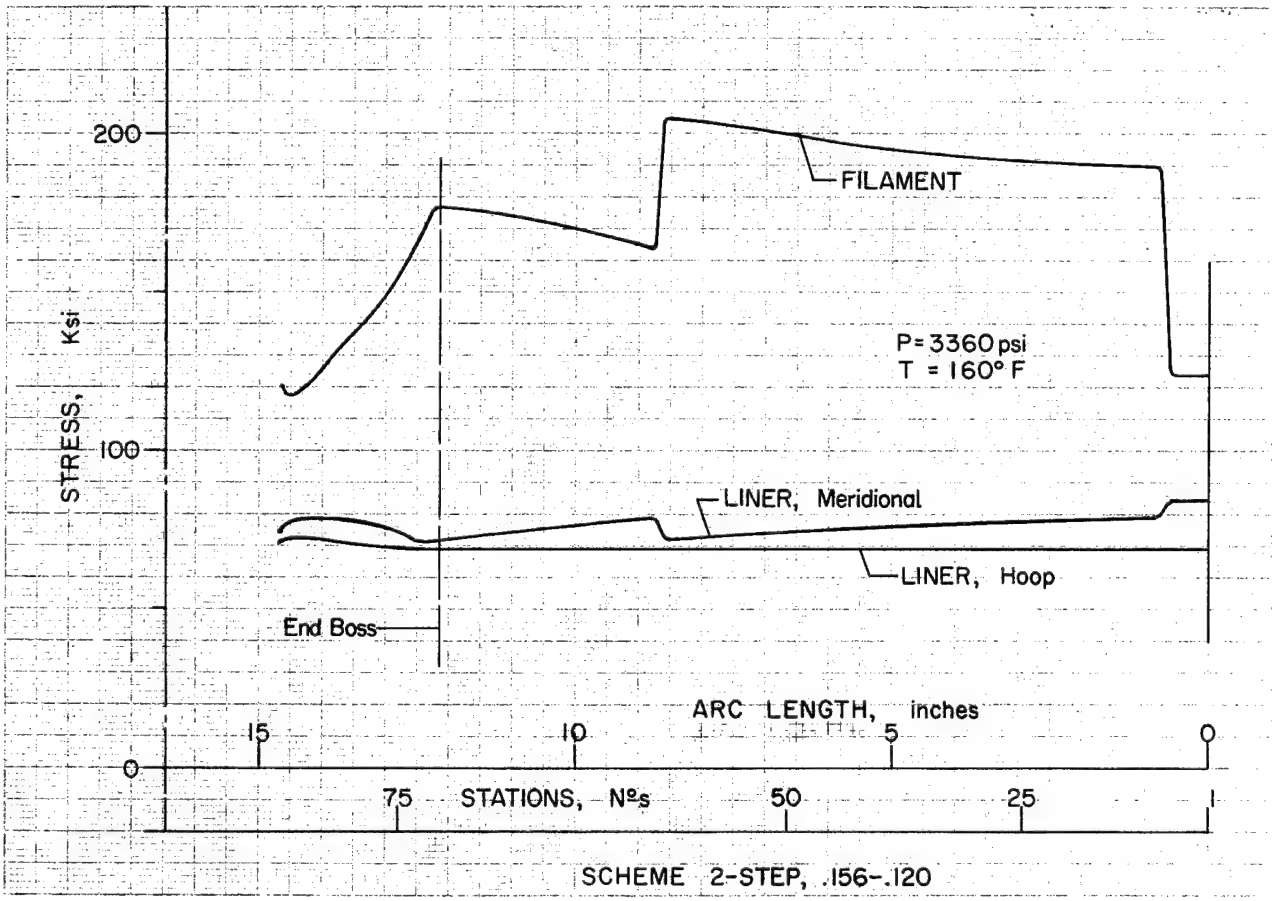

SCHEME 2-STEP, .156-.120

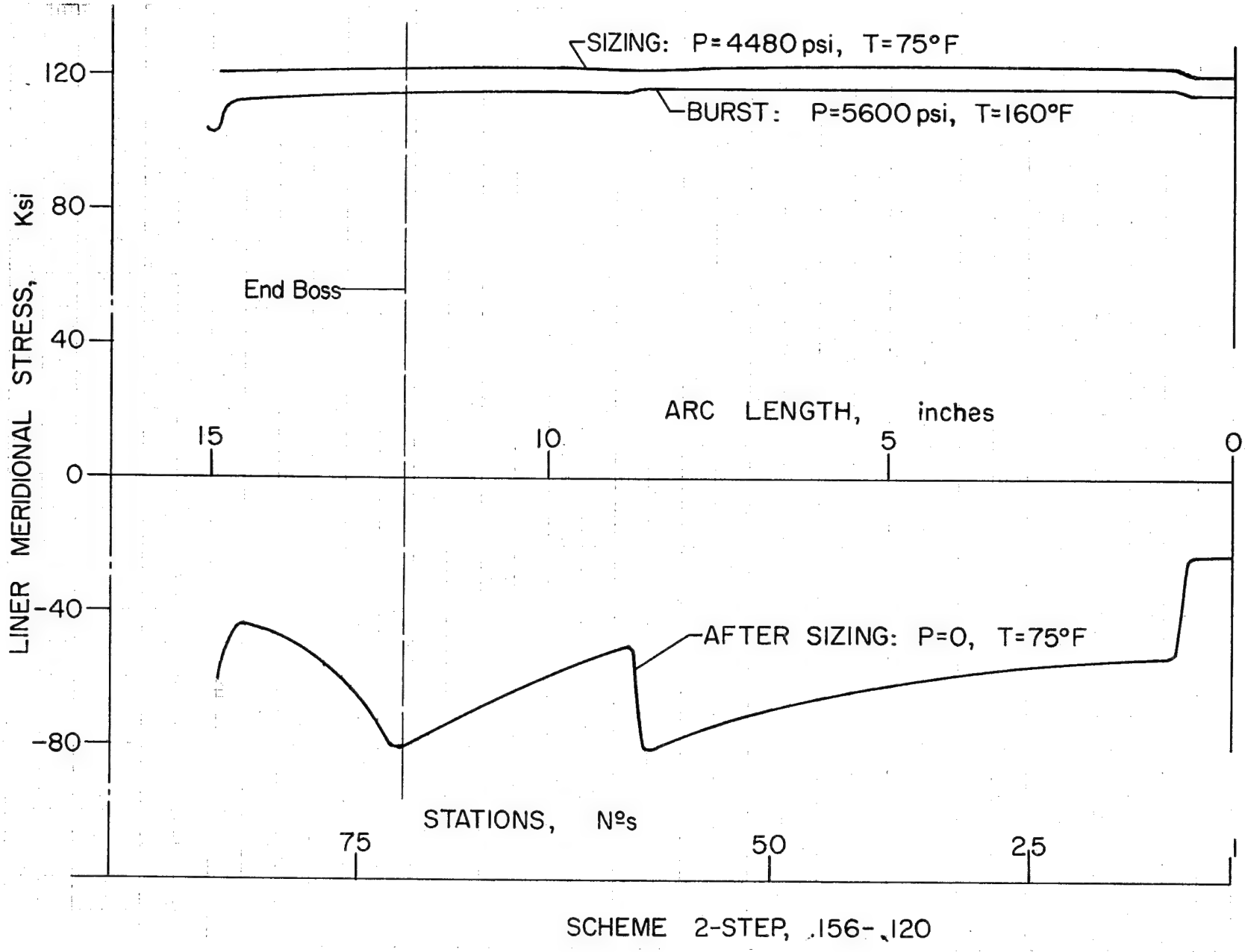
SIZING: P=4480 psi, T=75°F
BURST: P=5600 psi, T=160°F
120
80
40
0
-40
-80
LINER MERIDIONAL STRESS, Ksi
End Boss
ARC LENGTH, inches
15
10
5
0
AFTER SIZING: P=0, T=75°F
STATIONS, Nºs
75
50
25
1
SCHEME 2-STEP, .156-.120

Failure Analysis of Titanium Domes
That Cracked during Explosive-Forming
Development Phase

(February and March 1970)

FAILURE ANALYSIS OF TITANIUM DOMES THAT CRACKED DURING EXPLOSIVE-FORMING DEVELOPMENT PHASE (FEBRUARY AND MARCH 1970)

INTRODUCTION

Two titanium domes (5Aℓ-2.5Sn) fabricated by explosive forming for NASA Contract NAS3-12023, along with strips of the as-received material, were received in the laboratory for investigation.

OBJECT

The object of the investigation was to determine cause of failure and to recommend a fix for the problem.

CONCLUSION

The as-received material was not properly annealed as supported by microstructural analysis.

RECOMMENDATIONS

Anneal all raw material at 1650°F for 4 hours in a vacuum and furnace-cool. Do not use any domes that have been formed without this annealing cycle from the start because of possible induced microcracks.

PROCEDURE

The origins of failure in each of the two failed domes were determined by the following procedures:

1) Specimens taken from near the origin of failure were microexamined for stabilized alpha contamination on the surface. Interstitial contamination was determined by making microhardness measurements;

2) The procedure in 1) was repeated on specimens taken from the unformed as-received plate sections representing a failed dome and a good dome.

The as-received plate representing one failed dome and one good dome was chemically analyzed. This analysis was compared with that of the vendor.

Several specimens in the as-received condition were chem-milled and machine milled. These specimens were mechanically tested in the longitudinal, long transverse, and 45° directions for:

1) Fast strain rate (approximately 1 in./in./minute);

2) Normal strain rate (0.005 in./in./minute).

The anneal cycle was determined as follows:

1) Three specimens each were annealed for 1 hour at each of the following temperatures--1300, 1400, 1450, 1500, 1550, 1600, and 1650°F. All specimens were microexamined and mechanically tested in the same direction;

2) At highest elongation and lowest yield strength, three specimens each were annealed for 1, 2, 4, 8, and 24 hours. All specimens were microexamined and mechanically tested in the same direction as in 1).

RESULTS

Microexamination of cross sections taken from the failed ares of the two domes C-2 and D-3 revealed no evidence of alpha scale. The microstructure was predominantly hot-rolled-textured (Fig. 1). Several areas of crosshatch cracking were observed in the microstructure near the failed areas (Fig. 2).

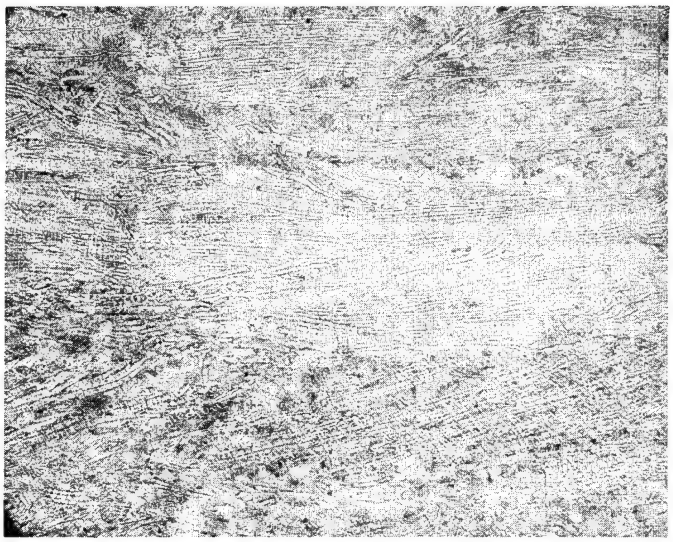

Figure 1 Photomicrograph of Cross Section at 100X from Failure Area of Dome C-2 Showing Hot-Roll Texture

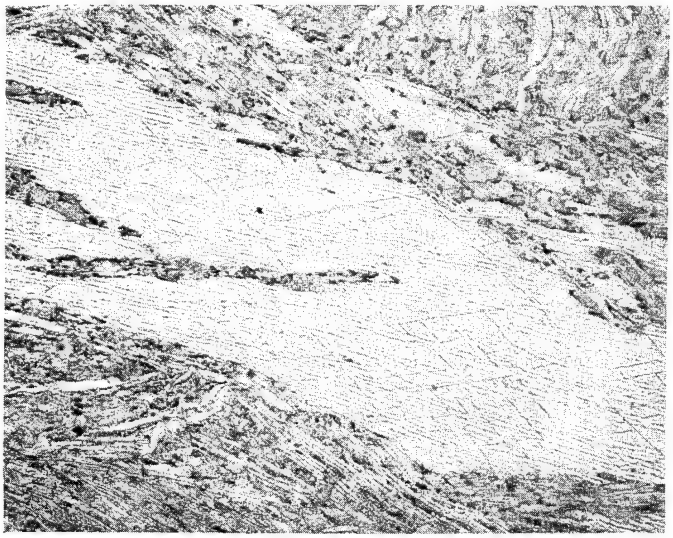

Figure 2 Photomicrograph of Cross Section at 100X from Failure Area of Dome D-3 Showing Crosshatch Cracking

Microexamination of a cross section taken from the as-received plate used for the failed domes revealed no evidence of alpha scale. The microstructure was similar to that in the dome failed areas without the areas of crosshatch cracking (Fig. 3). The structure did not appear to be annealed.

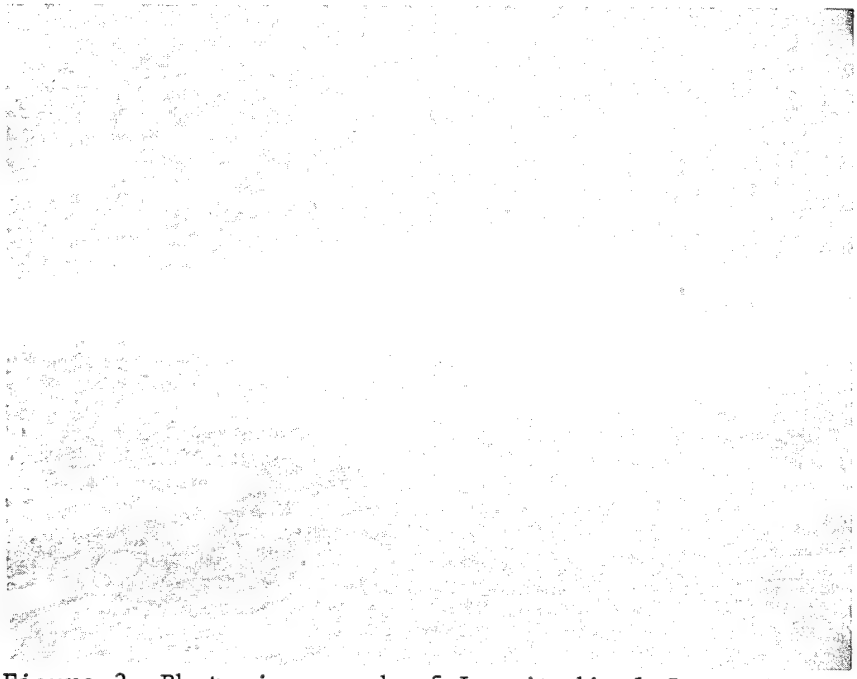

Figure 3 Photomicrograph of Longitudinal Cross Section at 100X of As-Received "C" Plate

The chemical analysis reported by the vendor and the analysis made by Martin Marietta of samples from the as-received plate are tabulated.

ELEMENT	VENDOR	MARTIN MARIETTA
Aℓ, %	5.2	5.34, 6.43, 5.39, 5.86
SN, %	2.6	2.71, 2.68, 2.65, 2.66
H, ppm	81	83, 79, 71, 93
O, ppm	1090	565, 556, 448, 649
N, ppm	120	431, 262, 304, 335

Although the Martin Marietta analysis showed some differences from the analysis of the vendor, it showed the material to be in the range of 5Aℓ-2.5SN alloy and no excessive amount of interstitial content was observed.

Tukon microhardness tests run on cross sections of the C dome and C dome as-received material showed no significant differences in hardness at the edge and the hardness in the center. However, the hardness was inconsistent throughout the cross section indicating that the material was significantly nonhomogeneous.

The averaged* tension test results reported by the vendor and the Martin Marietta tension test results are compared in the following tabulation.

	Ftu, ksi	Fty, ksi	%e, 2 in.
TRANSVERSE, MARTIN MARIETTA	128.5	125.4	15.0
VENDOR	126.1	120.9	12.5 (1500°F for 1/2 hr)
VENDOR	125.0	115.0	14.0 (1500°F for 1/4 hr)
LONGITUDINAL, MARTIN MARIETTA	127.9	121.8	17.5
VENDOR	122.8	111.6	14.0 (1500°F for 1/2 hr)
VENDOR	127.5	112.0	14.5 (1500°F for 1/4 hr)

*All Martin Marietta averaged data are from three test points.

These test results show a considerable difference in the yield strength between the Martin Marietta and vendor data, with the Martin Marietta results showing a higher value than the vendor results.

The following is a comparison of the Martin Marietta averaged* tension test results on the as-received plate material and the as-received plus chem-milled both sides.

TRANSVERSE LONGITUDINAL 45°	Ftu, ksi	Fty, ksi	%e, 2 in.
As-Received	128.5	125.4	15.0
0.005 in./minute	127.9	121.8	17.5
Strain Rate	121.9	117.3	16.0
As-Received	135.0	--	12.5
>1 in./minute	132.1	--	14.7
Strain Rate	123.8	--	16.3
Chem-Milled	128.7	123.2	11.1
0.005 in./minute	128.6	121.7	12.8
Strain Rate	121.7	117.0	15.7
Chem-Milled	134.7	--	10.9
>1 in./minute	135.3	--	13.5
Strain Rate	126.8	--	13.7

*All Martin Marietta averaged data are from three test points.

These data show an increase in Ftu when tested at the higher strain rate (> 1 in./minute). The data also show a slight decrease in ductility as a result of chemical milling. This can be explained by the fact that the outer edges of the plate exhibited a finer grain structure than the center portion of the plate and that the chemical milling therefore removed some of the more ductile layer of the plate.

The following is a comparison of the averaged (three specimens) tension test results of the annealing cycle determination. Their corresponding grain structure comparison is shown in Figures 4 thru 17.

Annealed 1 Hour at Temperature, Transverse Specimens

Temperature, °F	Ftu, ksi	Fty, ksi	%e, 2 in.	Micro
1300	126.8	123.3	--	Fig. 4
1400	125.6	121.7	14.8	Fig. 5
1440	121.0	118.7	--	Fig. 6
1500	121.7	117.6	16.7	Fig. 7
1545	119.9	116.9	17.5	Fig. 8
1600	120.0	116.5	17.3	Fig. 9
1660	117.3	114.3	18.2	Fig. 10

Annealed 2 Hours at Temperature, Transverse Specimens

Temperature, °F	Ftu, ksi	Fty, ksi	%e, 2 in.	Micro
1700	115.8	113.3	16.9	Fig. 11
1750	116.1	113.4	15.2	Fig. 12

Annealed at 1600°F for Designated Time, Transverse Specimen

Time, hr	Ftu, ksi	Fty, ksi	%e, 2 in.	Micro
1	117.9	114.2	16.3	Fig. 13
2	116.6	114.1	16.8	Fig. 14
4	116.0	114.0	17.5	Fig. 15
8	115.9	113.9	15.0	Fig. 16
24	113.5	110.6	13.5	Fig. 17

As a result of the 1-hour tests and the 2-hour tests at higher temperature, it was decided that the ductility (Fty and %e) would be best at around 1650°F. Subsequent tests at different times showed the best combination of Fty, %e, and grain structure to be around a 4-hour anneal at 1660°F.

Figure 4 Photomicrograph of Longitudinal Cross Section at 100X of C Plate, Annealed 1 hour at 1300°F

Figure 5 Photomicrograph of Longitudinal Cross Section at 100X of C Plate, Annealed 1 hour at 1400°F

Figure 6 Photomicrograph of Longitudinal Cross Section at 100X of C Plate, Annealed 1 hour at 1440°F

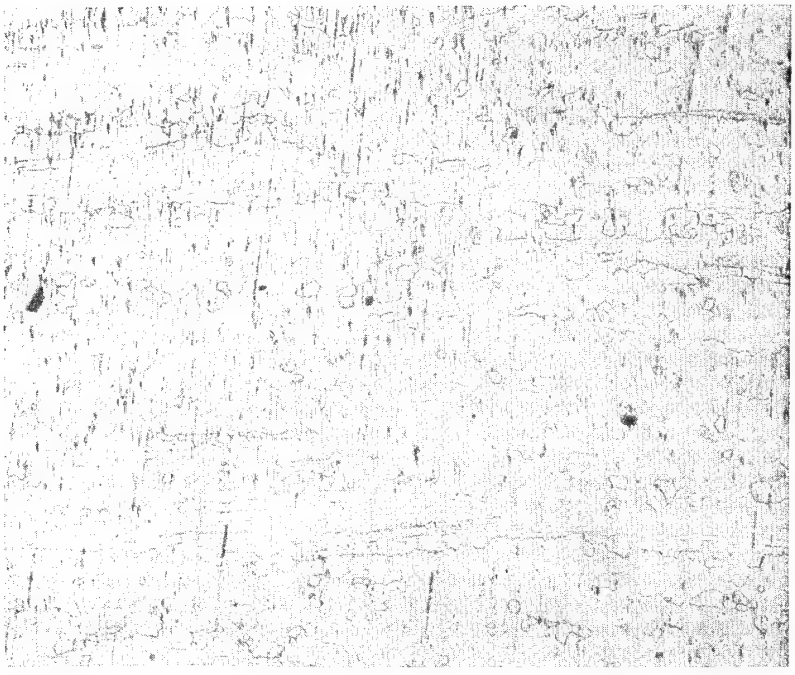

Figure 7 Photomicrograph of Longitudinal Cross Section at 100X of C Plate, Annealed 1 hour at 1500°F

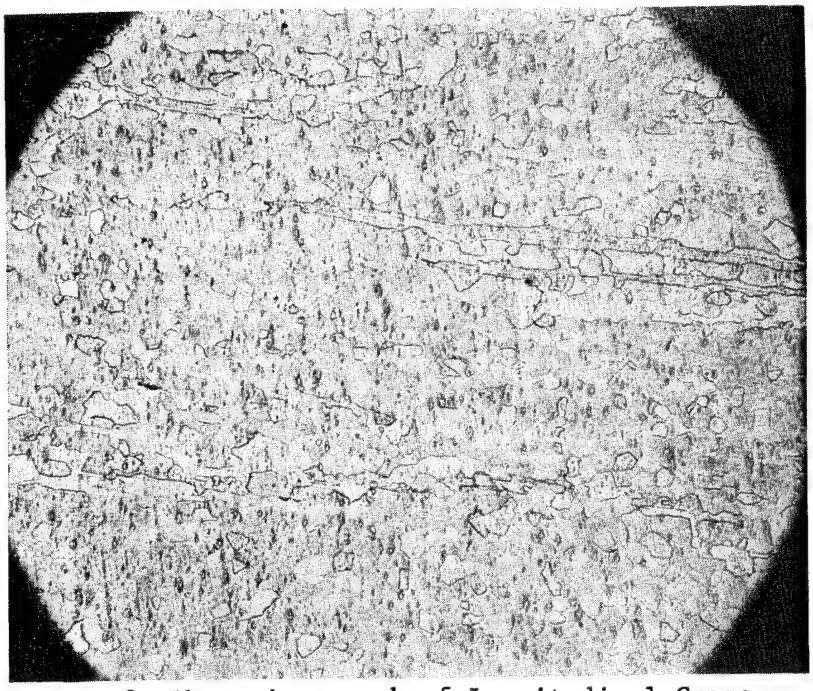

Figure 8 Photomicrograph of Longitudinal Cross Section at 100X of C Plate, Annealed 1 hour at 1545°F

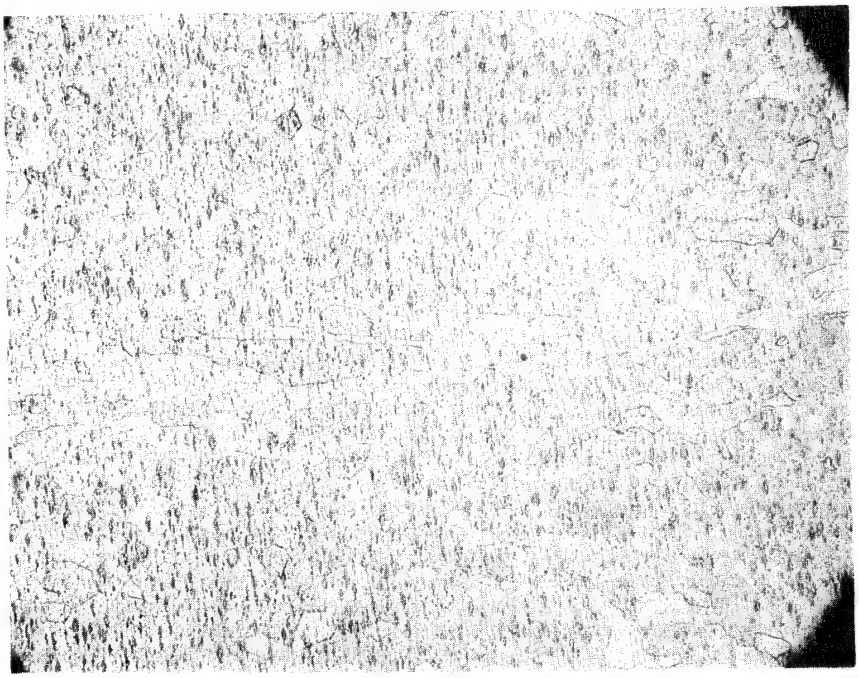

Figure 9 Photomicrograph of Longitudinal Cross Section at 100X of C Plate, Annealed 1 Hour at 1600°F

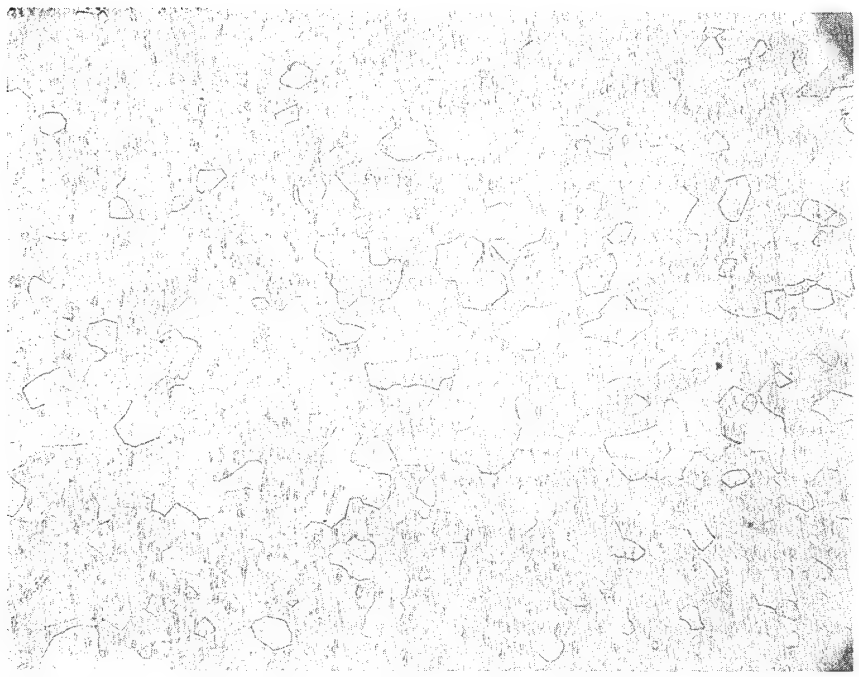

Figure 10 Photomicrograph of Longitudinal Cross Section at 100X of C Plate Annealed 1 hour at 1660°F

Figure 11 Photomicrograph of Longitudinal Cross Section at 100X of C Plate Annealed 2 hours at 1700°F

Figure 12 Photomicrograph of Longitudinal Cross Section at 100X of C Plate Annealed 2 hours at 1750°F

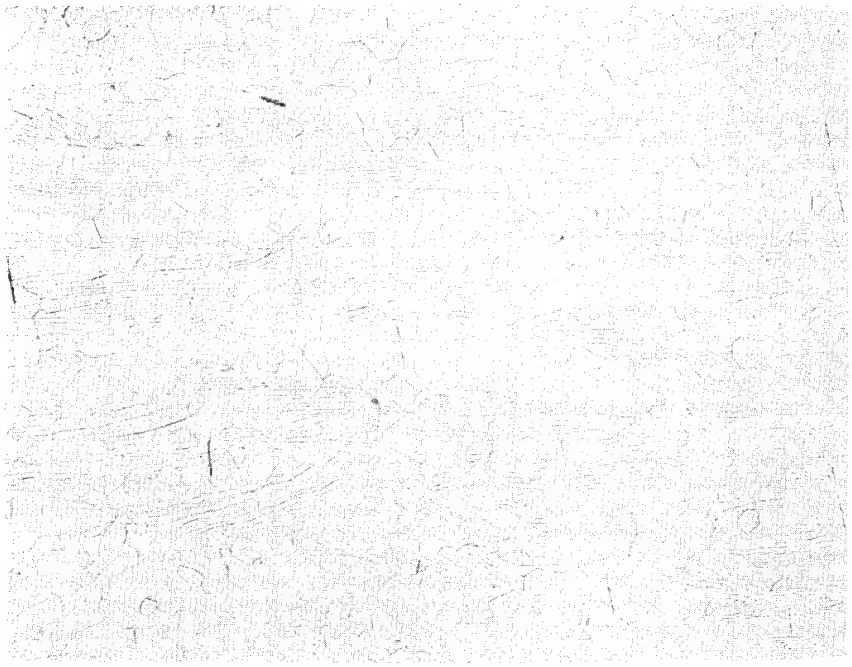

Figure 13 Photomicrograph of Longitudinal Cross Section at 100X of C Plate Annealed 1 hour at 1660°F

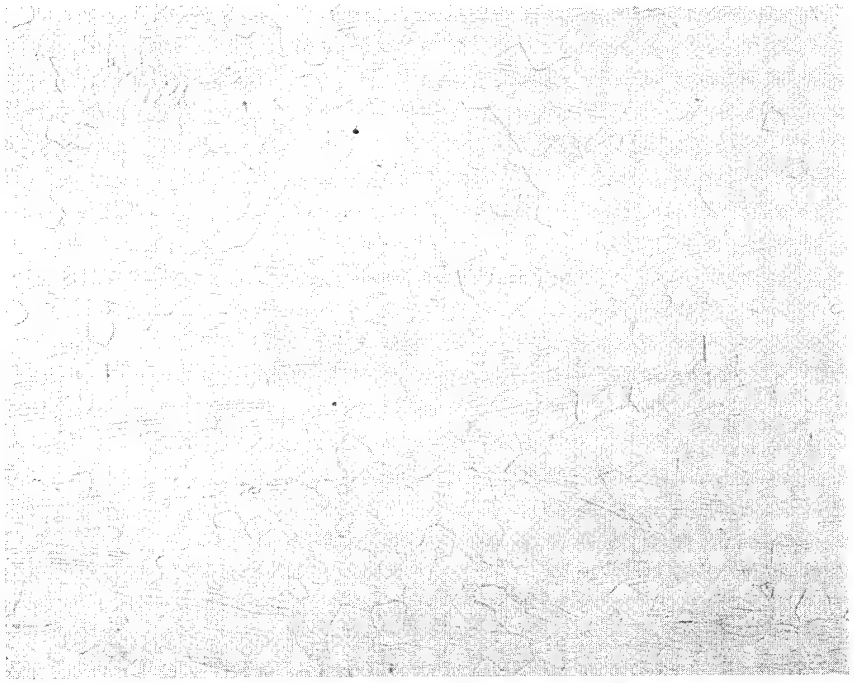

Figure 14 Photomicrograph of Longitudinal Cross Section at 100X of C Plate Annealed 2 hours at 1660°F

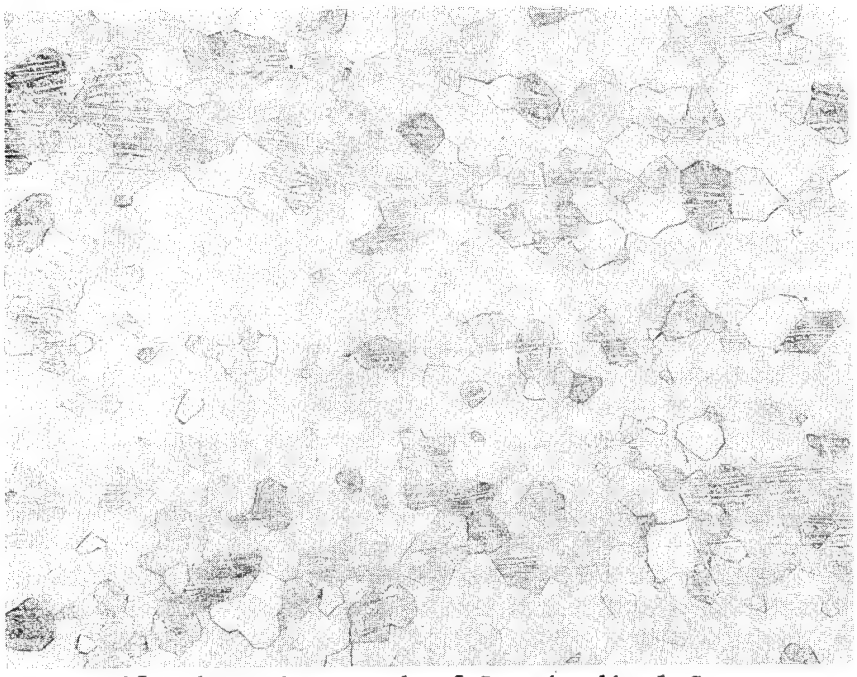

Figure 15 Photomicrograph of Longitudinal Cross Section at 100X of C Plate Annealed 4 hours at 1660°F

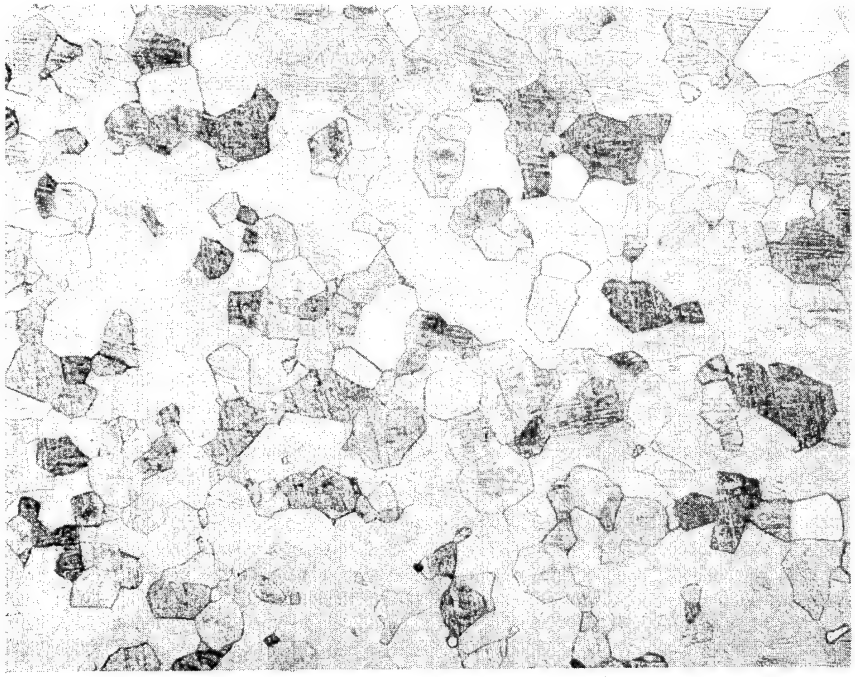

Figure 16 Photomicrograph of Longitudinal Cross Section at 100X of C Plate Annealed 8 hours at 1660°F

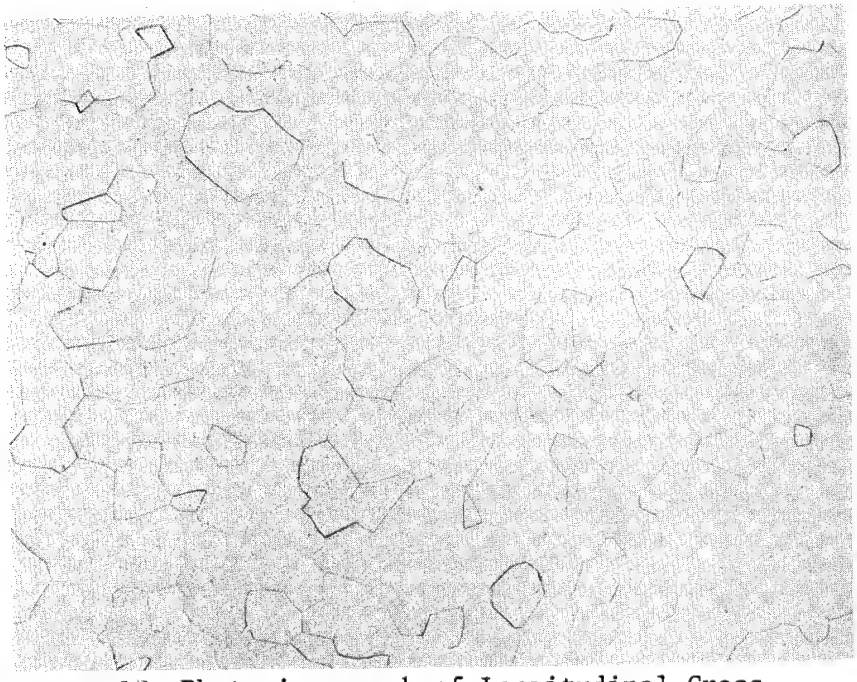

Figure 17 Photomicrograph of Longitudinal Cross Section at 100X of C Plate Annealed 24 hours at 1660°F

Investigation of Dome Failures during
Explosive Forming and Annealing

(June 1970)

INVESTIGATION OF DOME FAILURES DURING EXPLOSIVE FORMING AND ANNEALING (JUNE 1970)

INTRODUCTION

Although liners for the composite overwrapped tanks were to be made from ellipsoidal domes explosively formed from titanium 5Aℓ-2.5Sn alloy plate, cracking problems were experienced and, at the date this report was prepared, no domes had been successfully formed. Cracks developed at various points of the forming cycle. The original forming cycle consisted of two forming operations with an intermediate anneal. Using this cycle, two domes cracked during forming. An investigation was conducted to determine the cause of these failures, resulting in the conclusion that the plate stock had not been properly conditioned for forming. The annealed titanium 5Aℓ-2.5Sn plate had been procured to commercial requirements from Reactive Metals, Inc. It was subsequently learned that two process/annealing treatments had been used to treat the lot of 14 plates, either 15 minutes at 1500°F or 30 minutes at 1500°F. Twelve of the plates received the 30-minute anneal and two the 15-minute anneal. Regardless of which cycle was used, the plate had a highly directional rather than an equiaxed grain structure, and relatively low elongation. As a part of the study, an annealing cycle was developed to recover the plate material, that is, to develop a predominantly equiaxed grain structure with higher elongations and better formability. Through test, an annealing cycle of 4 hours at 1660°F was established. The tests demonstrated that this annealing treatment developed a predominantly equiaxed grain structure in the plate and raised the elongation from an as-received low of 12% to 17% (in 2 in.) minimum.

On the basis of the investigation, the forming cycle was changed to:

1) Vacuum-anneal 4 hours at 1660°F and furnace-cool at 300°F per hour;

2) First explosive-forming operation, partial draw;

3) Clean and vacuum-anneal, same cycle as 1) above;

4) Second explosive-forming operation, form to final shape;

5) Clean and vacuum-anneal, same cycle as 1) above.

Eight blanks were started through this cycle--E1, K1, K2, K3, L1, H2, BB1, and BB3. Not all of these completed the cycle, specifically:

1) K1 - Cracks found after step 3;

2) H2 and BB2 - Cracks found after step 4;

3) All others - Cracks found after step 5.

The cracks found in these eight domes were (1) shallow cracks that could be observed without magnificaiton on the outside surface of the domes, generally 2 to 4 inches above the flange, and (2) similar cracks that could be seen at other locations but only at magnifications of 10X or greater. Cracks tentatively identified as stress corrosion cracks were found in domes K1 and BB3. In K1 these cracks were 1½ to 2½ inches long, radial, and open to outside surface. In BB3, cracks similar to those in K1 were found, and cracks were also found in the flange radius and in the flange. These were all radial, relatively short, and appeared to be stress corrosion cracks. The cracks in the radius open to the inside surface of the dome and those in and above the flange open to the outside surface are shown in Figures 1 thru 3. The third cracking mode was typical of all domes except K1, H2, and BB3. These cracks opened to the inside surface, located on a radius of approximately 5 inches from the dome apex. The most severe case was dome E1 (Fig. 4), while dome L1 (Fig. 5) was more typical of this cracking. Again stress corrosion was suspected but creep and buckling had not been ruled out.

Macroexaminations of the eight cracked domes and specimens from four domes, as-received materials, and as-annealed stock were conducted. In summary, these examinations indicated that an oxygen-rich (stabilized alpha) case was developing on both the inside and outside surfaces of the domes, and that stress corrosion cracking was occurring in some domes. Buckling and stress rupture have not been eliminated as possible causes for the cracks near the apexes of the domes.

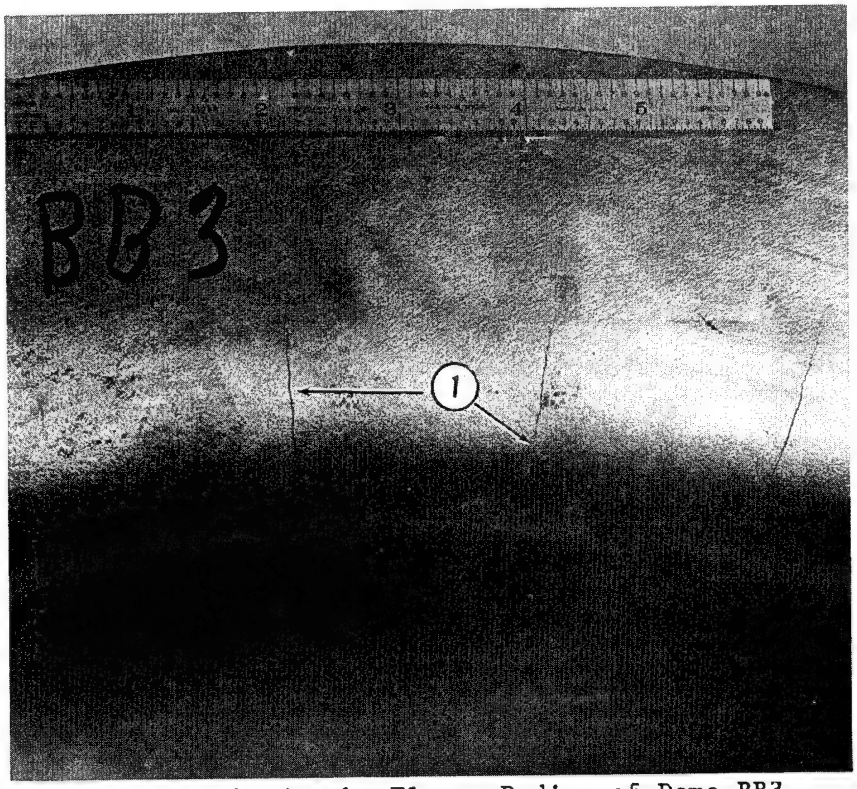

Figure 1 Cracks in the Flange Radius of Dome BB3

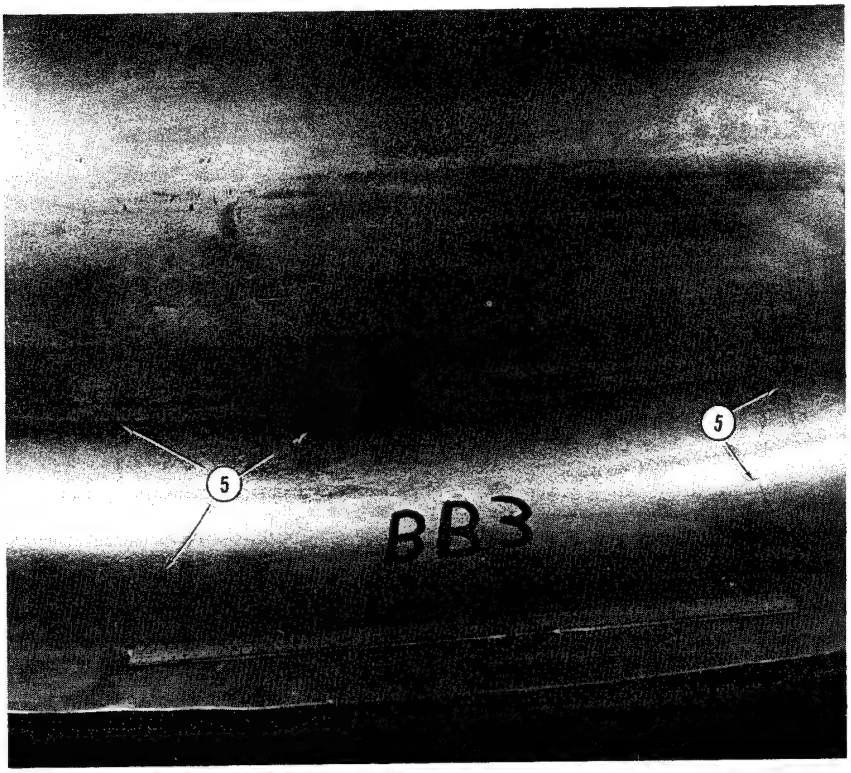

Figure 2 Cracks in the Flange and above the Flange of Dome BB3

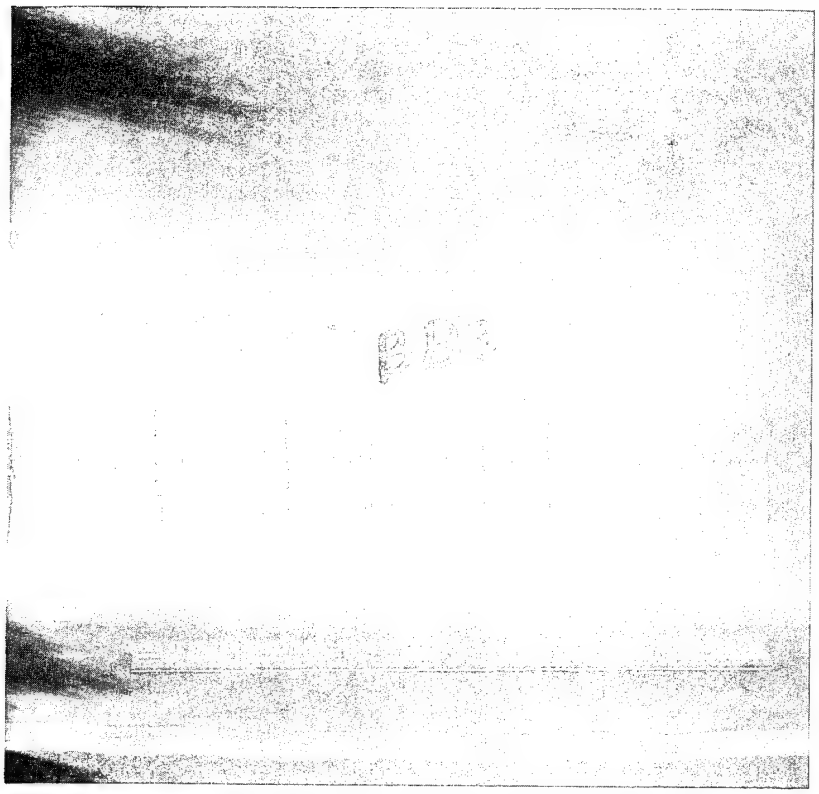

Figure 3 Cracks above the Flange of Dome BB3

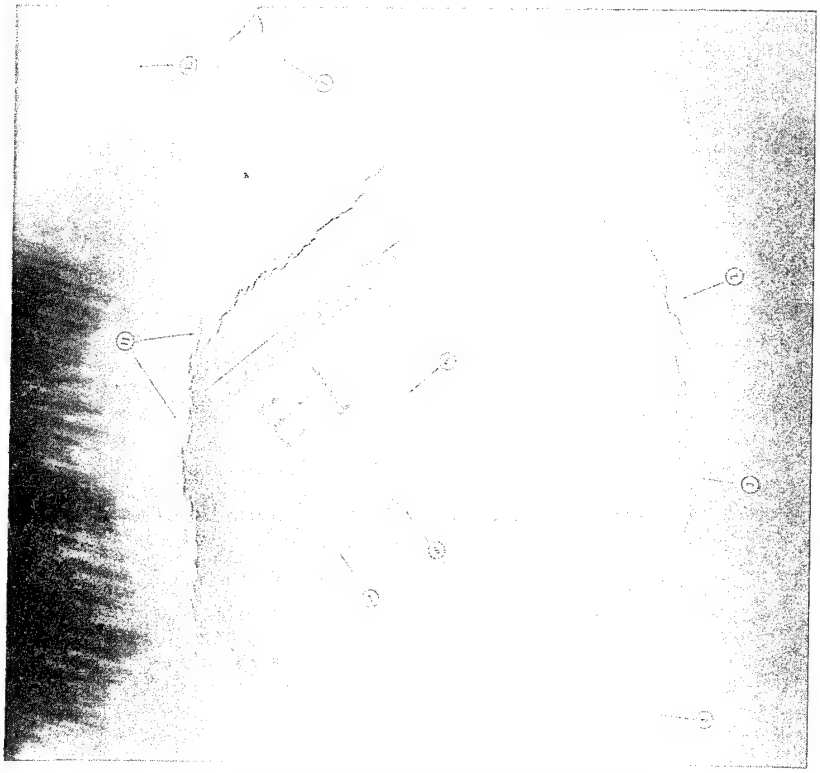

Figure 4 Cracks on the Inside Surface Near the Apex of Dome E1

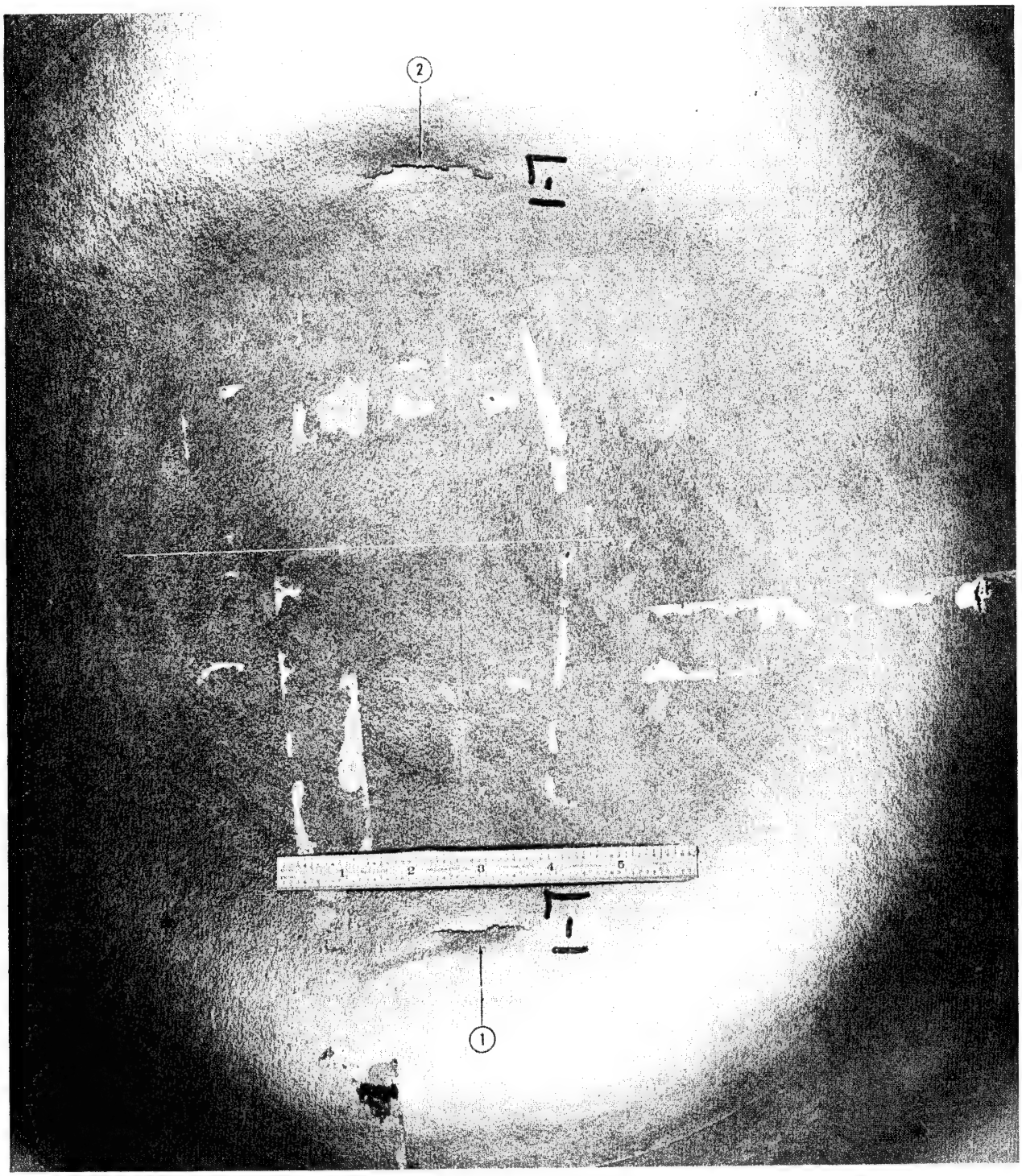

Figure 5 Cracks on the Inside Surface Near the Apex of Dome L1

TEST PROGRAM

A test program for investigating the cause for failure of domes in the vacuum furnace, and for evaluating Turco Pretreat and the air furnace as a substitute for the vacuum furnace for in-process annealing was instigated.

Vacuum Furnace Investigation

This investigation revealed the following:

1) Several small leaks were found and repaired;

2) The vacuum sensor for the Ipsen vacuum furnace was found to be located in a small line just upstream from the diffusion pump. The output from the sensor was recorded on an x-y pressure/time recorder. The instrumentation indicated 0.1 micron during all of the furnace runs in this program;

3) The vacuum measured at an access port on the opposite side of the furnace proved to be 1.25 microns. The sensor was located between the internal wall and baffles in the furnace chamber proper. The test was conducted with a CEC ionization gage that was in calibration as certified by the Secondary Standards Group;

4) Metallurgical examination revealed that a case hardening of the sheet material through oxidation and contamination occurred during the annealing cycle. Bend specimens tested in this condition failed by cracking. Chemical milling of these specimens (approximately 0.005 in. removed from each side) removed the case hardening and the bend specimens did not crack.

A review of the time, temperature, and vacuum recordings and study of the history of the dome blank and forming results indicated that in early activities (February - April) the furnace atmosphere was probably minimally satisfactory.

As our program advanced, however, the performance deteriorated. The changes were very subtle and the impact on dome fabrication and processing was not recognized until several domes failed during the explosive-forming and annealing operations.

Evaluation of Turco Pretreat and Air Furnaces

When it was suspected that the furnace was possibly the remaining cause for contamination and embrittlement, alternative methods were sought. Preliminary study results indicated application of this Turco Pretreat protective coating would likely allow an air furnace to be employed. Several bend specimens were coated, annealed, and tested. The result was favorable and the decision to further evaluate and develop the process was made.

To assure that the process was suitable for complete domes and that the most efficient Martin Marietta Denver Division furnace was used, bend and tensile specimens accompanied a full-scale (scrap) dome through the cleaning, etching, and annealing processes. Two sets of properly coated specimens and domes were prepared for the evaluation. One set was annealed in the air furnace in the beryllium facility operated by AMT and the second set was annealed in the Ordnance Applications Laboratory furnace.

The test procedure followed for the air furnace and Turco Pretreat evaluation is included here.

PROCEDURE FOR TRIAL ANNEALING OF TURCO PRETREAT-COATED

TITANIUM 5Aℓ-2.5Sn DOMES FOR THE OVERWRAP TANK PROGRAM

1. Remove sections of the flange of each dome as shown in the following sketch.

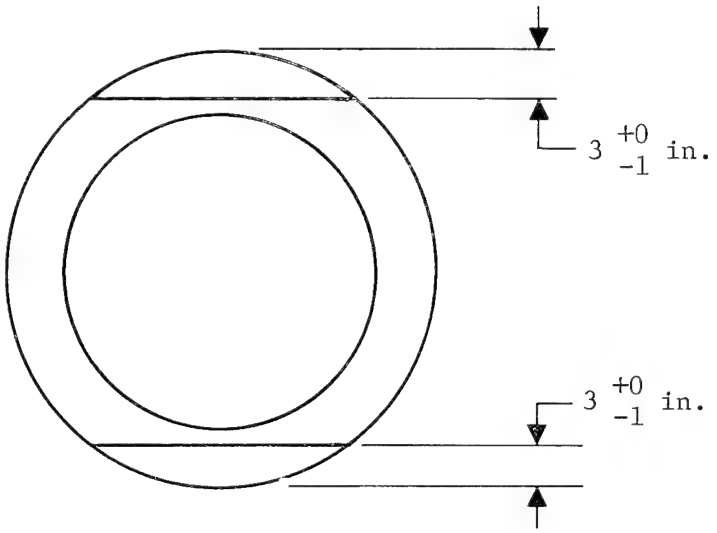

2. Chem-mill the domes and the sections from the flanges. Note: The normal prechem-mill cleaning procedure should be followed except the domes and specimens should not be vapor-degreased; a MEK wipe should be substituted for the vapor degreasing operation.

3. After chem milling, the domes and specimens shall be protected from contamination (white glove handling) and wrapped in polyethylene.

4. Apply Turco Pretreat to the domes and one specimen from the flange of each dome. Clean the surfaces with new MEK before applying the Turco Pretreat.

5. Heat-treat 1 hour +15 minutes, -0 minute, at 1550°F ± 20°F. Air-cool; support the dome at the flange in the "flange-up" position. Air blast is not required but may be used.

6. Cleaning: Method IIA of EPS50063, except do not vapor-degrease.

7. Chem-mill (do not vapor-degrease). Remove 0.005 inch minimum from all surfaces of the domes and specimens.

Using the steps described, two partially formed domes and six test bars were processed through the heat-treat cycle and cleaning. One dome and three bars were processed in each of two different air atmosphere furnaces. After the processing, the specimens were tested and examined for evidence of surface contamination as a result of heat treatment.

RESULTS

The results can be summarized as:

1) Test specimens processed in both furnaces showed no cracks when bent around a 4 T bend radius. This corresponds to similar tests on normal high-quality annealed Ti-5Aℓ-2.5Sn titanium alloy;

2) Metallographic examination showed no additional contamination as a result of oxygen absorption and complete removal of superficial contamination by use of the chemical milling operation;

3) Only in areas not completely descaled in the original chemical milling operation was there evidence of oxygen contamination in the form of stabilized alpha phase. These areas were compared to similar visual areas observed on specimens not processed through the cleaning and annealing cycle and were found to be similar. Therefore, it was concluded the Turco Pretreat coating did protect the titanium sufficiently through the annealing cycle in an air atmosphere furnace;

4) The presence of heat-treat scale is easily detectable, visually, with the unaided eye as rough matte appearing areas, whereas chemically milled titanium approaches a mirror finish. Therefore, any heat-treat scaled areas were detected and removed from the part.

CONCLUSIONS

The following conclusions are made:

1) All future thermal treatment of Ti-5Aℓ-2.5Sn titanium alloy should be performed in either the Advanced Manufacturing Technology Laboratory furnace or the Ordnance Laboratory furnace. Turco Pretreat shall be employed as the protective media to prevent oxidation of the titanium;

2) The Turco Pretreat should be applied so the surface of the titanium is uniformly coated;

3) The titanium should be chemically milled so a minimum of 0.005 inch and a maximum of 0.010 inch is removed from all surfaces of the titanium parts;

4) The cleaning and heat-treat process should be followed as outlined,

   a) Hand-clean with MEK,

   b) Alkaline-clean,

   c) Chem-mill a minimum 0.005 inch and a maximum of 0.010 inch from all surfaces,

   d) Wrap parts in kraft paper,

   e) Apply Turco Pretreat and allow to dry thoroughly,

   f) Anneal at 1550°F $\pm$ 25°F, soak 1 hour $^{+15}_{-0}$ minutes, cool in air at room temperature,

   g) Clean as indicated above, but hold in the chemical mill activator until all visible trace of the Turco Pretreat is removed,

   h) Chem-mill 0.005 inch minimum and 0.010 inch maximum from all surfaces of the parts.

HOT-SIZING PROCESS FOR TITANIUM DOMES

HOT-SIZING PROCESS FOR TITANIUM DOMES

The following steps were taken in assuring that the proper quality control procedures were applied:

1) Machine dome 1/8 in. oversize (height dimension);

2) Clean dome and apply Everlube T-50;

3) Coat sizing fixture with Everlube T-50;

4) Assemble dome to fixture and torque as required to seat dome to tool;

5) Hot-size at 1250°F $\pm$ 25°F for 30 minutes minimum in air furnace and install single thermocouple inside of dome. Quality-verify temperature & cycle time;

6) Remove from furnace after 30 minutes and air-cool (no forced air);

7) Disassemble from sizing fixture. (Note: Do not disassemble until part has cooled below 800°F.)

8) Clean dome, including,

   a) Toluol wash to remove Everlube T-50,

   b) Finish removal of Everlube T-50 via scale conditioner bath (Turco 43-16),

   c) Nitric hydrofluoric pickle bath & rinse with deionized water,

   d) Verify part cleanliness.

COMPOSITE OVERWRAPPED METALLIC TANKS
TASK IV

TEST PROCEDURE
H40152
SIZING OPERATION
&
BURST PROCEDURE (AMBIENT TEMPERATURE)

INTRODUCTION

Glass fiber-reinforced titanium pressure vessels were sized, proof pressure tested, and subjected to ambient burst tests at the Cold Flow Laboratory for NASA Lewis Research Center. These tanks were the first in a series of tanks to be tested by Cold Flow personnel. Future testing will include ambient and cryogenic cycling tests.

OBJECTIVES

The objective of these tests was to measure the strains necessary to obtain design information for composite pressure vessels fabricated by glass-fiber overwrapping (and compression) of titanium pressure vessels. Hoop strain and barrel section longitudinal strain were measured during ambient burst tests. The procedures followed are outlined below.

PRETEST PROCEDURE

_____ 1. Verify that displacement vs recorded output of the LVDTs has been accomplished.

_____ 2. Verify test item installation per CFL drawing 630043 (Fig. 1) and that pictures have been taken of the tank and setup.

_____ 3. Verify that Safety has been informed and concurs with the test schedule.

_____ 4. Verify that instrumentation has been installed and is ready for test.

_____ 5. Verify that adequate GN_2 and inhibited water are available (approximately 50 gal inhibited water).

TEST PROCEDURE

_____ 1. Verify all valves are closed except the water lockoff valve (WLOV).

_____ 2. Increase the hand loader to approximately 400 psig.

_____ 3. Open the pressurization valve PNV and pressurize the test item to 350 psig.

_____ 4. Close PNV.

CAUTION Do not allow leak detection fluid to come in contact with the test item glass wrapping.

_____ 5. Bubble-leak-check all connections.

_____ 6. Open through-flow valve and reduce the test item pressure to zero.

_____ 7. Install the immersion tank top and initiate an audible warm GN_2 purge through the immersion tank. Immersion tank temperature requirement for this test is 75 $\pm$ 10°F.

_____ 8. Remove the pressurization and vent lines.

_____ 9. Open the water fill valve (WFV) and fill the 6000-psi K-bottle and the test item with 75 $\pm$ 10°F inhibited water.

_____ 10. Allow water to flow through TFV until a gas-free condition is reached. Close WFV and TFV. Disconnect the water fill line and adjust the water level to point A. Cap the water fill line and reconnect the pressurization and vent lines.

_____ 11. Request instrumentation personnel to calibrate all functions.

_____ 12. Place the cell area in a red condition and erect suitable barricades. Verify that the area is cleared to the extent that a catastrophic failure of the test item will not cause injury to personnel.

_____ 13. Mark recorders "H40152 Tank S/N _____ Sizing, Date and Time." Start recorders at 2.5 mm/s.

_____ 14. Verify that the immersion tank temperature is 75 $\pm$ 10°F.

_____ 15. Verify that all valves except WLOV are closed.

NOTE Test item failure is indicated by either a sudden drop of test item pressure P_1 (rupture), or a stabilized differential between the supply pressure gage G_2 and the test item pressure P_1 (liner leakage failure).

_____ 16. Slowly open the pressurization valve PNV and adjust the supply hand loader as required to increase the test item pressure at a strain rate not to exceed 1%/minute until a pressure of 4480 psig is reached. Maintain this pressure for a period of not less than 10 seconds.

_____ 17. Close PNV and open the tank vent valve (TVV). Reduce the test item pressure to zero as rapidly as possible without dumping water.

_____ 18. Reduce the supply hand loader to zero and allow the recorders to run for 10 minutes.

_____ 19. Postcalibrate all functions and annotate "End Sizing Operation Tank S/N _____."

_____ 20. Disconnect the pressurization and vent lines. Refill the system to point A using a graduated cylinder to measure the amount of water required to refill the system.

_____ 21. Replace the pressurization and vent line.

_____ 22. Request instrumentation to rezero the LVDTs and calibrate all functions.

_____ 23. Annotate recorders "Start Burst Test, Tank S/N _____ Date and Time." Start recorders at 2.5 mm/s.

_____ 24. Verify that all valves are closed except WLOV.

_____ 25. Verify that actuation and supply pressures to the boost pump are proper.

_____ 26. Open PNV and adjust the supply hand loader as required to increase the test item pressure at a strain rate not to exceed 1%/minute until test item pressure is 4050 $\pm$ 100 psig. Maintain 4050 $\pm$ 100 psig for 3 minutes.

NOTE Expected test item burst is approximately 5600 psig. If facility GN_2 pressure is not sufficient to rupture the test item, close PNV, open the boost pump outlet valve POV, and continue test item pressurization using the boost pump until test item failure occurs.

_____ 27. Adjust the supply pressure as required to increase the test item pressure at a strain rate not to exceed 1%/minute until the test item pressure is 5600 $\pm$ 100 psig. Maintain 5600 psig for 3 minutes.

_____ 28. Adjust the supply pressure as required to increase the test item pressure at a strain rate not to exceed 1%/minute until test item rupture occurs.

_____ 29. When test item failure occurs, immediately close WLOV and stop the boost pump (or close PNV).

_____ 30. Open TVV and reduce system pressure to zero.

_____ 31. Open WLOV and TFV.

_____ 32. Postcalibrate all recorders and annotate "End Burst Test S/N _____ Date and Time."

NOTE IMPORTANT: Do not balance the pressure data channel during or after postcalibration. A deadweight of P_1 is required in the "as-is" condition.

_____ 33. Discontinue the immersion tank purge.

_____ 34. Remove the immersion tank top and verify test item failure.

_____ 35. Remove P_1 and deadweight through the indicated failure pressure.

_____ 36. Photograph the failed test item in the holding fixture. All photographs will contain specimen identification, test, date, and time of failure.

_____ 37. Carefully remove the test item from the holding fixture and photograph as necessary to show all of the failure.

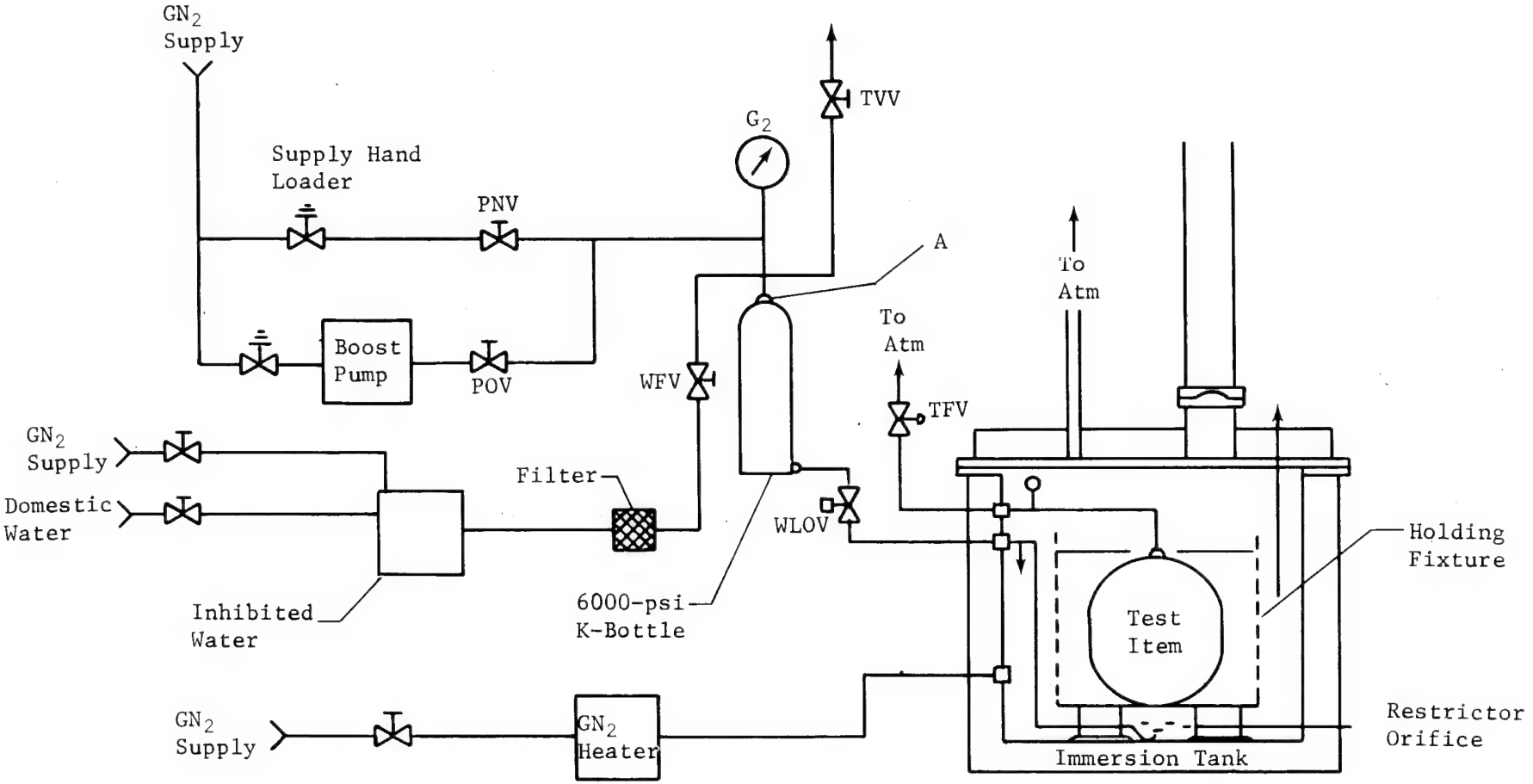

Figure 1 Test Setup

COMPOSITE OVERWRAPPED METALLIC TANKS
TASK IV

TEST PROCEDURE
H40152
AMBIENT CYCLING
(S/N 6)

INTRODUCTION

Eight test items were subjected to an ambient sizing test in the Composite Overwrapped Metallic Tank program (NAS3-12023). Six of the tanks ruptured during the sizing portion of the test. One tank successfully completed the sizing test and subsequently ruptured at 5062 psig during the ambient temperature burst test. One tank successfully completed the sizing test but was not subjected to a burst test. This tank (S/N 6) was subjected to the ambient cycling test described in this procedure.

OBJECTIVE

The objective of the test was to determine if tank S/N 6 could be subjected to 1000 ambient temperature operating pressure cycles without failure. The procedures followed are included here.

PRETEST PROCEDURE

_____ 1. Verify that displacement vs recorded output of the LVDTs has been accomplished.

_____ 2. Verify test item installation per CFL drawing 6300423 (Fig. 1) and that pictures have been taken of the tank and setup.

_____ 3. Verify that Safety has been informed and concurs with the test schedule.

_____ 4. Verify that instrumentation has been installed and is ready for test.

_____ 5. Verify that adequate GN_2 and inhibited water are available (approximately 50 gal inhibited water).

TEST PROCEDURE

_____ 1. Verify all valves are closed except the water lockoff valve (WLOV).

_____ 2. Increase the hand loader to approximately 400 psig.

_____ 3. Open the pressurization valve PNV and pressurize the test item to 100 psig.

_____ 4. Close PNV.

CAUTION Do not allow leak detection fluid to come in contact with the test item glass wrapping.

_____ 5. Bubble-leak-check all connections.

_____ 6. Open through-flow valve (TFV) and reduce the test item pressure to zero.

_____ 7. Initiate an audible warm GN_2 purge through the immersion tank. Test item temperature requirement for this test is 75 $\pm$ 10°F.

_____ 8. Verify WLOV and TFV are open.

_____ 9. Open the water fill valve (WFV) and fill the test item with 75 $\pm$ 10°F inhibited water.

_____ 10. Allow water to flow through TFV until a gas-free condition is reached. Close TFV. Disconnect point A and fill the K-bottle. Reconnect point A and close all valves.

_____ 11. Request instrumentation to calibrate all functions.

_____ 12. Place the cell area in a red condition and erect suitable barricades. Verify that the area is cleared to the extent that a catastrophic failure of the test item will not cause injury to personnel.

_____ 13. Mark recorders "H40152 Tank S/N _____ Cycling, Date and Time." Start recorders at 1.0 mm/s.

_____ 14. Verify that the test item temperature is 75 $\pm$ 10°F.

_____ 15. Open WLOV.

NOTE Test item failure is indicated by either a sudden drop of test item pressure P_1 (rupture), or a stabilized differential between the supply pressure gage G_2 and test item pressure P_1 (liner leakage failure).

_____ 16. Verify PNV and TVV are closed and load the supply hand loader to 4000 psig.

_____ 17. Open PNV as required to increase test item pressure to 3360 ± 50 psig at a strain rate not to exceed 2%/minute. Close PNV.

_____ 18. Open TVV as required to reduce test item pressure to 0 to 100 psig.

_____ 19. Repeat steps 17 and 18 a total of 1000 times. Maintain test item temperature at 75 ± 10°F. Every 50 cycles, pause for 15 seconds between steps 17 and 18. Pressure decay exceeding 30 psi during the 15-second period indicates a possible test item failure and that the test should be discontinued for a failure investigation. The test instrumentation should be recalibrated at least once every hour. Pressure cycles need not be continuous but the test item temperature must be maintained at 75 ± 25°F whenever the tank contains water.

_____ 20. On successful completion of the 1000 pressure cycles, the test will be discontinued or the test item will be subjected to an ambient burst test at the test requestor's discretion.

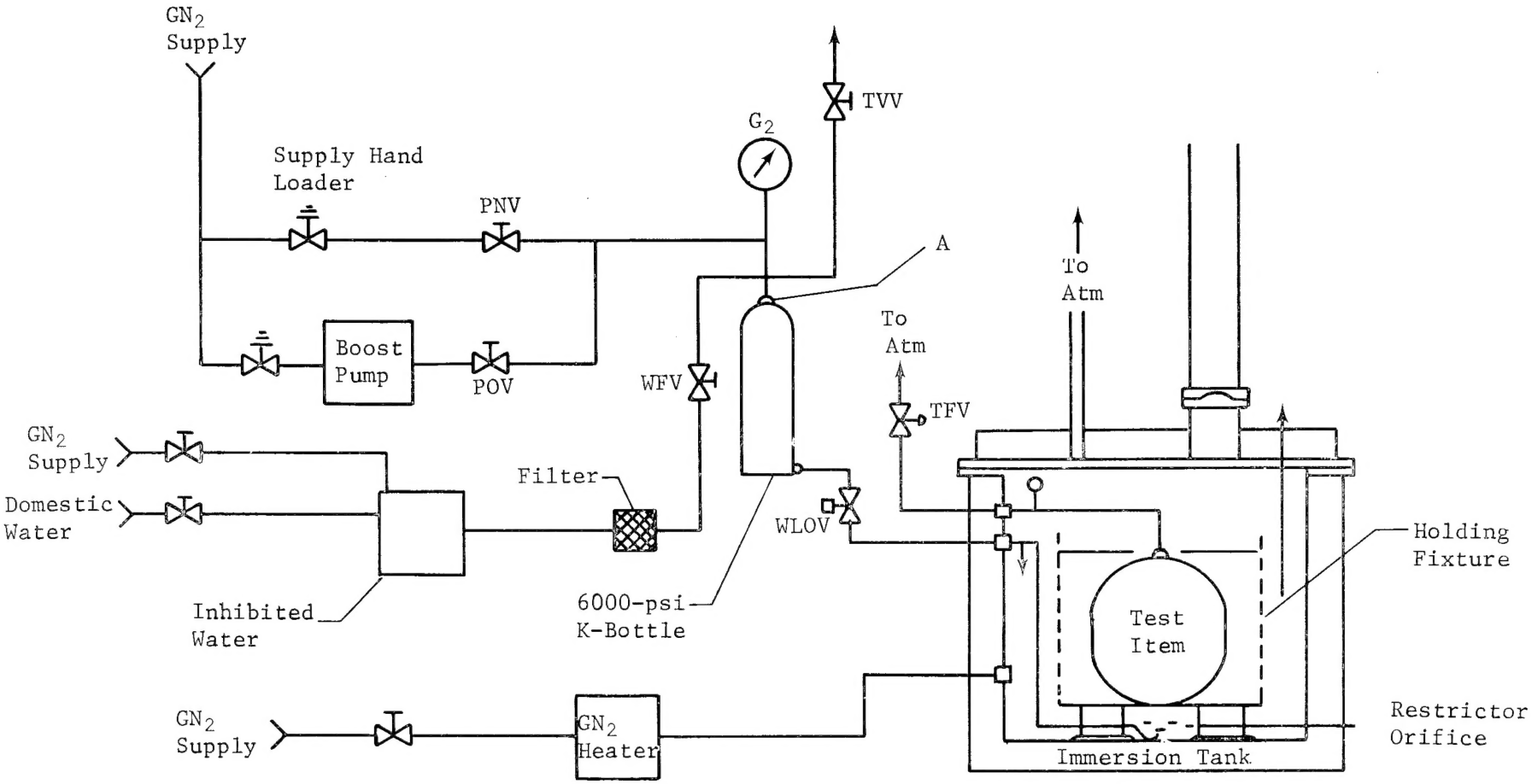

Figure 1 Test Setup

MARTIN MARIETTA CORPORATION DENVER DIVISION

POST OFFICE BOX 179, DENVER, COLORADO 80201 TELEPHONE (303) 794-5211

14 April 1972

Refer to: 72-Y-11225

To: National Aeronautics and Space Administration
Lewis Research Center
21000 Brookpark Road
Cleveland, Ohio 44135

VIA AIR MAIL

Attn: Contracting Officer, Jack Lerner/M. S. 500-313

Subj: Contract NAS3-12023, Composite Overwarapped Metallic Tanks, Transmittal of Data

Ref: (a) Contract NAS3-12023, Exhibit "B" Paragraph C
(b) NASA Lewis Approval Letter dated 14 March 1972 signed by Thomas J. Flanagan

Encl: (1) NASA CR-120888, Final Report (1 copy)

The Final Report (Enclosure 1) is transmitted in compliance with the referenced requirement of the subject contract. Distribution has been made per the list furnished with the Approval Letter (reference b), each designee will receive a copy of the attachment to this letter.

Very truly yours,

MARTIN MARIETTA CORPORATION

Henry Aliano

Henry Aliano, Chief
Configuration and Data Management
Denver Division

HA/JW:bb

Internal Distribution (w/o Encl)
C. Caudill, 1630

AFPRO, A-18